University of Calgary

PRISM Repository **https://prism.ucalgary.ca**

The Vault Open Theses and Dissertations

2014-09-30

Exploring Mitochondrial Regulation of Reovirus Infection in Cancer Cells

Clarkson, Matthew

Clarkson, M. (2014). Exploring Mitochondrial Regulation of Reovirus Infection in Cancer Cells (Master's thesis, University of Calgary, Calgary, Canada). Retrieved from https://prism.ucalgary.ca. doi:10.11575/PRISM/26090

http://hdl.handle.net/11023/1891

Downloaded from PRISM Repository, University of Calgary

UNIVERSITY OF CALGARY

Exploring Mitochondrial Regulation of Reovirus Infection in Cancer Cells

by

Matthew Frederick Clarkson

A THESIS

SUBMITTED TO THE FACULTY OF GRADUATE STUDIES

IN PARTIAL FULFILMENT OF THE REQUIREMENTS FOR THE

DEGREE OF MASTER OF SCIENCE

DEPARTMENT OF BIOCHEMISTRY AND MOLECULAR BIOLOGY

CALGARY, ALBERTA

SEPTEMBER, 2014

© Matthew Frederick Clarkson 2014

Abstract

Oncolytic reovirus demonstrates mixed results in clinical trials. To achieve better clinical outcomes a more complete understanding of reovirus infection is needed. Efficient reovirus infection often culminates in cell death by apoptosis. Mitochondria play essential roles regulating apoptosis and oxidative phosphorylation. Although mitochondria are implicated in integrating reovirus-induced apoptotic signaling, no study has explored how modulating apoptotic pathways or mitochondrial metabolism influences reovirus infection.

I demonstrate that directly priming apoptotic pathways may be an effective strategy for augmenting reovirus-induced cytolysis in pediatric leukemia cells and possibly other cancer cells. Further study is warranted to explore the clinical potential of this strategy. The experiments attempting to modulate mitochondrial function may be consistent with a role for mitochondrial respiration in reovirus infection. However, the influence of mitochondrial metabolism on reovirus infection requires more directed study in the future.

Acknowledgements

I would like to sincerely thank Dr. Randal Johnston for giving me the opportunity to pursue grauate studies in his lab. He has been an inspiring, encouraging, supportive, and patient mentor and friend.

I wish to thank my committee members Dr. Morley Hollenberg, Dr. Aru Narendran, and Dr. Daniel Muruve for their guidance and encouragement during my studies.

I would like to thank past and present Johnston Lab members, as well as members of the Narendran and Kurz labs, for their helpful discussion and troubleshooting.

I would like to acknowledge the financial support I received from graduate studentships from NSERC and the CIHR/ACHRI Training Program in Genetics, Child Development, and Health.

I wish to thank my friends both near and far for their encouragement and support.

Finally, I must thank my family for their constant love, support, encouragement, and faith in me.

Table of Contents

List of Tables

List of Figures and Illustrations

List of Symbols, Abbreviations and Nomenclature

AA	antimycin A
ABT	ABT-737
AIF	apoptosis inducing factor
ALL	acute lymphoblastic leukemia
AML	acute myeloid leukemia
ANOVA	analysis of variance
APAF-1	apoptotic proteinase activating factor 1
ATP	adenosine triphosphate
AZ	sodium azide
B1	B-cell ALL cell line
BAK	Bcl-2 agonist/killer
BAX	Bcl-2 associated X protein
BCL-2	B-cell lymphoma-2
BCL-XL	B-cell lymphoma- extra large
BH3	Bcl-2 homology domain 3
BID	Bcl-2-interacting domain death ligand
CAD	caspase-activated DNase
CEM	T-cell ALL cell line
CI	combination index
CV	crystal violet
DHX33	DEAH box protein 33
DHX9	DEAH box helicase 9
DISC	death-inducing signaling complex
DKO	double knockout
DMEM	Dulbecco's Modified Eagle's Medium
DOX	doxorubicin
DR	death receptor
dsRNA	double stranded RNA
DV	dead virus, UV light-inactivated
Ψm	mitochondrial inner membrane potential
EGFR	epidermal growth factor receptor
eIF2α	eukaryotic initiation factor 2α
eIF4E	eukaryotic initiation factor 4E
EndoG	endonuclease G
ER	endoplasmic reticulum
ERK	extracellular signal-regulated kinase
ETC	electron transport chain
FADD	fas-associated death domain
GCIY	gastric cancer cell line
HCT-LG	low glucose-adapted HCT116 cells
HCT116	colon adenocarcinoma cell line
HeLa	cervical adenocarcinoma cell line
HeLa-LG	low glucose-adapted HeLa cells
HS68	human foreskin fibroblast cell line (not immortalized)
HSP70	heat shock protein 70 kDa

HSV	herpes simplex virus
HT29	colon adenocarcinoma cell line
HtrA2	high temperature requirement protein A2
IAPs	inhibitor of apoptosis proteins
IFN	interferon
IMS	(mitochondrial) intermembrane space
IPS-1	interferon-beta promoter stimulator 1
IRF3	interferon responsive factor 3
ISG	interferon stimulated gene
ISVP	infectious subviral particle
JAM-A	junctional adhesion molecule-A
JURKAT	T-cell ALL cell line
L929	mouse fibroblast cell line
LC3	Microtubule-associated protein 1A/1B-light chain 3
LG	low glucose
LV	Live Virus
MAPK	mitogen activated protein kinase
MAVS	mitochodnrial antiviral signaling
MCL-1	myeloid cell leukemia 1
Mda5	melanoma differentation-associated protein 5
MIM	mitochondrial inner membrane
MKN1	gastric cancer cell line
MKN74	gastric cancer cell line
MN45	gastric cancer cell line
MOI	multiplicity of infection
MOLT3	B-cell ALL cell line
MOM	mitochondrial outer membrane
MOMP	mitochondrial outer membrane permeabilization
mRNA	messenger RNA
mtDNA	mitochondrial DNA
MTX	methotrexate
NF-κB	nuclear factor-kappa-light-chain-enhancer of B cells
NOXA	Phorbol-12-myristate-13-acetate-induced protein 1
OA	oligomycin A
Opti-MEM	modified Eagle's Minimum Essential Medium
OV	oncolytic virus
OXPHOS	oxidative phosphorylation
p.i.	post infection
p53	tumor protein p53
PARP	poly(ADP-ribose)polymerase
PBL	peripheral blood lymphocyte
PKR	dsRNA activated protein kinase
pmf	proton motive force
RAS	rat sarcoma (related protein)
RB	retinoblastoma protein
RC	respiratory chain

RIG-I	retinoic acid-inducible gene 1
RN	rotenone
RNase L	ribonuclease L
SEM	standard error of the mean, in figure legends
SEM	B-cell ALL cell line
SMAC	second mitochondrial-derived activator of caspases
SOS	son of sevenless
ssRNA	single stranded RNA
T1L	reovirus strain type 1 Lang
T2J	reovirus strain type 2 Abney
T3A	reovirus strain type 3 Abney
T3D	reovirus strain type 3 Dearing
tBID	truncated BID
TE-1	esophageal cancer cell line
TE-8	esophageal cancer cell line
TIB202	AML cell line
TMRM	tetramethylrhodamine methyl ester
TR	Trail ligand
TRAIL	tumor necrosis factor-related apoptosis-inducing ligand
UV	ultraviolet
VF	viral factory
VV	vaccinia virus
XIAP	X-linked inhibitor of apoptotis protein
ZVAD	z-VAD-fmk, caspase inhibitor

Units of Measure	Definition
%	percent
g	grams
hr(s)	hour(s)
kDa	kilodalton
M	molar
mg	milligram
min(s)	minute(s)
mL	millilitre
mM	millimolar
nM	nanomolar
oC	degrees celcius
pfu	plaque forming units
v/v	mL solute/100 mL solution
w/v	g solute/100 mL solution

Chapter One: **INTRODUCTION**

This thesis pursues an enhanced understanding of the role of apoptotic pathways and mitochondrial regulation in efficient reovirus oncolysis. Naturally occurring reovirus is relatively harmless to humans but replicates robustly in and kills many types of cancer cells by apoptosis *in vitro* and *in vivo*. Although reovirus is currently being evaluated in numerous clinical trials, the observed antitumor efficacy as monotherapy has been modest. As reovirus may soon achieve clinical approval as an adjuvant to chemotherapy, it will be important to improve our understanding of the factors regulating efficient reovirus oncolysis to improve antitumor efficacy and to better predict patient response.

1.1 Oncolytic Virotherapy

1.1.1 Introduction to Oncolytic Viruses

Oncolytic (cancer-killing) viruses (OVs) are naturally occurring or engineered, replication competent viruses that preferentially infect and kill cancer cells. The concept of using viruses for cancer therapy originated in the 1900's[1]. But only in the 1990's had significant improvements in the understanding of cancer, virology, and genetic manipulation allowed for convincing pre-clinical study of oncolytic viruses, providing support and promise for the clinical translation of these agents[2]. Significant progress has been made in the field and currently nine different virus families are being investigated in clinical trials against advanced malignancy. At least a few of these agents, including oncolytic reovirus, are likely to become approved anticancer agents[3, 4].

1.1.2 General Mechanisms of Oncolytic Virotherapy

Although each virus has a specific cellular tropism, many naturally occurring viruses preferentially infect and kill tumor cells, while others are engineered to do so. OVs take advantage of aspects of tumor biology, whereby preferential virus infection is often facilitated by i) overactive biosynthetic pathways, ii) defective antiviral pathways, and iii) altered or enhanced cell surface expression of receptors for virus[5]. Following efficient replication, OVs can kill

infected cancer cells through direct mechanisms, such as infection-induced apoptosis, necrosis, or autophagy. OVs can also induce immunogenic forms of cell death[6], leading to stimulation of antitumor immunity capable of destroying uninfected cells. OVs also induce bystander killing of uninfected cells through destruction of tumor associated vasculature and by engineered viral proteins conferring pro-drug activating activity[4]. Clinically, oncolytic virotherapy of tumors is complex and likely involves multiple pathways contributing to tumor destruction.

1.1.3 Advantages of Oncolytic Viruses

Oncolytic virotherapy provides numerous potential advantages over conventional chemotherapy, including limited toxicity, dose escalation within the tumor, and stimulation of antitumor immunity[6-8]. This is important, because cancer remains as a worldwide epidemic. In the United States 2 in 5 people will develop an invasive cancer in their lifetime, and only 3 in 5 patients will live to 5 years from diagnosis[9]. It is clear that patients are in need of improved therapeutic options. OVs such as reovirus and others hold great promise as safe, effective adjuvants to current cancer therapy.

The majority of OVs in the clinic (7 of 9) have been genetically modified. Oncolytic viruses can be genetically engineered for a number of broad purposes including: i) enhancing tumor specificity, ii) 'arming' viruses for improved anticancer effect, and iii) tumor visualization[4, 10]. Due to the size constraints and the segmented dsRNA genome of reovirus, it had previously been impossible to engineer reovirus. However, recent developments including i) the development of a reverse genetics system allowing for the manipulation of reovirus genes[11], and ii) the apparent dispensability of the C-terminal of the reovirus σ1 protein[12], may allow the future development and study of engineered reoviruses (RN Johnston and M Shmulevitz collaboration).

1.1.4 Clinical Observations from Oncolytic Virotherapy Trials

As expected, oncolytic virotherapy has been found to be safe in patients. However, disappointingly, the strong efficacy of oncolytic viruses observed *in vitro* and with *in vivo* mouse models of numerous cancer types has not carried over to human trials. Reasons for this are

thought to include i) inefficient delivery of virus to tumor, ii) inefficient virus spread within the tumor, and possibly iii) acquired resistance to virus infection. Resistance can occur when either cell, virus, or both adapt during the course of infection such that cells support infection but may no longer be killed. It is unclear if this occurs in humans, but resistance to reovirus infection has been demonstrated in cancer cell lines that were persistently infected by this virus and it is possible this may occur in patients[12].

Based on numerous early trials, it seems clear that oncolytic viruses will not be a stand alone therapy, but likely a powerful adjuvant to the current standards of care[3]. In this regard, trials combining oncolytic viruses, including reovirus, vaccinia virus (VV), and Herpes Simplex virus (HSV), with chemotherapy or radiation have provided a high frequency of tumor responses that include partial or complete tumour regression[10]. An oncolytic adenovirus has already been approved in China[13], and it is expected that other OVs including reovirus, VV, and HSV, which are currently in phase III clinical trials, will become clinically approved anticancer agents[3].

The full potential of oncolytic virotherapy has yet to be realized. Improvements in virus arming, virus delivery to tumor, and importantly, improving the understanding of tumor susceptibility to each virus will lead to improved therapy and prediction of patient responders. This thesis focuses on the study of oncolytic reovirus, and therefore the following section provides an overview of Oncolytic Reovirus.

1.2 Oncolytic Reovirus

1.2.1 Discovery of Oncolytic Reovirus

Studies performed in the lab of Dr. Patrick Lee at the University of Calgary, Alberta demonstrated that activation of the RAS pathway in nontransformed cells conferred sensitivity to efficient reovirus oncolysis. Transforming reovirus resistant NIH-3T3 cells with constitutively active EGFR, SOS, or RAS, conferred sensitivity to efficient reovirus replication and reovirus-induced apoptosis[14-16]. As activation of the RAS pathway was thought to be present in >30% of all tumors, Dr. Lee's group found that wildtype reovirus (Type 3 Dearing, T3D) preferentially infected and killed cancer cells *in vitro* and *in vivo*[17]. The company Oncolytics Biotech® Inc.

based in Calgary, Alberta was formed to assess the clinical application of reovirus as an oncolytic agent (Reolysin®, www.oncolyticsbiotech.com)[14, 15, 17].

1.2.2 The "Active RAS" Model for Susceptibility to Oncolytic Reovirus

Experiments performed by Dr. Lee's group originally led him to propose that RAS transformation released a block in viral translation mediated by dsRNA-activated PKR. However, more recent studies found that RAS transformation does not affect translation of reovirus proteins[18], and in fact reovirus can overcome host translation shutoff regardless of PKR status[19]. Research now suggests that active signaling through RAS promotes four aspects of reovirus infection: i) enhanced proteolytic uncoating of the virus, ii) inability to synthesize or respond to antiviral IFN-β, iii) enhanced infectivity of reovirus progeny virions, and iv) enhanced apoptosis-mediated release of reovirus progeny[18, 20]. These observations form the basis of the current "Active RAS" model for reovirus oncolysis. **Figure 1** illustrates the current "Active RAS" model for susceptibility to reovirus oncolysis.

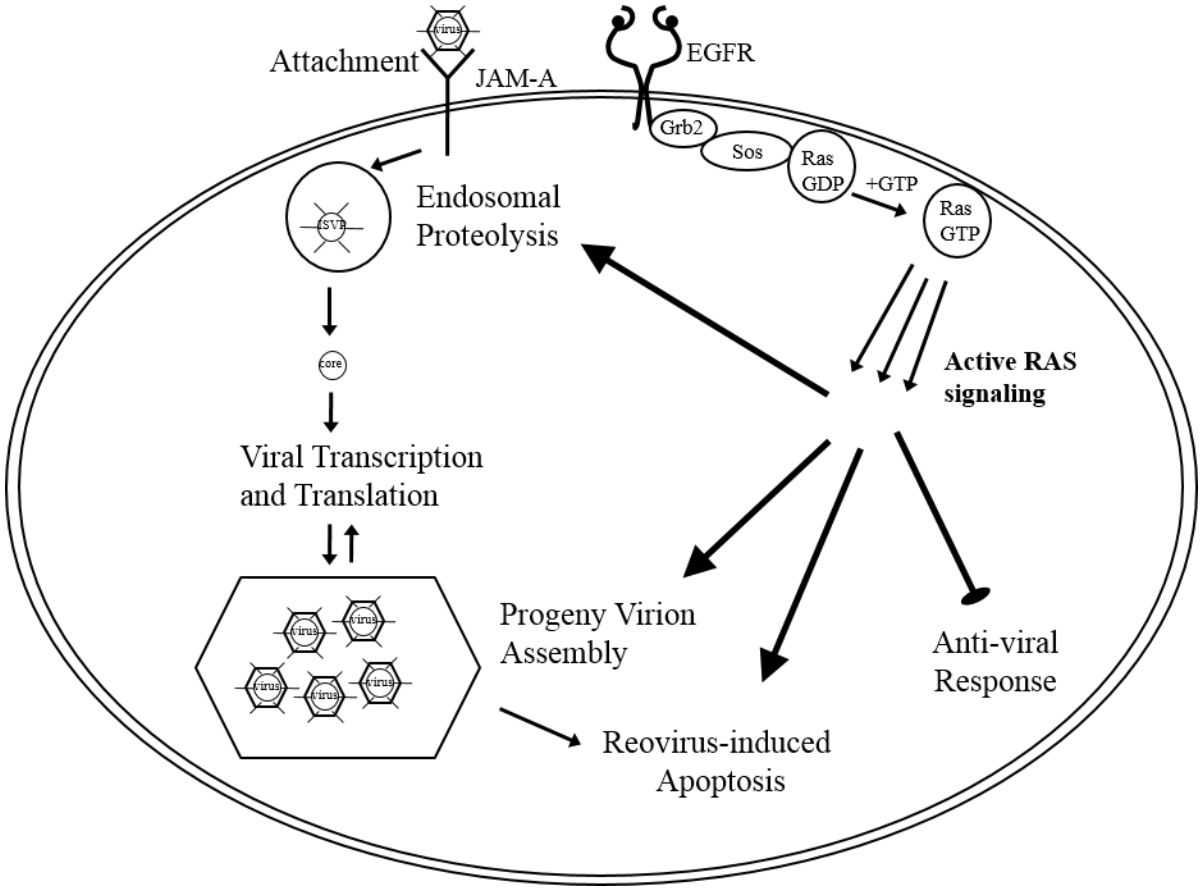
Attachment
JAM-A
EGFR
Grb2
Sos
Ras
GDP
+GTP
Ras
GTP
Endosomal
Proteolysis
SVP
core
Active RAS
signaling
Viral Transcription
and Translation
Progeny Virion
Assembly
Anti-viral
Response
Reovirus-induced
Apoptosis

Figure 1. Current Model for Reovirus Oncolysis: Active RAS Signaling Confers Susceptibility to Reovirus Infection

Active RAS signaling promotes efficient reovirus infection by enhancing i) proteolytic disassembly of virions during entry into host cells, ii) enhanced infectivity of progeny virions, iii) enhanced reovirus-induced apoptosis and release of progeny virions, and iv) reovirus spread by suppression of cellular antiviral responses[18, 20]. The pathways downstream of RAS that mediate these effects are unclear. Studies clearly support a role for RAS in promoting efficient reovirus infection in cancer cells. Importantly, however, recent studies strongly indicate that the RAS model alone is insufficient to fully explain susceptibility to reovirus oncolysis.

1.2.3 Gaps in the "Active RAS" Model

Although RAS activation clearly plays a role in efficient reovirus infection, there are significant gaps in this model. Multiple studies performed *in vitro*, *in vivo*, and in tumor biopsies found no correlation between sensitivity to reovirus cytolysis and the level of EGFR/RAS pathway activation[21-25].

The current model fails to include other signaling and regulatory pathways that have been implicated in regulating reovirus oncolysis. For example, the status of cellular tumor suppressor genes, such as p53 and RB, impinges on the efficacy of reovirus oncolysis, though this effect may be cell line dependent[26, 27]. The mitogen-activated pathway kinase (MAPK) pathways have been shown to regulate apoptosis (JNK)[28], reovirus replication (p38)[29], and downregulate interferon pathways (ERK)[20]. However these effects are completely dependent on the cell line, as each of these studies found no effect of inhibition of the other 2 pathways on reovirus infection.

Microarray studies of gene expression changes following reovirus infection highlight many other pathways and proteins potentially involved in reovirus infection. The three major pathways highlighted by these studies were: downregulation of DNA damage response genes, upregulation of genes involved in ER stress response, and upregulation of cellular innate immune response genes[30, 31]. The precise role of downregulating DNA damage responsiveness is unknown, but may be related to the influence of p53 status on reovirus induced cell killing, as p53 is implicated in regulating cell fate decisions at the mitochondria[30, 32]. ER stress induces host translation shutoff, and recent evidence suggests that reovirus can overcome this block and allow preferential synthesis of viral proteins, which may explain why reovirus infection leads to upregulation of ER stress proteins[19, 33]. Finally, although reovirus induces significant enhancement of type I interferon pathway genes, data suggest that reovirus infection is largely unaffected by these changes[33].

1.2.4 Overview of Oncolytic Reovirus in Clinical Trials

To date, reovirus has been enrolled in 31 completed or ongoing trials within the US, UK, or Canada for patients with various tumor types. Results demonstrate an excellent safety profile, with the ability of reovirus to overcome pre-existing antiviral humoral immunity leading to many

partial and a few complete responses when combined with chemotherapy[34-36]. Oncolytic reovirus is currently in a phase III trial for head and neck cancer that has recently concluded, and this virus is likely to become an approved therapy.

As is the case with other oncolytic viruses, antitumor efficacy in clinical trials has been less than expected. Furthermore, it is clear that reovirus monotherapy alone is not sufficient for cure[34]. The partial tumor responses observed in clinical trials and the ability of reovirus to combine effectively with chemotherapy provide optimism for the clinical utility of reovirus. However, to improve the efficacy of reovirus-based therapy and to better predict patient response to reovirus, it is essential to improve the understanding of the molecular determinants underlying cancer cell susceptibility to efficient reovirus infection.

This thesis aims to further understand and improve the efficiency of reovirus infection at the level of apoptosis and the mitochondria. Therefore the following section introduces basic reovirus biology, highlighting the prominent role of apoptosis in reovirus pathology and reovirus oncolysis.

1.3 Reovirus

1.3.1 Introduction to Mammalian Reovirus

Respiratory enteric orphan virus (reovirus) is a non-enveloped, segmented double-stranded RNA (dsRNA) virus that is capable of infecting most mammals and replicates in the cytoplasm of infected cells. Reovirus is found ubiquitously in nature in water stores and sewage, reflecting the fecal-oral route of transmission. There are three main serotypes of mammalian reovirus, namely Type 1 Lang (T1L), Type 2 Jones (T2J), and Type 3 Abney (T3A) and Dearing (T3D). Although all three serotypes have been studied extensively, only strain T3D is being investigated for its oncolytic potential.

Reovirus virions contain 10 segments of dsRNA enclosed within two concentric protein capsids: an inner protein core and an outer capsid. The outer capsid proteins stabilize the virus and facilitate virus entry into the host cell, while the core functions to further shield and participate in transcription of the reovirus genome. Reovirus dsRNA segments are classified into large (L1, L2, and L3), medium (M1, M2, and M3), and small (S1, S2, S3, and S4). Each

segment of dsRNA encodes a single protein except for the S1 and M3 gene segments. S1 encodes two proteins in alternate reading frames and M3 encodes two proteins in the same reading frame. Together, these genes encode eight structural proteins (protein core and outer capsid) and four nonstructural proteins (virus replication and assembly).

1.3.2 Reovirus Infection in Humans and Mice

Studies in mice suggest that reovirus infections initiate in the respiratory and enteric tracts by virus binding to microfold (M) cells in the pulmonary and intestinal epithelium[37]. Virus is carried by transcytosis across M cells and exposed basally to epithelial cells, as well as to lymphoid tissue and Peyer's patches in the airway and intestine, respectively. Reovirus infects and replicates in epithelial cells of the respiratory and enteric tract. In the intestine, basolateral infection and replication in epithelial cells leads to apical release of progeny virions to facilitate host to host dissemination[37]. If antiviral defences are insufficient, reovirus dissemination within the infected host occurs in a serotype-dependent manner involving neural and hematogenous routes. Hematogenous dissemination accounts for spread of type 1 reovirus, while neural dissemination is used primarily by type 3 reovirus. Both types of reovirus lead to infection and disease within the central nervous system, heart, and liver[37].

Reovirus infection is normally associated with only mild flu-like symptoms and diarrhea but no severe disease (hence 'orphan' virus). This is due in part to the protective effects of the innate immune response. In the intestine, the type I IFN response elicited by dendritic cells following exposure to reovirus in Peyer's patches is essential for controlling intestinal viral infection[38] and limiting reovirus-induced encephalitis[39] and myocarditis[40].

Although innate immunity acts as the first level of protection at the site of primary infection, antibody-mediated immunity plays an important role in restricting viral spread to other sites in the body such as the central nervous system, heart, liver, and muscle[37]. This is highlighted by *in vivo* work showing that B cell- and antibody-deficient, but not T cell- deficient, mice are very sensitive to efficient reovirus replication in many tissues leading to lethality[37].

Together, the innate and acquired immune defences in humans and mice are efficient at restricting reovirus infection. Most people are exposed to reovirus during childhood leading to only mild or asymptomatic infection, and therefore many adults contain circulating reovirus-

specific antibodies. Further, the excellent safety profile of this virus has contributed to and been fully supported by clinical observations[34].

1.3.3 Reovirus Replication: Attachment and Entry Into the Host Cell

The complete reovirus replication cycle is summarized in schematic form in **Figure 2.** Infection of a host cell begins with attachment of the reovirus virion to the cell surface. Initially, virions bind to sialic acid, facilitating a higher affinity interaction with the tight junction molecule Junction Adhesion Molecule A (JAM-A) on the cell surface. Interaction with sialic acid and JAM-A are mediated by binding to the stalk and head domain, respectively, of viral σ1[33]. Virus internalization occurs by endocytosis and requires interaction with β1-integrin, likely via integrin-binding sequences in viral λ2, which occurs following engagement of JAM-A[41]. Virions in early endosomes require transport along microtubules toward acidified (late) endosomes[42], a process that is aided by proper sorting of early endosomes by activated Src kinase[43].

1.3.4 Reovirus Replication: Proteolytic Disassembly and Penetration into the Cytoplasm

Following successful transport to acidified/late endosomes, virions undergo proteolytic uncoating via endo/lysosomal proteases such as cathepsins B and L[22, 42]. Proteolytic disassembly generates an infectious subviral particle (ISVP) defined by degradation of σ3, rearrangement of σ1 and μ1/μ1C (C-terminal fragment of μ1 formed from autolytic cleavage of μ1), and cleavage of μ1C into particle-associated ϕ and δ fragments. The ISVP particle is also generated in the intestinal lumen during natural infection, and is fully infectious[22]. Efficient generation of the ISVP is essential for productive reovirus replication and infection-induced apoptosis[22, 44]. Following ISVP formation, further conformational changes allow release of μ1N and other μ1 fragments, and loss of attachment protein σ1 (these virus particles are called ISVP*). Released μ1N and ϕ associate and form pores in the endosomal membrane that recruit reovirus particles and facilitate entry into the host cell cytoplasm[37, 45].

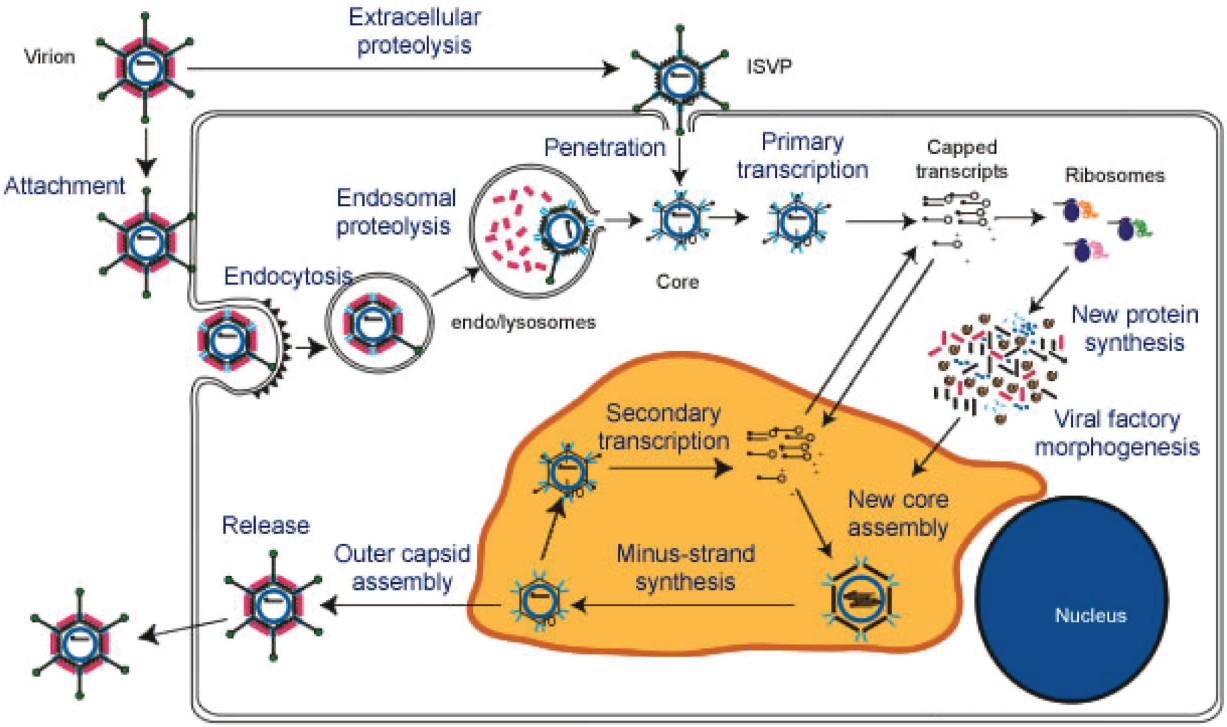
Virion
Extracellular proteolysis
ISVP
Attachment
Penetration
Primary transcription
Capped transcripts
Ribosomes
Endosomal proteolysis
Endocytosis
endo/lysosomes
Core
New protein synthesis
Viral factory morphogenesis
Secondary transcription
New core assembly
Release
Outer capsid assembly
Minus-strand synthesis
Nucleus

Figure 2. Reovirus Replication Cycle.

Reovirus particles attach to cells through JAM-A on the cell membrane and undergo receptor-mediated apoptosis to enter cells. Disassembly of reovirus by proteolytic cleavage of virions into infectious subviral particles (ISVP) is required for penetration into the host cytoplasm. Of note, extracellular proteolysis can create ISVPs capable of penetrating the plasma membrane.

Transcriptionally active core particles undergo primary transcription to provide [+] mRNA and viral proteins that assemble to form nascent core transcriptase particles within viral factories formed by μNS (yellow). Secondary transcription from nascent cores is responsible for most viral transcription and protein synthesis and formation of progeny virions. Replication of mRNA into dsRNA and addition of outer capsid proteins to packaged core particles inhibits transcription and precedes viral release by multiple mechanisms, notably cell death by apoptosis.

Figure adapted from: https://instruct1.cit.cornell.edu/research/parker_lab/Reovirus.htm

1.3.5 Reovirus Replication: Viral Transcription, Translation, and Factory Formation

Endosomal degradation and penetration into the cytoplasm yields reovirus 'core' particles. Reovirus cores are transcriptionally active and contain all enzymes required for transcription and capping of *de novo* transcripts and replication of the viral genome. Viral λ3 is a viral RNA-dependent RNA polymerase (with helicase activity) that associates with viral cofactor μ2 within the core. Viral polymerase is localized next to each of the 12 transcript exit channels formed from pentameric λ2 turrets and peripentonal λ1 within the inner capsid. Following the helicase and RNA polymerase activities of λ3, viral mRNAs are capped by the combined actions of λ1 (RNA triphosphate phosphohydrolase activity) and λ2 (guanylyltransferase and methyltransferase activity) as nascent mRNA exits the core particle. Within the cytoplasm, host ribosomes recognize capped viral mRNA, recruit translation initiation factors, and protein synthesis ensues.

Upon release into the cytosol, the initial wave of transcription (called primary transcription) takes place within 1-2 hours. Primary transcription favours generation and translation of capped viral mRNA coding for λ3, σ3, σNS, and μNS during the first 4-5 hours post-infection (hpi). The function of early transcripts coding for λ3, σ3 and σNS is thought to be in stabilization of other viral transcripts[37].

Early translation of the μNS matrix protein facilitates formation of a cytoplasmic structure called a viral factory (VF; also called viral inclusion) surrounding the transcriptionally active core particle. Reovirus factories were recently shown to be a membranous network derived from ER-associated cell membrane[46]. This structure grows in size as viral transcription and translation continue, is visible as puncta within 2 hours, localizes to the perimeter of the nucleus, interacts with microtubules, and has multiple contacts with the endoplasmic reticulum and especially mitochondria[46].

μNS binds and recruits nascent inner capsid (core) structural proteins and viral [+] mRNA into newly formed core particles (a result of primary transcription). Nascent core particles have transcriptase activity and following generation of dsRNA, produce a second wave of transcription (called secondary transcription) that accounts for the majority of viral mRNA synthesized during infection. As infection progresses viral translation gradually increases along

with a corresponding decrease in cellular translation, and within 10 hpi viral mRNA translation is predominant. By 10 hpi, all viral transcripts are generated at levels proportional to their nucleotide length, whereas protein levels are maintained at fairly constant relative levels to each other regardless of transcript levels. Viral translation is tightly regulated and involves features of the transcript, including content and length of the non-translated region, total transcript length, and regulation by cellular and viral RNA-binding proteins[37].

1.3.6 Reovirus Replication: Progeny Virions and Release from the Host Cell

The mechanisms underlying the highly precise genome assortment and packaging into new viral cores remain unknown, but are thought to involve specific viral mRNA-protein and/or RNA-RNA interactions. Generation of dsRNA by [-] strand synthesis using [+] mRNA templates is accomplished by the viral polymerase, and may occur only following assortment and packaging of a complete set of viral mRNA. Following assembly of a complete core with dsRNA, viral RNA polymerase is inhibited and outer capsid proteins are added to complete progeny virions. Precise mechanisms of release of progeny virions are not well understood, but can occur as a result of apoptotic cell death, non-apoptotic cell death, or independently of cell death[47, 48].

1.3.7 Host Cell Responses to Infection: Interferon Induction

Reovirus infection induces antiviral IFN in infected cells *in vitro* and in mice[37]. IFN induction is dependent on viral RNA, but is not dependent on viral replication. IFN induction during reovirus infection is stimulated by recognition of viral dsRNA by numerous pattern recognition receptors including RIG-I and Mda-5 [20, 49], DHX9[50], DHX33[51] and probably others[51]. Viral RNA binding stimulates interaction of these proteins with interferon-promoter stimulating factor 1 (IPS-1, also called MAVS), which mediates downstream activation of transcription factors IRF3 and NF-κB leading to IFN induction[52]. IFN-β is the predominant secreted factor following reovirus infection of normal and cancer cells. The extent of IFN induction is dependent on cell type and reovirus strain[37].

1.3.8 Host Cell Responses to Infection: Interferon Stimulated Genes

The implications of reovirus-induced IFN in the whole organism have been discussed above. At the cellular level, reovirus-induced interferon leads to expression of antiviral IFN-stimulated genes (ISGs), such as dsRNA-activated protein kinase (PKR). Reovirus infection leads to PKR activation in non-treated and especially in IFN-treated cells[53]. However, while PKR normally functions to limit host and viral protein translation by phosphorylating translation initiation factor eIF2α, observations suggest that PKR activation does not inhibit reovirus replication or cytopathic effects[31]. In fact, reovirus replication seems to benefit from PKR activation[31, 54].

Reovirus dsRNA also activates another ISG called 2',5'-oligoadenylate synthetase that activates the ssRNA endonuclease RNase L. However, similarly to PKR, while RNase L would be expected to negatively impact reovirus replication, replication is unaffected and may actually benefit from RNase L[54].

1.3.9 Host Cell Responses to Infection: Cell Cycle Inhibition

Reovirus infection can lead to inhibition of host cell cycle progression and DNA synthesis, an effect dependent on viral replication that segregates with the S1 gene. S1 encoded σ1s localizes to the nucleus and stimulates phosphorylation and inactivation of cell cycle control kinase cdc2, causing G_2/M arrest through an unknown mechanism[55]. Microarray analysis of reovirus infected cells found altered transcripts of several genes regulating cell cycle progression through G_1/S, G_2/M, and mitotic spindle checkpoints[56]. It remains unclear what benefit may be provided to reovirus infection by blocking cell cycle progression.

1.3.10 Host Cell Responses to Infection: Introduction to Reovirus-induced Apoptosis

Efficient reovirus infection induces apoptosis *in vitro* and *in vivo*[33]. Reovirus-induced apoptosis contributes to tissue injury and virus spread in the infected host[57], and tumor debulking and stimulation of antitumor immunity in mouse tumor models[8, 58]. Reovirus also combines synergistically with cytotoxic chemotherapy and radiotherapy *in vitro* and *in vivo* due to

enhanced viral replication and apoptosis[59]. Together, these observations support a partial role for apoptosis in tumor responses observed in clinical trials.

This thesis pursues the hypothesis that targeting apoptotic pathways more directly will enhance reovirus oncolysis *in vitro*, and also pursues an enhanced understanding of the regulation of reovirus-induced apoptosis at the level of the mitochondria. Therefore, the following sections introduce apoptosis, regulation of this process, and the regulation and role of apoptosis in reovirus pathogenesis and particularly reovirus oncolysis.

1.4 Apoptosis

Apoptosis is a well-conserved, programmed, active form of cell death responsible for elimination of cells when they are damaged, pose a threat to the organism, or are no longer needed[60]. Apoptosis is essential during embryonic development, immune system maintenance, and response to pathogens or other harmful stimuli. At the cellular morphology level, apoptosis induces cytoplasm and nuclear shrinkage, DNA condensation, DNA and nuclear fragmentation, and cellular fragmentation into roughly spherical, intact vesicles of different size termed 'apoptotic bodies'[60]. Apoptotic bodies are taken up by phagocytosis into cells and degraded in a non-immunogenic manner[60].

Apoptosis is highly regulated, and dysregulation is associated with multiple diseases, including cancer[61]. The nature and degree of stimulus or condition, the signaling pathway architecture (including mutational status) within a cell, and the mitochondrial state (influenced by metabolism) within a cell determine its fate. The primary pathways regulating apoptosis downstream of harmful stimuli are i) the extrinsic, death-receptor-mediated pathway, and ii) the intrinsic, BCL-2 family/mitochondria-mediated pathway. These pathways will be outlined below, and are summarized in **Figure 3**.

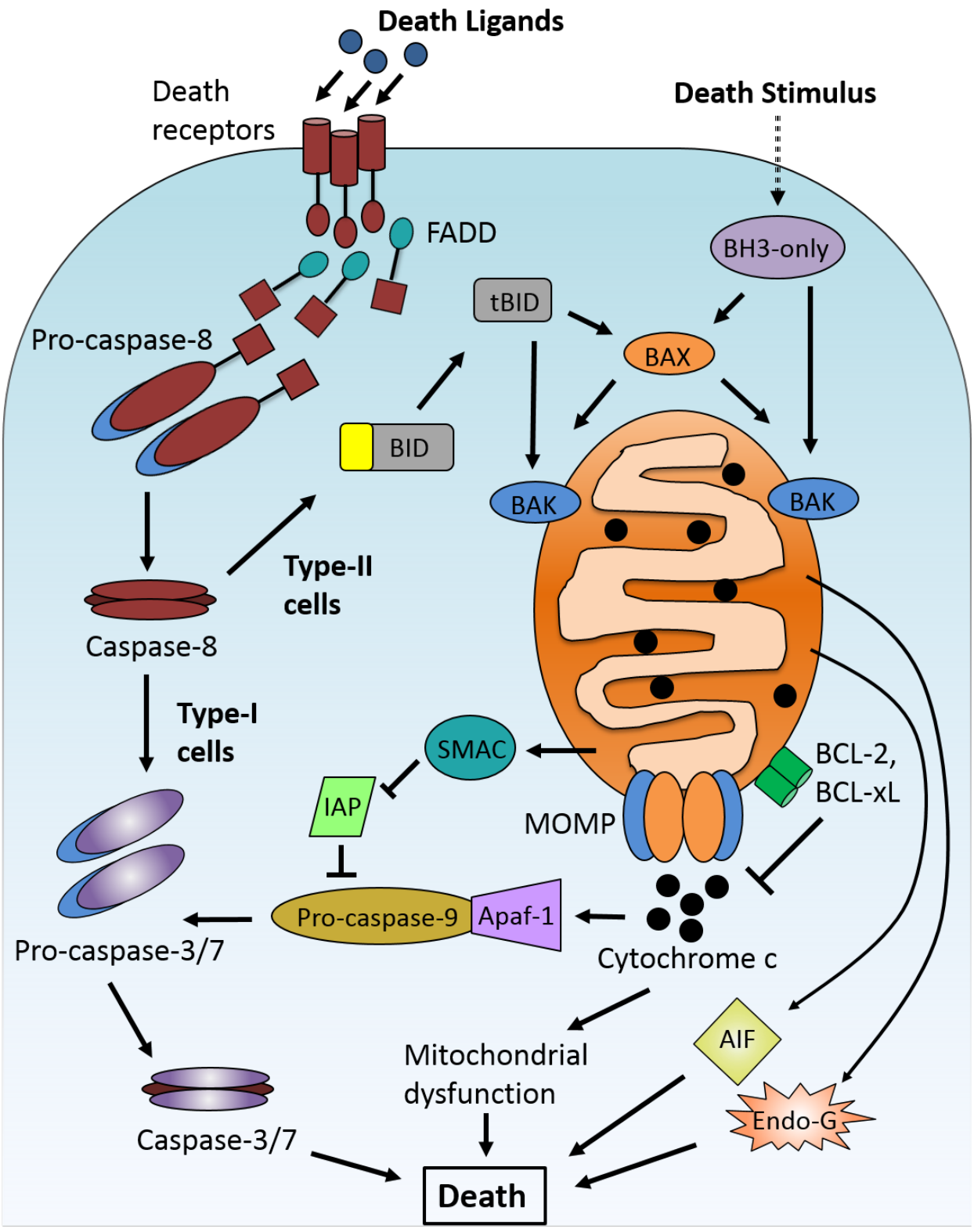
Death Ligands
Death receptors
Death Stimulus
FADD
BH3-only
tBID
Pro-caspase-8
BAX
BID
BAK
BAK
Type-II cells
Caspase-8
Type-I cells
SMAC
IAP
BCL-2, BCL-xL
MOMP
Pro-caspase-9
Apaf-1
Pro-caspase-3/7
Cytochrome c
AIF
Mitochondrial dysfunction
Endo-G
Caspase-3/7
Death

Figure 3. Extrinsic and Intrinsic (Mitochondrial) Pathways of Apoptosis.

The extrinsic apoptotic pathway involves the activation of death receptors at the cell surface leading to caspase-8 activation. In certain cellular contexts (type I cell death), high levels of caspase-8 activation are sufficient to directly initiate effector caspases leading to cell death. In type II cell death, death signal amplification is required and low levels of active caspase-8 truncate the proapoptotic BH3-only protein BID (tBID), which converges on the intrinsic/mitochondrial apoptotic pathway to induce efficient cell death. The intrinsic pathway is regulated at the level of the mitochondria by the BCL-2 family proteins. Components of this family act with each other and in membranes, and the location, concentration and specific affinities of these proteins dictate the events at the mitochondria. The BH3-only proteins act as stress sensors, responding to numerous stress/death stimuli and acting to indirectly and directly promote the activation of BAX and BAK, proteins that oligomerize and form pores leading to mitochondrial outer membrane permeabilization (MOMP). The antiapoptotic members of this family include BCL-2, and act to sequester either BH3-only proteins or BAX and BAK directly, and are capable of preventing MOMP and cell death. When triggered, MOMP is a "point of no return", sealing cell fate through the release of numerous apoptogenic proteins from the mitochondrial intermembrane space (IMS), as well as the resulting decrease in bioenergetic capacity (not illustrated). Released cytochrome c associates with APAF-1 and procaspase-9 to activate effector caspases, an event that is further promoted by the suppression of the caspase inhibitory proteins IAPs by released SMAC, leading to cellular dismantling. Release of the endonucleases AIF and ENDO-G further contributes to DNA condensation and fragmentation leading to death.

1.4.1 Extrinsic Pathway of Apoptosis

The extrinsic apoptotic pathway is initiated by apoptotic ligand binding to death receptors on the cell surface. A family of death receptors with specific ligands exist and two signaling pathways in this family function primarily as inducers of apoptosis, namely FasL/Fas, and TRAIL/DR4,DR5. Receptor engagement by ligand leads to receptor trimerization and conformational changes in the cytoplasmic tail of receptors containing death domains. Death domains bind and recruit the FAS-associated death domain (FADD) proteins that recruit and activate initiator caspase-8. All together, formation of this protein complex is termed the death-inducing signaling complex (DISC), responsible for cleavage and activation of caspase-8. In certain cellular contexts, a high level of death receptor signaling substantially activates caspase-8, which cleaves and activates effector caspases leading directly to apoptotic cell death, called type I death[62, 63]. In other cellular contexts (type II cell death), less efficient stimulation of the extrinsic pathway and caspase-8 activity requires signal amplification through the intrinsic BCL-2 family/mitochondria-mediated pathway to induce efficient apoptosis. Mitochondrial amplification is mediated by the caspase-8 cleavage target BID, yielding proapoptotic tBID, which interacts with other BCL-2 family proteins at the mitochondrial outer membrane (MOM) to promote apoptosis (see below). The difference between type I and II cell death is not an intrinsic difference in cells, but seems to be related to the amount of cell surface death receptor expression as well as the propensity to efficiently assemble DISCs and activate caspase-8[63, 64].

1.4.2 Intrinsic (Mitochondrial) Pathway of Apoptosis

The mitochondria act as "gatekeepers" of cell life and death and play the central role in eliciting apoptosis downstream of intrinsic apoptotic signals. Numerous proteins that function normally within the mitochondrial intermembrane space (IMS) are released as a result of mitochondrial outer membrane permeabilization (MOMP), which act together or independently to induce cell death. One of the major events contributing to efficient apoptosis is release of cytochrome c from the IMS into the cytosol. Cytosolic cytochrome c and ATP associate with the adaptor protein APAF-1, facilitating dimerization and activation of the initiator casapase-9, which then cleaves to activate the executioner caspases-3/7. The executioner caspases are largely

responsible for the morphological features associated with apoptosis by inducing DNA fragmentation, degradation of nuclear and cytoskeletal proteins, exposure of phagocytic recognition signals, and formation of apoptotic bodies[60, 65]. Efficient caspase activation downstream of MOMP is promoted by the release of other IMS proteins called SMAC and HTRA2 that act to neutralize the caspase-inhibitory function of inhibitor of apoptosis proteins (IAPs). Release of further proapoptotic proteins from the IMS, including endonucleases AIF, EndoG, and CAD, leads to DNA condensation and fragmentation, further contributing to cell death[65].

Triggering MOMP is considered a "point of no return" that commits cells to die[66]. This is consistent with reports that caspase activity downstream of MOMP is not essential for appropriate cell death *in vivo*[67]. Furthermore, dysfunction of mitochondrial respiration (due to cytochrome c loss)[68] and/or release of proapoptotic endonucleases[69, 70] following MOMP leads to cell death independently of caspases. Due to the essential role for mitochondria in metabolism as well as cell death, it is not surprising that MOMP is highly regulated.

The intrinsic pathway is directly regulated by the BCL-2 family of proteins. This family includes two categories of proapoptotic proteins: i) the multi-BCL-2 homology (BH) domain containing proteins BAX and BAK, which are the main effectors of apoptosis induction, and ii) the BH3 domain-only proteins of which there are many. The proapoptotic proteins are kept in check by a single category of antiapoptotic, multi-BH domain containing proteins, including BCL-2, BCL-XL and MCL-1[71].

MOMP is formed by the direct pore-forming activity of BAX and BAK oligomers in the MOM yielding pores of sufficient size to release key IMS proteins. Their activation is controlled by: i) direct activation by "activator" BH3-only proteins, required for proper MOM insertion and oligomerization of BAX and BAK, ii) direct sequestration via interactions with antiapoptotic proteins (ex. BCL-2), iii) indirect effects of "sensitizer" BH3-only proteins that interact with antiapoptotic proteins to displace "activator" BH3-only proteins (more efficient displacement) and/or to displace BAX and BAK (less efficient) to promote MOMP[71].

It should be noted that BCL-2 proteins have roles distinct from cell death regulation, including in mitochondrial dynamics (fission and fusion), ER functions, and autophagy[71]. The role of BCL-2 proteins in cell fate decisions versus other functions appears to be governed by the

specific proteins expressed, their concentration, and affinity of binding partners found at/in specific organelle membranes[71].

BH3-only proteins are essential initiators of intrinsic apoptosis in response to many cellular stressors, including DNA damage, growth factor withdrawal, ER stress, and intracellular pathogens, including reovirus[37, 72]. This family is normally under transcriptional and post-translational regulation to limit apoptotic functions, however diverse death stimuli can signal to release this control and promote apoptosis[72]. For example, the convergence point whereby extrinsic pathway signaling achieves signal amplification through the mitochondria is through truncation and activation of the BH3-only protein tBID. tBID localizes and inserts into the MOM, recruiting BAX and inducing conformational changes in BAX, thereby facilitating membrane insertion and activation, leading to MOMP and cell death[73].

1.5 Apoptosis in Reovirus Infection

Reovirus infection induces the morphological and biochemical features of apoptosis *in vitro* and *in vivo*[33]. Cell death and tissue injury following reovirus infection requires apoptosis. This is supported by the *in vitro* report that BCL-2 overexpression blocks reovirus induced apoptosis[74]. Further, reovirus-induced central nervous system tissue injury in neonatal mice is associated with extrinsic and intrinsic apoptosis, and injury is dramatically reduced in caspase-3 deficient animals[75]. Similarly, caspase inhibition protects against reovirus-induced myocardial injury *in vivo*[76].

Apoptosis also plays a prominent role in the combinatorial effects of reovirus with chemotherapy or radiotherapy. Preclinical *in vitro* and *in vivo* combinations of reovirus with platin- or taxane-based chemotherapy have been shown to be highly synergistic in melanoma [77], prostate cancer[78], and non–small cell lung cancer[79] through enhanced viral replication and apoptosis. Combining reovirus with radiation synergistically enhances cytotoxicity associated with enhanced apoptosis in a variety of tumor cells *in vitro* and *in vivo*[80].

In fact, apoptosis is the major preferred mode of action to eliminate tumor burden in cancer patients as both radio- and chemotherapy work predominantly by inducing apoptosis[81]. Induction of apoptosis likely plays an important role in the antitumor efficacy of reovirus/chemo- and reovirus/radio-therapy combinations in responding patients by direct tumor de-bulking as

well as by stimulation of antitumor immunity[6]. Therefore, exploiting and improving our understanding of reovirus-induced apoptosis should contribute to better clinical success with reovirus.

1.5.1 Reovirus Activates Extrinsic and Intrinsic Apoptotic Pathways

Reovirus-induced apoptosis is mediated by TRAIL ligand binding to its cognate death receptors, DR4 and DR5[82]. Activation of caspase-8 downstream of TRAIL stimulation leads to truncation and activation of the BH3-only protein BID, thus amplifying the cell death signal through the intrinsic apoptotic pathway. Caspase-8 and tBID are required for reovirus-induced apoptosis *in vitro* and *in vivo*[83], pointing to an essential role for the intrinsic pathway and MOMP as the effector mechanism for reovirus-induced apoptosis. Reovirus-induced apoptosis is associated with release of proapoptotic proteins from the mitochondrial IMS, including cytochrome c and SMAC, which execute apoptosis[33]. **Figure 4** illustrates reovirus-induced extrinsic and intrinsic apoptotic signaling as described here and in the next section.

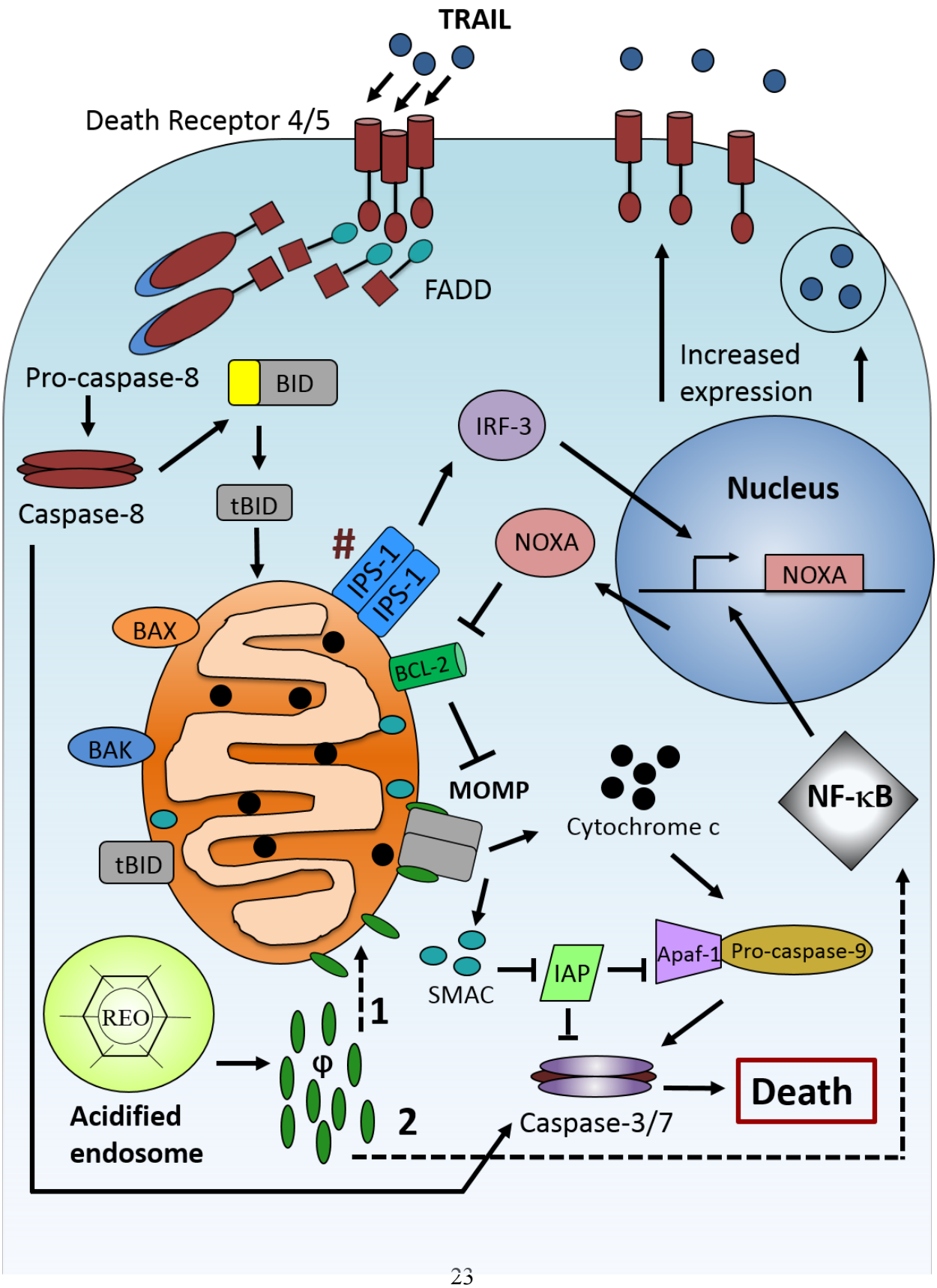
TRAIL
Death Receptor 4/5
FADD
Pro-caspase-8
BID
Caspase-8
tBID
Increased
expression
IRF-3
Nucleus
NOXA
NOXA
#
IPS-1
IPS-1
BAX
BCL-2
BAK
MOMP
tBID
Cytochrome c
NF-κB
SMAC
IAP
Apaf-1
Pro-caspase-9
REO
1
φ
2
Acidified
endosome
Caspase-3/7
Death

Figure 4. Reovirus activates extrinsic and intrinsic apoptotic pathways.

Reovirus disassembly releases the μ1 ϕ fragment, which has been shown to elicit mitochondrial outer membrane permeabilization (MOMP) following 1) direct insertion or interaction with tBID in the MOM[83, 84] or 2) activation of NF-κB[85]. It is important to note that the mechanism of reovirus-induced MOMP remains unclear, but the effectors BAX and BAK appear to be dispensable. #:Activation of innate immune proteins including IPS-1 (via reovirus RNA-activated proteins including Mda-5 and RIG-I, not shown), IRF3, and NF-κB leads to upregulation of proapoptotic proteins, including NOXA, death receptor 4/5, and TRAIL. TRAIL binding to DR4/5 activates extrinsic apoptotic signaling leading to active caspase-8-mediated truncation of BID (tBID). Extrinsic pathway stimulation requires mitochondrial amplification of the apoptotic signal, directly via proapoptotic tBID and/or through the membrane perturbation effects of ϕ for efficient cell killing. IRF-3 and NF-κB stiulate NOXA expression, leading to inhibition of antiapoptotic BCL-2 proteins, further promoting reovirus-induced MOMP. MOMP releases cytochrome c, SMAC, and other IMS proteins (not shown) that lead to cellular dismantling in a caspase-dependent and caspase-independent manner.

1.5.2 Regulation of Reovirus-induced Apoptosis

Genetic reassortment of reovirus strains implicates the σ1-encoding S1 gene and the μ1-encoding M2 gene in regulating apoptotic efficiency during reovirus infection. Binding of σ1 to sialic acid and JAM-A can influence apoptosis, yet neither are required since antibody-mediated uptake of reovirus also leads to apoptosis in infected cells[86]. Viral σ1s promotes cell cycle arrest and contributes to apoptosis, but is not strictly required[87]. This is consistent with recent reports that point to a more prominent role for the viral μ1 protein.

Ectopically expressed μ1 activates the extrinsic and intrinsic apoptotic pathways leading to cell death, similarly to natural infection[84]. The ϕ domain of μ1 generated during efficient proteolytic disassembly of natural infection localizes preferentially to the ER and mitochondrial membranes increasingly during infection and is essential for the apoptosis-inducing effects of full length μ1[88]. Natural infection or ectopic expression of μ1 induce efficient apoptosis in cells lacking BAX and BAK[84]. BAX and BAK are normally required for MOMP, and their loss prevents apoptosis in response to many chemotherapy drugs[89]. These reports implicate a novel, undefined mechanism for MOMP induced by reovirus infection that involves an indirect and/or direct role for reoviral μ1/ϕ. Consistent with this, a report demonstrated that a peptide derived from ϕ can autonomously destabilize membranes and it is postulated that reovirus ϕ might interact with other BCL-2 proteins such as tBID, which is structurally homologous to BAX and can form pores in lipidic membrane, to elicit MOMP and release of proapoptotic factors[85]. However, expression of μ1 derived from differentially apoptosis-inducing reovirus strains induce a similar amount of apoptosis, suggesting that other events modulate the extent of apoptosis in infected cells[88].

Reovirus-induced apoptosis requires NF-κB activity in most contexts via stimulation of the extrinsic apoptotic pathway. Preventing degradation of an NF-κB inhibitory protein, overexpressing this inhibitory protein, or using NF-κB-deficient cells abrogates apoptosis induced by reovirus[90]. NF-κB is activated early in infection by viral μ1[91] and μ2[92], and translocates to the nucleus to induce transcriptional changes[30]. However, it is not known how NF-κB activation triggers cell death, as previous microarray studies have failed to identify significant changes in expression of apoptosis-regulating transcriptional targets of NF-κB such

as death receptors, death ligands, or BCL-2 family proteins[33]. Indeed, although increased expression and release of TRAIL, and increased expression of the TRAIL receptors DR4 and DR5 on the cell surface have been reported and mediate reovirus-induced apoptosis, it remains unclear how these proteins are regulated by NF-κB[83]. One exception to this is the finding that reovirus infection leads to upregulation of the proapoptotic BH3-only protein NOXA at late times post infection in an NF-κB and IRF3 dependent manner, and cells lacking NOXA are severely diminished in reovirus-induced apoptosis[93].

The above reports highlight the importance of virus entry and efficient proteolytic disassembly in triggering reovirus-induced apoptosis in a replication-independent manner. Studies have demonstrated the apparent dispensability of virus replication in reovirus-induced apoptosis. For example, dead virions (nucleic acid damage from UV light exposure) or virus particles devoid of RNA can induce apoptosis[33], emphasizing the importance of viral proteins in triggering apoptosis signaling. However, these statements are somewhat misleading, as very high doses (1000 infectious virus particle equivalents per cell) are used in these studies and are not physiologically relevant[33]. Indeed, in our lab and in many other studies, UV-inactivated virus at more commonly used doses (<100 infectious particles per cell) are used in control treatments and do not harm cells. This is consistent with the idea that virus replication enhances the quantity of proteins that participate in signaling events leading to efficient apoptosis, which is likely to be the case in physiological conditions.

There have been studies showing that reovirus infection induces endoplasmic reticulum (ER) stress due to accumulation of viral proteins, leading to transcriptional upregulation of proapoptotic proteins that contribute to efficient apoptosis in pancreatic cancer[94] and multiple myeloma[95]. Other pathways have been implicated in reovirus apoptosis, and many pathways that influence or regulate extrinsic or intrinsic pathways of apoptosis are likely to play a role in the cellular response to reovirus infection.

1.5.3 Evidence for Mitochondrial Involvement in Reovirus-induced MOMP

The following observations imply an essential role for the mitochondria in regulating reovirus-induced apoptosis: 1) BCL-2 family proteins are required (tBID), promote (NOXA),

and prevent (BCL-2) reovirus-induced apoptosis, 2) mitochondria are permeabilized and release proapoptotic factors from the IMS that execute reovirus-induced apoptosis, 3) the viral ϕ domain localizes to mitochondrial membranes and likely harbours membrane destabilizing activity, and 4) reovirus induces release of IMS proteins independently of the typically essential effectors BAX and BAK. The mechanism of IMS protein release from the mitochondria is unclear. There seems to be an important role for BCL-2 family proteins, however, how these proteins interact with one another and/or with viral μ1/ϕ at the mitochondrial outer membrane during reovirus infection appears to be more complex than simple opening of a BAX/BAK-dependent pore.

It is remarkable that the single agent reovirus is capable of infecting and killing many types of cancer cells *in vitro*, *in vivo*, and in the clinic. This fact might suggest that many cancer cells share certain characteristics that facilitate susceptibility to reovirus oncolysis. Indeed, it is assumed that like many viruses, reovirus takes advantage of upregulated anabolic and proliferative pathways within cancer cells[5], such as the RAS pathway[18]. Reovirus replication and apoptosis are somewhat dissociable events: apoptosis induction in cancer cells is usually associated with efficient virus replication, whereas high virus replication does not always induce apoptosis. Determining the factors that regulate efficient reovirus-induced apoptosis in reovirus-sensitive cancer cells remains an important goal of reovirus research.

1.6 Metabolism and Mitochondria in Cancer Cells

1.6.1 Alterations in Cancer Cell Metabolism and Mitochondria

One of the hallmarks of many cancer cells is a metabolic shift toward glycolysis independently of oxygen availability, called the Warburg effect[61]. This metabolic transition is mediated in large part by mutational status in common tumor suppressors (p53, PTEN) and oncogenes (RAS, MYC, PI3K), and/or oxygen availability (HIF)[96]. Enhanced glycolytic metabolism is beneficial for rapid proliferation through rapid ATP generation and for the synthesis of biosynthetic intermediates supporting cell growth. Mitochondria in cancer cells are often considered dysfunctional as a result of this metabolic shift, despite the fact that under glucose withdrawal cancer cell mitochondria are capable of maintaining cell survival, and in general are well suited to rapidly adapting bioenergetic metabolism based on nutrient

availability[97, 98]. It has recently become more recognized that cancer cell mitochondria retain functional ATP-producing ability despite an apparent Warburg phenotype and cancer cells actually display a wide variation in the relative contributions of glycolysis and oxidative phosphorylation (OXPHOS) to ATP production[98]. This is consistent with the notion that the Warburg effect is not a fundamental difference between normal and cancer cells, but is a consequence of a metabolic shift in rapidly dividing cells.

On the other hand, inactivation of common tumor suppressors and/or activation of oncogenes leads to transcriptional suppression of OXPHOS components and mitochondrial generation of ATP. For instance, transformation with constitutively active H-RAS or K-RAS leads to enhanced glycolysis and pyruvate fermentation, decreased glucose flux through OXPHOS, increased reactive oxygen species levels, and more aggressive tumor growth *in vivo*, which was associated with RAS-induced transcriptional suppression of OXPHOS genes and increased expression of glycolytic enzymes[99-102]. Less common tumor suppressors and oncogenes have been identified as integral components of glycolysis and OXPHOS, which function to inhibit mitochondrial ATP production and promote glycolysis[103]. Mutations in mtDNA have also been found in up to 56% of all tumors, primarily occurring in the mtDNA coding for the catalytic subunits of Complex I, or occurring in a regulatory region of mtDNA[104]. These mutations leads to dysfunction of respiration and increased production of reactive oxygen species that can promote tumorigenesis, while the concurrent shift toward glycolysis promotes lactic acid production, tumor progression, and metastasis.

1.6.2 Mitochondrial Metabolism Can Influence Apoptosis

Dysfunction of the respiratory chain complexes by mutations in mitochondrial DNA (mtDNA) can accumulate in cancer and contribute to mitochondrial dysfunction alongside oncogenic alterations[103]. A report by Kwong et al. 2007 showed that osteosarcoma cells with dysfunctional respiratory complexes resulting from mtDNA mutations, or cells completely lacking mtDNA called ρ^0 cells, are resistant to apoptosis induced by etoposide[105]. However, conversely, they found that an mtDNA mutation in an ATP synthase subunit that affects ATP synthesis but not formation of the protein complex actually promotes apoptosis. This study also

showed that electron transport chain function affected the complement of BCL-2 family proteins and modulated mitochondrial morphology.

It is possible that mitochondrial morphology can modulate efficiency of apoptosis. Efficient apoptosis requires release of cytochrome c from the IMS during MOMP. However, cytochrome c is normally sequestered in the mitochondrial cristae where it functions as a soluble electron carrier between respiratory complex III and IV in the electron transport chain (ETC)[66]. Mitochondrial processes that disrupt cristae structure can therefore impact the efficiency of apoptosis[106]. One example is oxidizable substrate limitation, growth factor withdrawal, or chemical inhibition of electron transport in a murine pro-B cell line causing a decrease in mitochondrial inner membrane polarization (Ψ_m) leading to matrix condensation, cristae unfolding, enhanced cytochrome c release via MOMP, and enhanced apoptosis[107]. The link between Ψ_m and mitochondrial configuration (and its implications for induction of apoptosis) is further supported by the finding that decreasing the cytosolic pH to regenerate a high Ψ_m reverses mitochondrial configuration[107]. Mitochondrial remodelling can therefore occur in response to metabolic alterations and modulate responses to apoptotic agents such as reovirus.

The preference of reovirus for growth in cancer cells over normal cells is incompletely understood. Reovirus is selective for efficient replication and induction of apoptosis in cancer cells. Although mitochondria are key to metabolic and cell death processes, are dysregulated in cancer cells, and reovirus-induced apoptotic signaling culminates at the mitochondria, no study has asked directly whether mitochondrial (dys)function in cancer cells might regulate or be exploited for reovirus infection.

1.7 Project Rationale

Observations from *in vitro* and *in vivo* studies strongly support an important role for apoptosis in executing efficient reovirus cytolysis. However, no study to date has directly explored the utility of combining proapoptotic drugs with reovirus to enhance reovirus cytolysis. Furthermore, the mitochondria are essential for integrating upstream apoptotic signals and regulating the execution of apoptosis in response to many lethal insults, such as reovirus. Mitochondria also play an essential role in cell metabolism. Reovirus preferentially infects and kills many types of cancer cells, and cancer cells frequently harbour altered mitochondria, yet

how mitochondrial function affects reovirus infection or cytolysis has not been explored. This thesis aims to exploit and explore the mitochondrial regulation of reovirus infection efficiency.

1.8 Hypothesis: Mitochondrial Pathways Modulate and Can Be Exploited to Improve Reovirus Cytolysis

1.8.1 AIM 1: To Directly Target Apoptotic Pathways to Enhance Reovirus Cytolysis in vitro

1) Assess the suitability of pediatric leukemia cell lines as a model for elucidation of the utility of promoting apoptosis to enhance reovirus cytolysis.
2) Determine the combinatorial ability of drugs promoting the extrinsic and intrinsic pathways of apoptosis to enhance reovirus cytolysis.

1.8.2 AIM 2: To Probe the Role of Mitochondrial Function in Reovirus Cytolysis

1) Assess the influence of chronic glucose deprivation on reovirus infection.
2) Assess the influence of chemical inhibitors of mitochondrial respiration and ATP synthesis on reovirus infection.
3) Characterize the influence of the ATP synthase inhibitor Oligomycin on reovirus infection and cell death.

Chapter Two: **MATERIALS AND METHODS**

2.1 Cell Lines and Culture Conditions

The human pediatric leukemia cell lines (B1, CEM, JURKAT, MOLT3, SEM, TIB202) used were provided by Dr. Aru Narendran (University of Calgary, Calgary, Canada). and maintained in OPTI-MEM (Life Technologies, #31985-070) with 10% Fetal Bovine Serum (FBS, Life Technologies, #12483-020) and 1% PenStrep (Life Technologies, #15140-122). The HCT116 colon carcinoma, HeLa cervical adenocarcinoma, HT29 colon adenocarcinoma, DLD1 colon adenocarcinoma, and L929 murine fibroblasts were obtained from American Type Culture Collection (ATCC). The MKN1, MKN74 and GCIY gastric cancer cells were from the RIKEN Cell Bank (Japan). The esophageal cancer cell lines TE-1 and TE-8 were provided by Dr. Takahashi Joh (Nagoya City University, Nagoya, Japan). HS68 normal human foreskin fibroblasts were provided by Dr. Karl Riabowal (University of Calgary, Calgary, Canada) at passage 4 and experiments were performed between passages 7-12. The following cell lines were cultured in high glucose (25 mM) Dulbecco's modified Eagle's medium (DMEM, Life Technologies, #11966-025) supplemented with 10% FBS and 1% PenStrep: HCT116, HeLa, HT29, L929, MKN1, MKN45, GCIY, TE-6, TE-10, and HS68.

Peripheral blood lymphocytes (PBL) were obtained with donors' consent and separated by Ficoll gradient. PBLs were used immediately for experiment and grown in OPTI-MEM.

Cells were grown in 10 cm or 6 cm tissue culture-treated plates (Griener Bio-One, #664160 and #628160, respectively) in monolayers (with the exception of suspension cells) in an incubator at 37^{o}C and 5% CO_2. Cells at 60-90% confluency were used to seed cells for experiments. Experiments were routinely performed in tissue culture plates of 6, 12, 24, or 96 wells (Griener Bio-One, #657165, #665165, #662165, #655180).

Wildtype and $BAX^{-/-}$/$BAK^{-/-}$ double knockout (DKO) HCT116 cells were a gift from Dr. David Andrews (University of Toronto, Toronto, Ontario, Canada). These isogenic cells were originally generated in a $BAX^{-/-}$ background. HCT116 cells are mismatch repair deficient and the BAX gene contains a guanine-rich region (G_8 tract) in nucletodies 114-121 that is prone to mutation, leading to inactivation of the BAX gene. $BAX^{-/-}$ HCT116 cells were isolated from an unselected subclone of HCT116 cells containing mutated guanine residues in the G_8 tract of each

BAX allele, and do not express BAX[108]. These cells were then BAK gene targeted using a recombinant Adeno Associated Virus vector and homologous recombination to introduce an antibiotic resistance cassette under the endogenous BAK promoter (with internal ribosomal entry sequence for translation) flanked by LoxP sites and incorporating two STOP codons into each of the BAK genes. Following selection and Cre-recombination to remove resistance cassette, BAK genes were left containing two STOP codons in exon 5 that disrupt protein expression[89]. Wildtype and DKO cells were cultured in high glucose DMEM with FBS and PenStrep, as above.

Stocks of cells were maintained in liquid nitrogen tanks for long term storage in 10% dimethyl sulfoxide (DMSO, Sigma), 45% medium, 45% FBS.

2.2 Reovirus

2.2.1 Reovirus Propagation

Reovirus strain type 3 Dearing was originally obtained from Dr. Patrick Lee (Dalhousie University, Halifax, Nova Scotia, Canada) and propagated from a laboratory stock of purified reovirus by infecting confluent plates of L929 cells until significant cytopathic effect was observed (~48h). Cells and supernatant were collected, frozen at -80 ^{o}C and thawed at 37 ^{o}C three times to lyse cells and release virus. This solution was spun twice for 10 minutes and 4000 *g* to pellet and remove cell debris. Supernatant containing reovirus was subjected to two 48 hour rounds of dialysis (1 volume virus supernatant to 200 volumes reovirus storage buffer [150 mM NaCl, 15 mM $MgCl_2$, 10 mM Tris, pH 7.4]) using a Pur-A-Lyzer^{TM} Mega 6000 Dialysis Kit (Sigma, #PURG60020-1KT). Following dialysis, virus solution was filtered through 0.2 μm filter, and filtered virus was aliquoted for storage at -20 ^{o}C.

2.2.2 Reovirus Titre and Quantifying Reovirus Replication

Reovirus lab stock titres as well as production of reovirus progeny virions following a variety of experimental conditions was quantified by viral plaque assay. Following experimental conditions, cells and media were collected for analysis of total progeny virion production.

Samples were freeze-thawed in three cycles as above, cell debris was removed by a single round of centrifugation (10 min., 4000 *g*) and supernatant was retained for titration onto monolayers of L929 cells. L929 cells were seeded into 12-well plates ($1x10^5$ cells/well), allowed to adhere overnight, and the following day viral samples were titrated onto L929 cells using 10-fold serial dilution with 200 μL infection solution per well. Infection was performed at 4 ^oC for 1 hour on a rocker platform, at which time 1 mL of a 1% (w/v) Avicel (FMC Corporation, CL-611) in 1X SMEM solution was overlaid onto wells and plates were placed in an incubator (37^oC and 5% CO_2) for 3 days. Wells were then fixed with 1 mL 3:1 Methanol:Acetic Acid (v:v) for 10 minutes, washed with H_2O, stained with 1 mL 5% Crystal Violet (Sigma) for 10 min then washed with H_2O. Plaques were counted and viral titre was determined as follows:

[# plaques x dilution factor (10^x) / infection volume (200 μL) = pfu/μL]

For measuring replication of reovirus following given experimental conditions, virus replication was expressed based on the number of cells initially infected, as follows:

[pfu/μL (as per above calculation) x total volume of experimental sample / number cells initially infected = pfu/cell]

2.2.3 Reovirus Infection

Following cell seeding, infection was initiated either immediately in suspension cells, or one day after seeding adherent cells. Depending on the experiment and cell line, different concentrations of reovirus were used. Typically, a multiplicity of infection (MOI, the number of infectious virus particles per cell [pfu/cell]) from 10-50 was used to ensure infection of the majority of cells, however certain experiments utilized a wide range of MOI from very low to very high (10^{-4} – 10^4 pfu/cell). Reovirus was added to cells in media at the total final volume desired, placed on a rocker platform at room temperature for 1 hour and then placed in incubator at 37^oC and 5% CO_2 until the endpoint of experiment. Dead virus (DV) was obtained by subjecting virus aliquots to ultraviolet light for 3 hours and used as a negative control for infection experiments with live virus (LV).

2.2.4 Reovirus Protein Synthesis

Reovirus protein synthesis was monitored by Western Blot (described below) using a polyclonal rabbit anti-reovirus (serotype 3) antibody serum, as in Alain et al., 2006[109]. As an internal reference point for *de novo* reovirus protein synthesis, a sample of cell lysate was prepared from cells immediately following the one hour infection period.

2.3 Cell Seeding

2.3.1 Suspension Cells

Cells grown to 60-90% of confluency were used for experiments. Cells in old growth media were counted by hemacytometer, using Trypan Blue dye (Life Technologies) to exclude dead cells. For cell counting by hemacytometer, 10 μL of cells was added to 90 μL trypan blue, mixed, and 10 μL of mixture was added to each side of the hemacytometer for counting under a microscope. Based on cell concentration, the number of cells needed for experiment was determined. Cells were placed into centrifuge tubes, spun for 3 minutes at 1000 *g*, and resuspended in the appropriate amount of fresh media and aliquoted into culture plates for experiments.

2.3.2 Adherent Cells

Cells grown to 60-90% of confluency were used for experiments. Cells were washed 1x in phosphate buffered saline (PBS, 137 mM NaCl, 2.7 mM KCl, 10 mM Na2HPO4, 2 mM KH2PO4, pH 7.4) then incubated with Trypsin-ethylenediaminetetraacetic acid (EDTA) (Life Technologies, #25200-056; 0.25% Trypsin, 0.913 mM EDTA) at 37 ^{o}C for 3-5 minutes. Trypsinized cells were then mixed with fresh media, and cells were counted by hemacytometer. The appropriate amount of cells in fresh media were seeded into culture plates and allowed to adhere overnight before the initiation of experiments.

2.4 Protein Assays

2.4.1 Cell Lysis

Following treatment, cells were washed 2X with PBS, and pellets (leukemia cells) or cells attached to plates were lysed using approximately 100 µL Lysis Buffer (1 M Tris, 8.75% glycerol, and 10% SDS, with 2 mM phenylmethylsulfonyl fluoride (Sigma) and PhosStop (Roche, 1 mM activated Na_3VO_4, 25 mM NaF)) per $2x10^5$ cells for 5 minutes on ice. Lysates were heated at 80 ^oC for 10 minutes, and stored at -20 ^oC. Cell lysates were quantified by Detergent Compatible (DC) Protein Assay Kit (Bio-Rad, #500-0111) using a Bovine Serum Albumin (Sigma) standard curve.

2.4.2 Western Blot

Cell lysates were separated by sodium dodecyl sulphate-poly acrylamide gel electrophoresis (SDS-PAGE) using the Mini-PROTEAN® Tetra Cell system (Bio-Rad). Gels were transferred to nitrocellulose membranes using the Mini-Trans® Blot Module (Bio-Rad). Membranes were blocked with 10% skim milk in Tris-buffered saline containing 0.1% Tween-20 (TBST) for 1 hour at room temperature, washed three times for 5 minutes with TBST, and incubated with primary antibody. Primary and secondary antibodies used are listed in **2.4.3.** Primary antibodies were maintained in TBST with 5% (w/v) BSA and 0.01% (v/v) Sodium Azide. Membranes were incubated overnight at 4^oC in primary antibody typically at 1:1000 (v/v), washed three times in TBST, then incubated for 1 hour in species-specific secondary antibody conjugated to horseradish peroxidase (HRP), and washed four times in TBST. Amersham ECL Prime Western Blotting Detection Reagent (GE Healthcare) was used for protein detection using Amersham Hyperfilm (GE Healthcare).

2.4.3 Primary and Secondary Antibodies

Antibodies used to detect characteristic markers of apoptosis included: anti-PARP rabbit polyclonal (Cell Signaling Technology, #9532), anti-caspase-3 rabbit monoclonal (Cell Signaling Technology, #9665S), and anti-caspase-8 mouse monoclonal (Cell Signaling

Technology, #9746S). Antibodies used as protein loading controls included: anti-β-actin mouse monoclonal (Abcam, #ab3280), anti-α-Tubulin mouse monoclonal (Santa Cruz, #sc-8035), and anti-GAPDH mouse monoclonal (Santa Cruz, #sc-137179). Antibodies used to detect cellular changes following low glucose treatment, reovirus infection, or other treatment(s) include: anti-phospho-p44/42 MAPK rabbit polyclonal (Erk1/2; Thr202/Tyr204 of Erk1 and Thr185/Tyr187 of Erk2, Cell Signaling Technology, #9101S), anti-p44/42 MAPK rabbit polyclonal (Cell Signaling Technology, #9102S), anti-phosphos-p53 (Ser15) rabbit monoclonal (Cell Signaling Technology, #9284P), anti-p53 mouse monoclonal (Santa Cruz, #sc-126), anti-phospho-eIF2α (Ser51) rabbit monoclonal (Epitomics, #1090-1), anti-eIF2α rabbit polyclonal (Cell Signaling Technology, #9722), anti-phospho-eIF4E (Ser209) rabbit polyclonal (Cell Signaling Technology, #9741S), anti-eIF4E mouse monoclonal (BD Transduction Labs, #610270), anti-XIAP mouse monoclonal (BD Transduction Labs, #610762), anti-Mcl-1 rabbit polyclonal (Santa Cruz, #sc-819), anti-BAX rabbit polyclonal (Oncogene/Nuclea diagnostics, #PC103-20ug), anti-BCL-2 rabbit polyclonal (Santa Cruz, #sc-783), anti-LC3B rabbit monoclonal (Cell Signaling Technology, #3868), and anti-p62 rabbit monoclonal (Sigma, #P0067).

2.4.4 RAS-Activation Assay

Levels of activated RAS (RAS-GTP) proteins in cancer cell lines were measured using the RAS Activation Assay Kit (Millipore, #17-218) following manufacturer's instructions. Briefly, untreated cells grown to ~80% confluency in 10 cm plates were washed in ice cold PBS and harvested in 500 µL of Mg^{2+} lysis buffer (MLB) according to protocol. Protein concentration in lysate was quantified as above, and 500 µg total protein per sample was incubated with the GST-Raf RAS-binding domain bound to glutathione agarose beads. Beads containing pulled-down RAS-GTP as well as whole cell lysates were subjected to Western Blot as described. Blots were blocked and incubated with the included primary anti-RAS antibody (1:1000), washed, followed by secondary goat anti-mouse-HRP and protein expression was visualized as described above.

2.5 Cell Survival

2.5.1 Leukemia Cell Studies: Cell Survival

To quantify the cytopathic effect of reovirus infection, drug treatment, or the combination of virus and drug in pediatric leukemia cell lines, cell survival was measured using the CellTiter-Glo® Viability Assay (Promega, #G7572). This assay measures the number of live cells based on quantitation of ATP levels in living, metabolically active cells. A SpectraMax M2e microplate reader (Molecular Devices) was used to measure luminescence.

Apoptosis-priming drugs, chemotherapy drugs, or reovirus, were serially diluted into 50 µL of media/well in an opaque 96-well plate. Cells were then added to wells to a final concentration of 5000 cells in 100 µL. All treatments were performed in duplicate. Solvent or dead virus controls were included and matched the highest concentration of drug/live virus used. Cell survival was then measured 1-4 days post treatment/infection, depending on experiment. Typically, three independent experiments were performed. Within each replicate, cell survival was calculated by normalizing data to control treatment as 100% survival. Drug response curves were generated using Graphpad Prism 5 software and non-linear regression curve fitting was used to determine the inhibitory concentration of each drug required to reduce cell survival by 10, 25, and 50% of cells (IC10, IC25, and IC50, respectively).

2.5.2 Leukemia Cells: Drug Combination Studies

Drug combination studies were designed using the method of Zhao et al. 2004[110] based on the Combination Index (CI) theory and equations derived by Chou and Talalay (1984) for assessing multiple drug interactions[111]. For a two drug combination (Drug=1, virus=2), the following method was used. First, dose response curves and IC values first for a single agent A were obtained. Next, dose response curves for agent B alone or in combination with a low dose of agent A, typically IC10 or IC25, were obtained. Combination Index (CI) values were obtained using the following equation:

[$CI = (C_{A,x}/IC_{x,A}) + (C_{B,x}/IC_{x,B})$], where $C_{A,x}$ and $C_{B,x}$ are the concentrations of agent A and agent B used in combination to achieve x% drug effect. $IC_{x,A}$ and $IC_{x,B}$ are the concentrations of single agents that achieve the same effect.

For our studies, proapoptotic or chemotherapy drugs acted as agent A and reovirus as agent B. Drug alone dose response curves provided IC10, IC25 (C_{drug}) and IC50 ($IC50_{drug}$) values. C_{drug} (IC10 or IC25) was used to combine with reovirus and generate dose-response curves of virus alone or with drug. Curves were used to generate IC50 values, where IC50 of reovirus alone is $IC50_{virus}$ and the IC50 of virus with drug present is C_{virus}, such that the above equation becomes:

$$[CI = (C_{drug}/IC50_{drug}) + (C_{virus}/IC50_{virus})]$$

A CI value less than 1 denotes synergy, where CI equal to or above 1 indicate additivity and antagonism, respectively.

2.5.3 Adherent Cell Studies: Cell Number

For adherent cell studies, we measured cell number following drug alone, virus alone, or combination treatments using a Crystal Violet staining assay in 96-well plate format. The Crystal Violet staining assay allows rapid, reproducible, quantitation of cells adhering to multi-well plates, based on the property of crystal violet to stain cell nuclei[112, 113]. At the end of experiment, cells were fixed by addition of equal volume 3:1 (v/v) Methanol:acetic aid for 10 minutes. Cells were then washed well with water, stained with 1% crystal violet for 10 minutes, washed well with H_2O, and allowed to dry. Crystal violet stain was then completely dissolved by addition a 1% SDS solution by shaking on a rocker platform. The optical density of crystal violet in each well was measured by microplate reader by measuring absorbance at 570 nm. Typically, three independent experiments were performed. Within each replicate, cell number was calculated by normalizing data to control treatment as 100% survival. Dose response curves, histograms and other graphing and statistical analyses were performed using Graphpad Prism 5.

2.6 Flow Cytometry

Flow cytometry was performed by the University of Calgary Flow Cytometry Facility using a BD LSRII flow cytometer (Becton Dickinson). Data analysis was performed by the Flow

Cytometry Facility, with the exception of JAM-A expression analysis. One-color analysis (JAM-A) was done using FloJo version 9.3 software. Two-color analysis was done using BD FACSDiva version 6.1.3 software. Cell Cycle data were analyzed using ModFit LT version 3.2 software (Verity Software House Inc.).

2.6.1 Junctional Adhesion Molecule-A (JAM-A) Expression

Untreated cells at ~80% confluency were used for detection of cell surface expression of the reovirus receptor JAM-A. Adherent cells were detached from plates using 1 mM EDTA in PBS and washed twice with PBS, while leukemia cells were washed in a similar fashion. Cells were incubated with 1:1000 anti-JAM-A mouse monoclonal antibody (Abcam, ab17261) or PBS as a negative control for 1 hour at room temperature. Following 2x PBS washes, cells were incubated with secondary anti-mouse phycoerythrin-conjugated antibody at 1:1000 for 1 hour at room temperature, washed 3X with PBS, and samples were analyzed at the Flow Cytometry Facility.

2.6.2 Mitochondrial Mass and Mitochondrial Inner Membrane Potential (Ψ_m)

HCT116 cells were infected with 25 pfu/cell reovirus, treated with Oligomycin A, Rotenone, or Obatoclax, or the combinations of virus and drug for 24 and 48 hours in the presence of the pan-caspase inhibitor Z-VAD-FMK (ZVAD, 50 μM; Imgenex, IMI-2310) to prevent rapid disassembly of dying cells. Medium was aspirated and cells were washed once with PBS. Cells were then incubated for 30 min. at 37 ^{o}C with 1 mL of mitochondria staining solution, including 100 nM tetramethylrhodamine, methyl ester, perchlorate (TMRM, Life Technologies, #T668), 100 nM MitoTracker Green FM (Life Technologies, #M7514), 1 μM Cyclosporin H (Enzo Life Sciences, #ALX-380-286-M001, used to prevent TMRM efflux from cells[114]) in Hank's Buffered Salt Solution (HBSS, Life Technologies, #24020-117). Staining solution was removed, cells were trypsinized and washed twice with PBS by centrifugation (1000 *g* for 3 min.), and the cell pellet was resuspended in 400 μL HBSS and samples were analyzed at the Flow Cytometry Facility.

2.6.3 Cell Cycle Analysis

HCT116 cells ($5x10^5$) were infected with 10 pfu/cell, treated with 10 nM Oligomycin A, or the combination for 8 hours and 16 hours. HeLa cells ($5x10^5$) were infected with 50 pfu/cell, treated with 10 nM Oligomycin A, or the combination for 8 hours and 18 hours. Cells were trypsinized as in **2.3.2**, washed twice in PBS by centrifugation at 1000 *g* for 3 min, and cell pellet was resuspended in 500 µL PBS followed by dropwise addition of ice cold 100% ethanol with gentle vortexing. Cells were stored at 4^oC overnight, washed once with PBS by centrifugation, and incubated in propidium iodide (PI) staining buffer (50 µg/mL PI [Sigma], 0.1% [v/v] Triton X-100 [Sigma], 0.2 mg/mL RNase A [Qiagen, DNase free]) for 30-45 minutes. Cells were then immediately analyzed by flow cytometry.

2.6.4 Pan-Caspase Activity

Active caspase activity was monitored by flow cytometry using the APO LOGIX^{TM} FAM-VAD-FMK kit (Cell Technology, #FAM100-2). Briefly, HCT116 cells were seeded into 12-well plates at a density of $1.5x10^5$ cells/1 mL media/well and adhered overnight. Cells were then treated with reovirus alone (10 MOI), Oligomycin A alone (10 nM), the pan-caspase inhibitor ZVAD (50 µM) alone, and every combination of these agents. All of the appropriate dead virus and solvent controls were included. Caspase activity controls included cells treated with Trail 0.2 µg/mL alone and Trail plus ZVAD. Note, samples including ZVAD treatment were pre-treated with ZVAD for 1 hour before infection or Oligomycin treatment. Untreated dual and single stain cells were also included for analysis. All cells were treated/infected for 14 hours, at which time cells were stained with FAM-VAD-FMK, washed in Wash Buffer, trypsinized to get single cell suspensions, washed further by centrifugation, and finally resuspended in 400 µL Wash Buffer and placed into flow cytometry tubes for analysis, as per kit instructions. Note, propidium iodide was added to cells immediately before analysis within the Flow Cytometry Facility.

2.7 Low Glucose Adaptation

To manipulate the reliance of cancer cell metabolism on high rates of glycolysis, HCT116 and HeLa cells were cultured in low glucose (LG) media. For LG media, DMEM (Life Technologies, #11966-025) containing no glucose but otherwise identical to 'normal' DMEM was used. LG DMEM was supplemented with 10% FBS (~1-5 mM glucose) and 1% PenStrep, making the final concentration of glucose ~0.1-0.5 mM. Cells were cultured for >30 days in low glucose media, changing media every 3 days and splitting cells (1:2 - 1:4) when >90% confluent. These LG-adapted cells are named HCT-LG and HeLa-LG. For experiments, cells were seeded in fresh LG media, and media were not replaced during the experiments.

2.8 Drugs

2.8.1 Drugs: Leukemia Cell Studies

Leukemia cell lines were treated with the following drugs, alone or in combination with reovirus as described above (**2.5.2**): Obatoclax (GX15-070, Selleckchem, S1057), ABT-737 (Santa Cruz, 207242), methotrexate hydrate (Santa Cruz, 215309), bortezomib (Santa Cruz, 217785), vincristine sulfate (Santa Cruz, 201434), and human recombinant Trail (Millipore, GF092). The pan-caspase inhibitor Z-VAD-FMK was obtained from Imgenex (IMI-2310).

2.8.2 Drugs: Mitochondrial Integrity Inhibitors

Adherent cell lines were treated with the following drugs targeting mitochondrial respiration, alone or in combination with reovirus, as described in **2.5.3**: Oligomycin A (Santa Cruz, #sc-201551A), Rotenone (Santa Cruz, #sc-203242), Antimycin A (Santa Cruz, #sc-202467A), and Sodium Azide (G-Biosciences, #786-299).

2.9 Phase Contrast Microscopy

Treated cells were observed using an Olympus CKX41 inverted phase contrast microscope, and images were taken at 100, 200, or 400X magnification using an Infinity 3-1

CCD camera and Infinity Capture Mac Software v2.0.0 (Lumenera Corporation). Image sizes were scaled down consistently between comparative images and converted to greyscale for clarity using Adobe Illustrator CS4.

2.10 Data Analysis and Statistics

Data are presented as the mean ± standard error of the mean (SEM). Raw data were maintained and normalized in Microsoft Excel. Normalized data were input into GraphPad Prism version 5 software for graphing and statistical analyses. Student's t-test was used to compare two groups (unpaired) using a two-tailed P value of 0.05. One-way Analysis of Variance (ANOVA) was performed when comparing more than two unmatched groups, using a Holm-Sidak post-test for multiple comparisons (P = 0.05) to assess significant differences among individual treatment means.

Chapter Three: **RESULTS**

3.1 AIM 1: To Directly Target Apoptotic Pathways to Enhance Reovirus Cytolysis *in vitro*

3.1.1 Pediatric Leukemia As a Model System for Testing AIM 1

To begin testing AIM 1, it was useful to choose a cancer type that might benefit from novel treatment options such as reovirus. Childhood leukemia is the most common form of cancer afflicting children. The majority of pediatric leukemia patients (~75%) present with Acute Lymphoblastic Leukemia (ALL)[115], while 15-20% of patients display Acute Myeloid Leukemia (AML)[116]. Recent improvements in treatments for children with ALL and AML have led to cure rates of >85%[117] and >65%[118], respectively. However, multiple issues exist and must be addressed regarding the treatment of these children. First, certain high-risk categories, including infant (<12months) ALL (iALL)[119], certain cytogenetic aberrations and gene mutations[115], and a diagnosis of AML confer disease with a high-risk of treatment-resistance and disease relapse with very poor prognosis. Furthermore, due to the highly toxic nature of chemotherapy used against these aggressive cancers, there are significant late effects in patients who survive into adulthood, such as secondary neoplasms (>5% of patients), cardiotoxicity, endocrine dysfunction, neurotoxicity, obesity, and infertility[120, 121]. For these reasons, novel therapies need to be investigated to increase efficacy and decrease toxicity associated with current therapies in children with leukemia.

Oncolytic reovirus in clinical trials shows an excellent safety profile (no maximum tolerated dose reached) and has led to some partial and complete responses in terminal patients in Phase I, II, and III trials[34]. Reovirus can be delivered systemically by intravenous injection and reaches distant sites of tumor load, which would be an important factor in targeting circulating leukemia cells. The safety and success of reovirus in adults has facilitated the creation of a Phase I trial of reovirus in pediatric patients with advanced solid tumors. Furthermore, recent studies have demonstrated the anti-cancer effects of reovirus *in vitro*, *in vivo*, and in primary tumor tissue of multiple hematological cancer types including myeloma, lymphoma, and chronic lymphocytic leukemia (CLL)[122, 123]. Therefore, the following work within AIM 1 first examines the ability of reovirus to target pediatric leukemia cell lines, then tests the hypothesis that

apoptotic enhancement will improve or accelerate reovirus cytolysis in pediatric leukemia and other cancer cells.

3.1.2 Pediatric Leukemia Cells Are Susceptible to Reovirus Infection

Through collaboration with Dr. Aru Narendran at the University of Calgary, we obtained a panel of pediatric leukemia cell lines for *in vitro* study. Cell line names, characteristics, high-risk features, and references are listed in **Table 1**.

The first step was to investigate whether pediatric leukemia cell lines are susceptible to reovirus infection. An important determinant of host cell susceptibility to viral infection is virus entry into the host. The majority of viruses, including reovirus, require interaction with cell surface proteins that act as viral receptors and facilitate virus entry into host cells. Reovirus normally requires interaction with the cell surface receptor JAM-A for entry into the host cell and to initiate infection. Flow cytometry was used to investigate JAM-A expression on the surface of pediatric leukemia cell lines. As shown in **Figure 5a**, five of six leukemia cell lines, as well as the positive control HCT116 cell line, seem to display cell surface expression of JAM-A.

Another marker that has been linked to susceptibility to reovirus infection is activation within the RAS pathway. To examine activation of RAS in leukemia cell lines, the levels of activated (GTP-bound) RAS were determined using an active RAS puldown assay (using the RAS-GTP-binding domain of RAF conjugated to agarose beads, followed by Western Blot. Leukemia cells were found to display varied levels of active RAS, as shown in **Figure 5b**. Active signaling through extracellular signal-regulated kinases 1 and 2 (ERK1/2) is associated with dual phosphorylation of threonine 202 (Thr202) and tyrosine 204 (Tyr204) in ERK1, and the corresponding residues in ERK2, and is one possible downstream target of active RAS signaling. However, levels of phosphorylated Erk1/2 (p-Erk1/2) were variable among cell lines and were not clearly related to RAS activation levels within cells, including control cell lines.

Although active RAS and downstream proteins have been linked to reovirus susceptibility[14, 18], there are many cases where RAS signaling does not dictate susceptibility to reovirus. As the majority of pediatric leukemia cell lines tested displayed receptor for reovirus on their cell surface, the next experiments investigated whether cell lines were permissive to reovirus infection.

Table 1. Pediatric leukemia cell lines and characteristics.

Cell Line	Class	MLL rearrangement	Description	Reference
B1	B-ALL	t(4;11)(q21;q23)	14 year old, biphenotypic features of early B and myeloid lineages, MLL-AF4	Freedman MH et al., 1993[124]
CEM	T-ALL	-	4 year old female	ATCC
JURKAT	T-ALL	-	14 year old male	ATCC
MOLT3	T-ALL	t(4;11)(q21;q23)	19 year old male, MLL-AF4	ATCC
SEM	B-ALL	t(4;11)(q21;q23)	5 year old female, biphenotypic, MLL-AF4	Greil J. et al., 1994[125]
TIB202	AML	t(9;11)(q23;p13)	1 year old male, MLL-AF9	ATCC

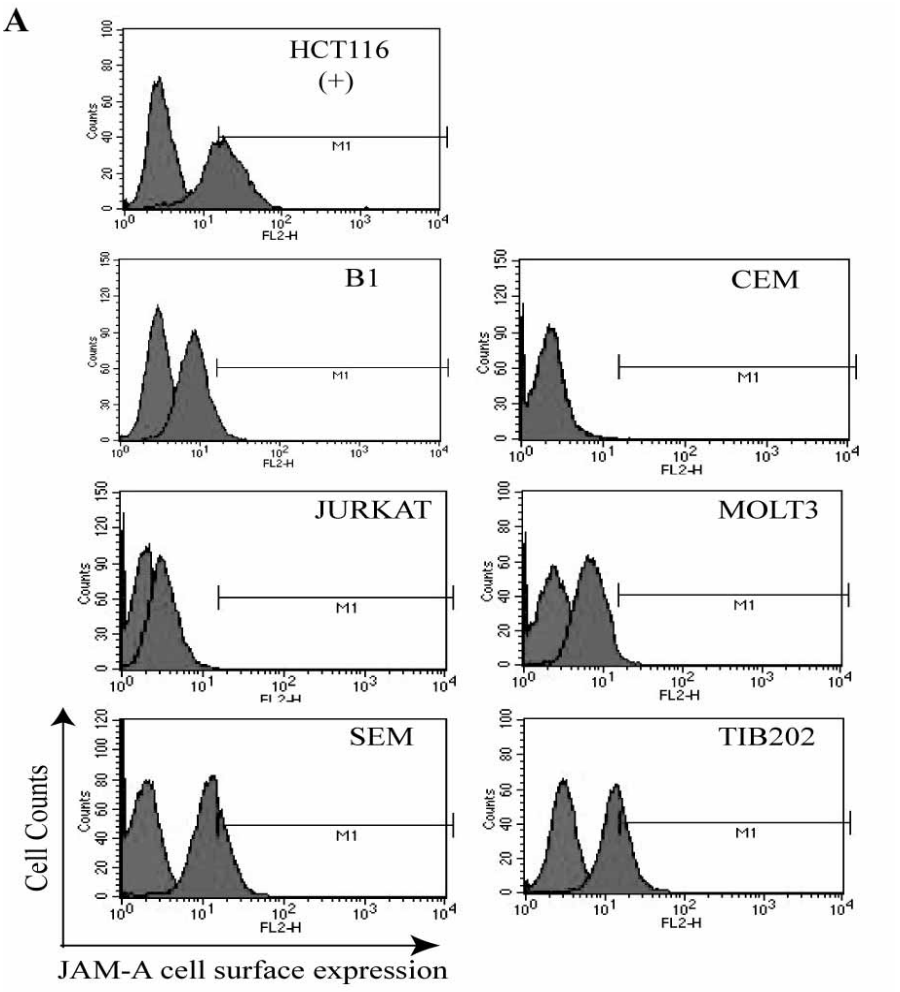
A
HCT116 (+)
B1
CEM
JURKAT
MOLT3
SEM
TIB202
M1
Counts
FL2-H
Cell Counts
JAM-A cell surface expression

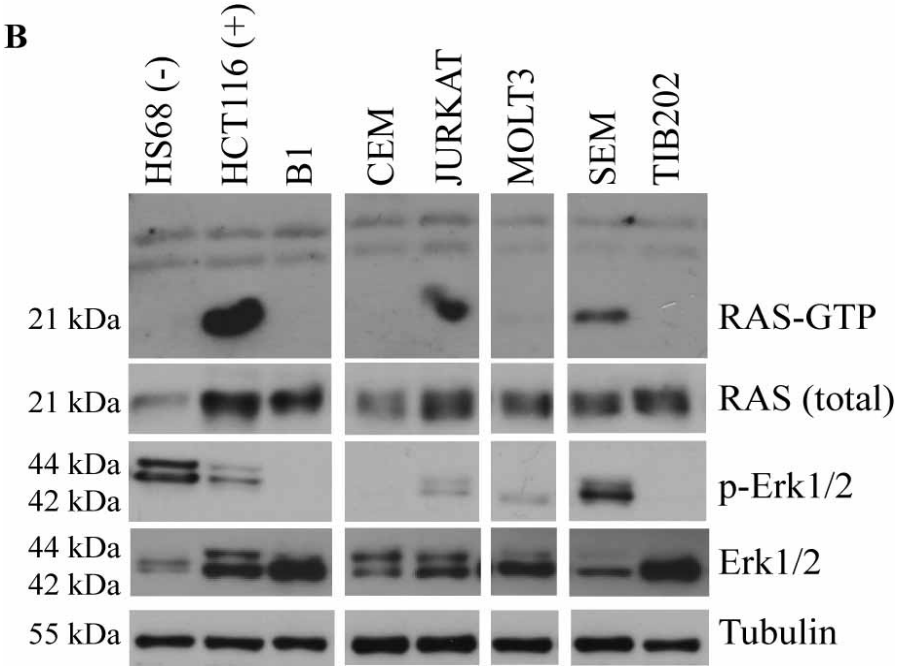
B
HS68 (-)
HCT116 (+)
B1
CEM
JURKAT
MOLT3
SEM
TIB202
21 kDa
RAS-GTP
21 kDa
RAS (total)
44 kDa
42 kDa
p-Erk1/2
44 kDa
42 kDa
Erk1/2
55 kDa
Tubulin

Figure 5. Pediatric Leukemia Cell Lines Display Variable Markers of Susceptibility

A) Cell surface JAM-A expression was assessed in untreated cell lines by flow cytometry. Peaks on the left are control cells (no primary antibody) and right-shifted, overlaid peaks are cells incubated with primary anti-JAM-A antibody followed by phycoerythrin-conjugated secondary antibody. HCT116 cells were used as a positive control. n=2, data from a representative experiment are presented.

B) Activated (GTP-bound) RAS was assessed by an active RAS pull-down assay as per protocol (see Methods). Briefly, lysates from untreated cells were quantified for protein content and 500 μg of each sample was incubated with RAS-GTP specific binding domain conjugated to agarose, followed by separation and detection by Western Blot. Leftover lysate not subjected to pull-down was used for detection of total RAS and activation (phosphorylation) of downstream Erk1/2 as well as Tubulin as loading control. HS68 human fibroblasts and HCT116 cells (harbouring constitutively active mutant HRAS) were used as negative and positive controls, respectively. n=2, data from a representative experiment are presented.

3.1.3 Pediatric Leukemia Cells Are Permissive to Reovirus Infection

Reovirus entry into host cells requires JAM-A but this does not ensure productive infection. For example, productive infection requires efficient proteolytic processing in endosomes, and certain cell lines are deficient in endosomal proteases, thereby limiting infection even when other conditions may be permissive. To assess whether leukemia cell lines are permissive to reovirus infection, the replicative ability of reovirus in cell lines was examined qualitatively by Western Blot and quantitatively by Plaque Assay.

In comparison to input virus protein levels (1 hpi lane), four of six cell lines displayed abundant *de novo* viral protein synthesis within 24 or 48 hours (**Fig. 6a**). CEM and JURKAT cells displayed low levels of viral proteins following infection. In **Fig. 6a**, Tubulin expression was intended as a loading control for Western Blot but was uneven in certain cell lines. This may be due to abundant reovirus proteins in those whole cell lysates that skewed the relative concentration of Tubulin in those samples, or cleavage due to apoptosis-induced cellular remodelling. Actin produced similar discrepancies (data not shown). An alternative approach to protein loading would be to begin experiments with the same number of cells, collect and lyse all cells at the end of experiment, and load equal volume of cell lysate. However, this was not performed for these experiments.

Using viral plaque assays to quantify reovirus replication, it was observed that five of six cell lines produce significant amounts of infectious reovirus progeny following a 24 hour infection, shown in **Fig. 6b**. Only the CEM cell line did not support efficient reovirus replication, consistent with inability of reovirus to enter JAM-A receptor-negative cells.

The cytolytic capability of reovirus in cell lines was first assessed by observing cell morphology under a phase contrast microscope following infection for 48 hours. Abundant membrane blebbing, cell death, and cell debris were clearly visible in B1, SEM, MOLT3, and TIB202 as well as the positive control HCT116 cells, shown in **Fig. 7a**. JURKAT and CEM cells, as well as the negative control HS68 cells, did not display morphological signs of cell death following reovirus infection. When quantified, reovirus infection reduced survival in four of six leukemia cell lines (**Fig. 7b**). Western Blots were used to confirm the characteristic cleavage of poly(ADP-ribose) polymerase (PARP) into an 89 kDa fragment resulting from caspase activity during reovirus-induced apoptosis (**Fig. 7c**).

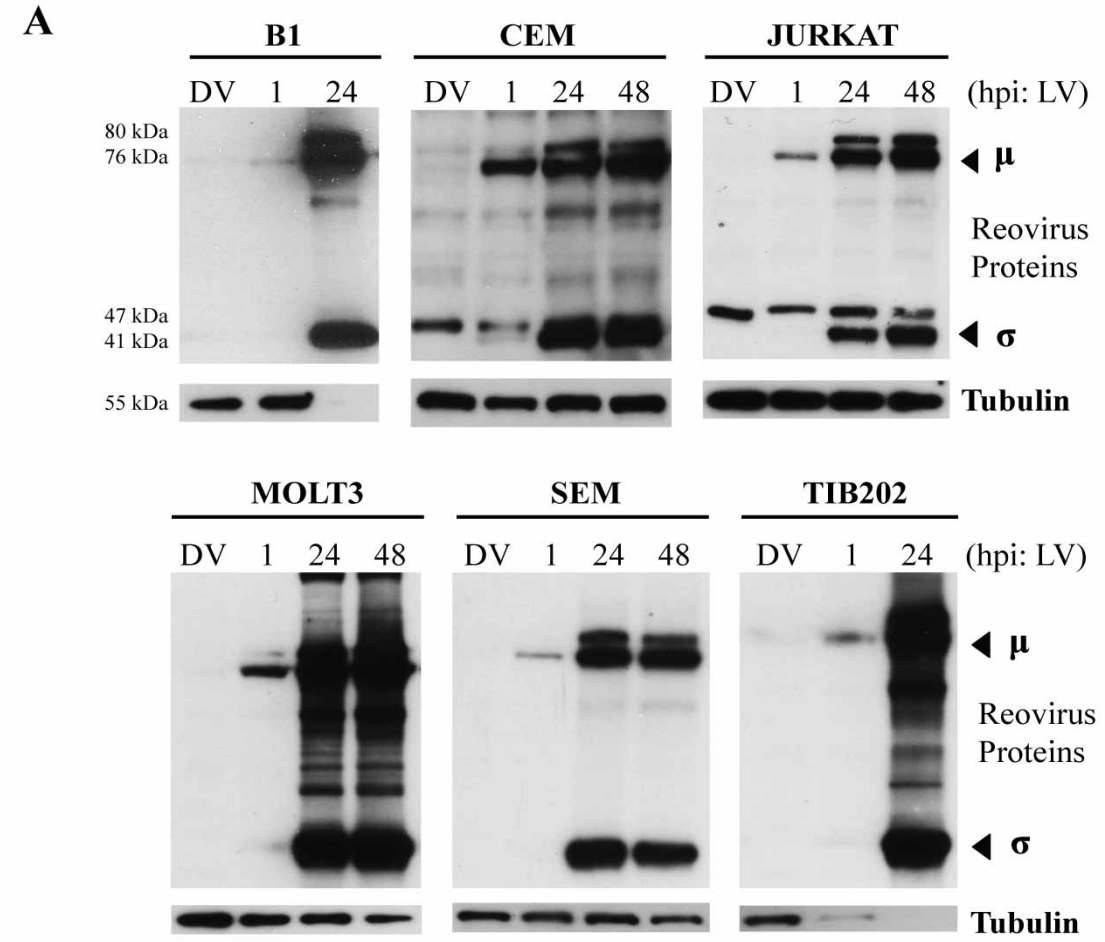
A
B1
CEM
JURKAT
DV 1 24
DV 1 24 48
DV 1 24 48
(hpi: LV)
80 kDa
76 kDa
47 kDa
41 kDa
55 kDa
μ
Reovirus Proteins
σ
Tubulin
MOLT3
SEM
TIB202
DV 1 24 48
DV 1 24 48
DV 1 24
(hpi: LV)
μ
Reovirus Proteins
σ
Tubulin

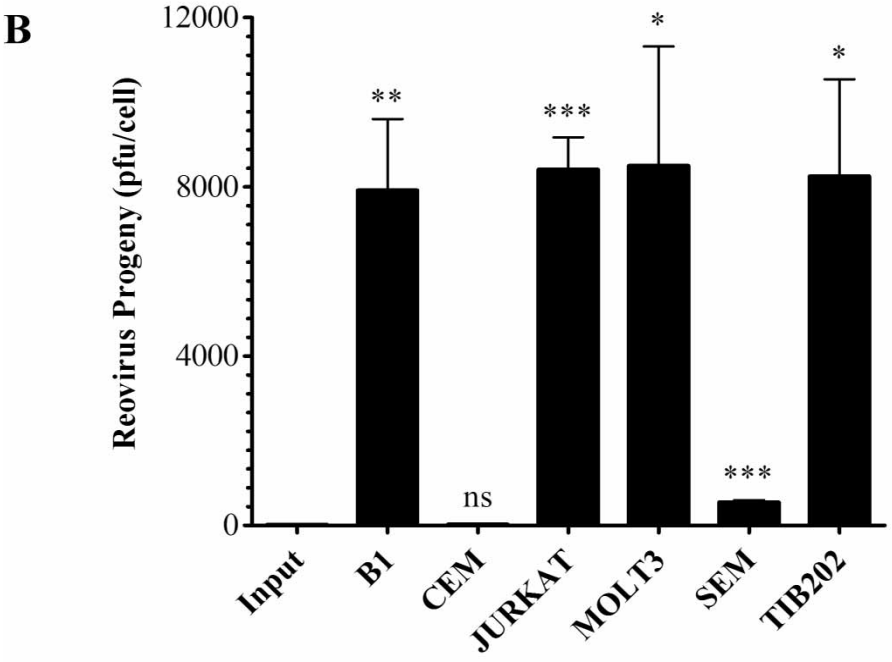
B
Reovirus Progeny (pfu/cell)
12000
8000
4000
0
**
***
*
*
ns
***
Input
B1
CEM
JURKAT
MOLT3
SEM
TIB202

Figure 6. Pediatric Leukemia Cell Lines are Permissive to Reovirus Infection.

A) Western blots were used to detect reovirus *de novo* protein synthesis in pediatric leukemia cell lines. Cells were infected with a multiplicity of infection of 10 pfu/cell (10 MOI = 10 pfu/cell) of live reovirus (LV) or UV-inactivated dead virus (DV) control, infected for the indicated time and samples were prepared for analysis by Western Blot. One hour (1 hpi) samples were used as a marker of input virus to gauge *de novo* virus protein synthesis. It should be noted that Tubulin, expected to be a loading control, was sometimes uneven between samples, which may be due to abundant reovirus proteins in those whole cell lysates that skewed the relative concentration of Tubulin in those samples, or cleavage due to apoptosis-induced cellular remodelling. Actin produced similar discrepancies (data not shown). n=2 for each cell line, data from a representative experiment are presented.

B) Reovirus production in cell lines infected with 10 MOI reovirus for 24 hours was assessed by plaque assay. Five of six cell lines supported reovirus replication leading to infectious viral progeny. Only CEM cells were completely non-permissive for reovirus replication, consistent with the lack of cell surface expression of JAM-A determined by flow cytometry (described above). Error bars represent standard error of the mean (SEM). *$p<0.05$, **$p<0.01$, ***$p<0.001$, all samples were assessed for significant difference compared to Input reovirus (10 pfu/cell) using individual t-tests. n=4 (B1 cells) and n=3 (other cell lines).

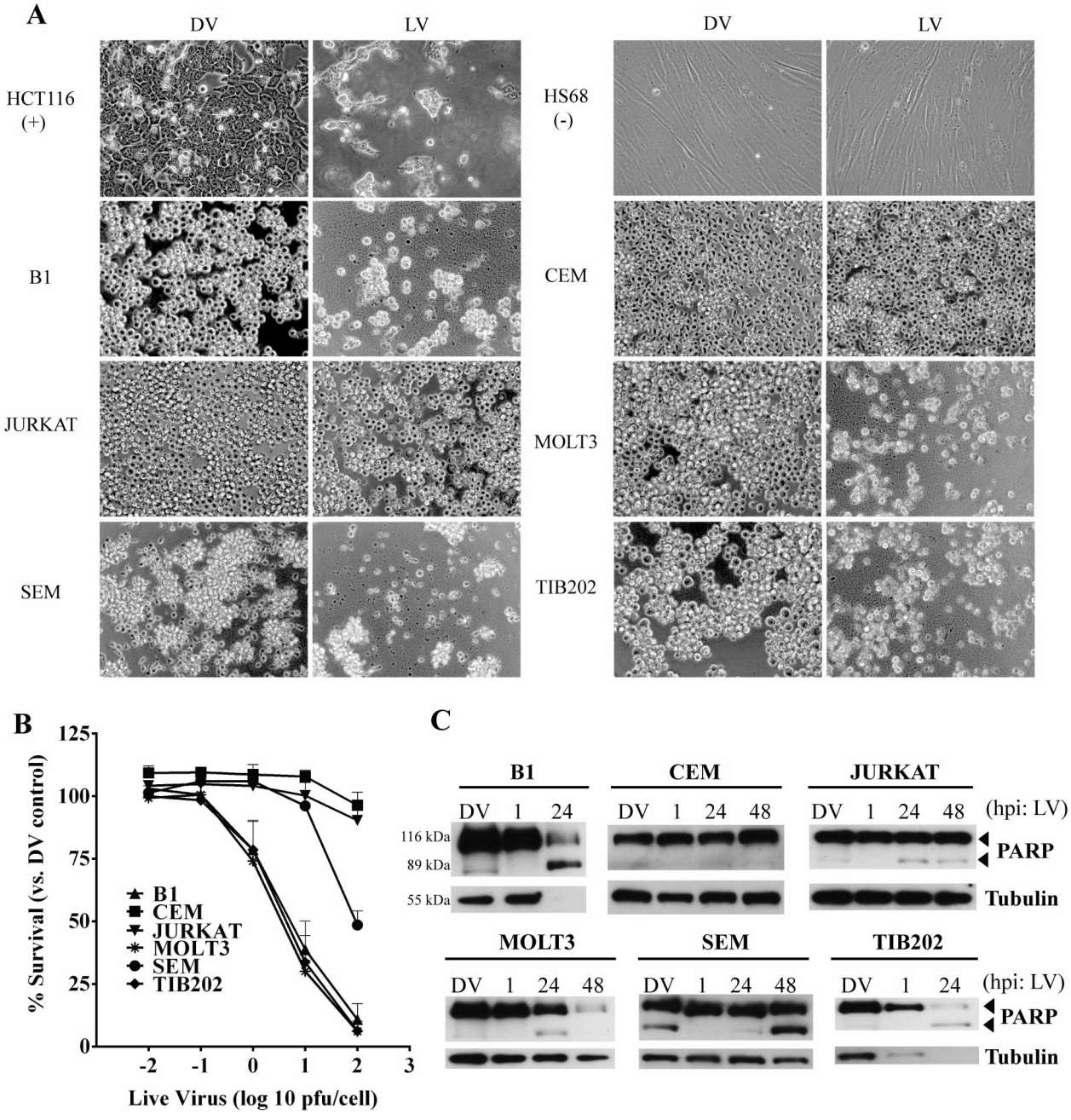
A
DV
LV
DV
LV
HCT116
(+)
HS68
(-)
B1
CEM
JURKAT
MOLT3
SEM
TIB202
B
% Survival (vs. DV control)
125
100
75
50
25
0
-2
-1
0
1
2
3
Live Virus (log 10 pfu/cell)
B1
CEM
JURKAT
MOLT3
SEM
TIB202
C
B1
CEM
JURKAT
DV 1 24
DV 1 24 48
DV 1 24 48
(hpi: LV)
116 kDa
89 kDa
55 kDa
PARP
Tubulin
MOLT3
SEM
TIB202
DV 1 24 48
DV 1 24 48
DV 1 24
(hpi: LV)
PARP
Tubulin

Figure 7. Reovirus-Induced Cell Death in Pediatric Leukemia Cell Lines

A) Cell morphology was observed and photomicrographs were taken 48 hpi following infection with 20 pfu/cell of live virus or dead virus. HCT116 and HS68 cells were included as positive and negative controls for reovirus-induced cytolysis. A decreased number of round healthy cells and significant debris due to cell death is observed in LV infected B1, JURKAT, MOLT3, SEM, and TIB202 cells, but not the non-susceptible CEM cells. n=2; data from a representative experiment are presented.

B) Cell survival was measured in leukemia cells, infected with a dosage range of live reovirus, for 48 hours. B1, MOLT3, SEM, and TIB202 cells clearly display loss of cell survival at high MOI (pfu/cell), while CEM cells and JURKAT cells retain viability even at 100 pfu/cell. Error bars are SEM. n=3.

C) Cleavage of PARP as a characteristic measure of caspase-mediated apoptosis was monitored by Western Blot following reovirus infection. Cells were infected with a multiplicity of infection of 10 pfu/cell (10 MOI = 10 pfu/cell) of live reovirus (LV) or UV-inactivated dead virus (DV) control, infected for the indicated time and samples were prepared for analysis by Western Blot. One hour (1 hpi) samples were used as a marker of input virus to gauge *de novo* virus protein synthesis. n=2 for each cell line, data from a representative experiment are presented.

3.1.4 Peripheral Blood Lymphocytes Do Not Support Reovirus Infection

Reovirus is used in clinical trials and demonstrates an excellent safety profile, including no adverse effects on circulating lymphocytes. Further, previous studies demonstrate the inability of reovirus to efficiently replicate in or harm peripheral blood lymphocytes (PBLs) as well as hematopoietic stem cells[122]. To confirm that reovirus does not harm peripheral blood lymphocytes, PBLs were obtained with donors' consent, isolated, and subjected to reovirus infection with 100 pfu/cell for up to 7 days in cell culture. When observing cells under the microscope, it was noted that the circular suspended lymphocytes seemed unaffected by reovirus infection, although this was not conclusive. Within 24 hours in all treatment conditions, adherent cells were noted in culture dishes. These cells are believed to be monocytes carried over during PBL isolation[126], but this was not confirmed. The number of adherent cells in untreated and dead virus treated conditions increased over time. However, by 7 days post infection the live reovirus infected dishes contained none of these adherent cells but contained significant cell debris (**Fig. 8a-b**). When cell survival was quantified using an ATP-based assay dependent on cell number, a significant decrease in survival was noted at late times post infection with live reovirus (**Fig. 8c**). It was not determined whether loss of cell survival was a result of cytolysis of adherent cells, suspended lymphocytes, or both. Western Blot was used qualitatively to determine if suspended PBLs support reovirus infection (**Fig. 8d**), and in line with previous findings, there was no evidence for *de novo* viral protein synthesis in PBLs, **Fig. 8d**.

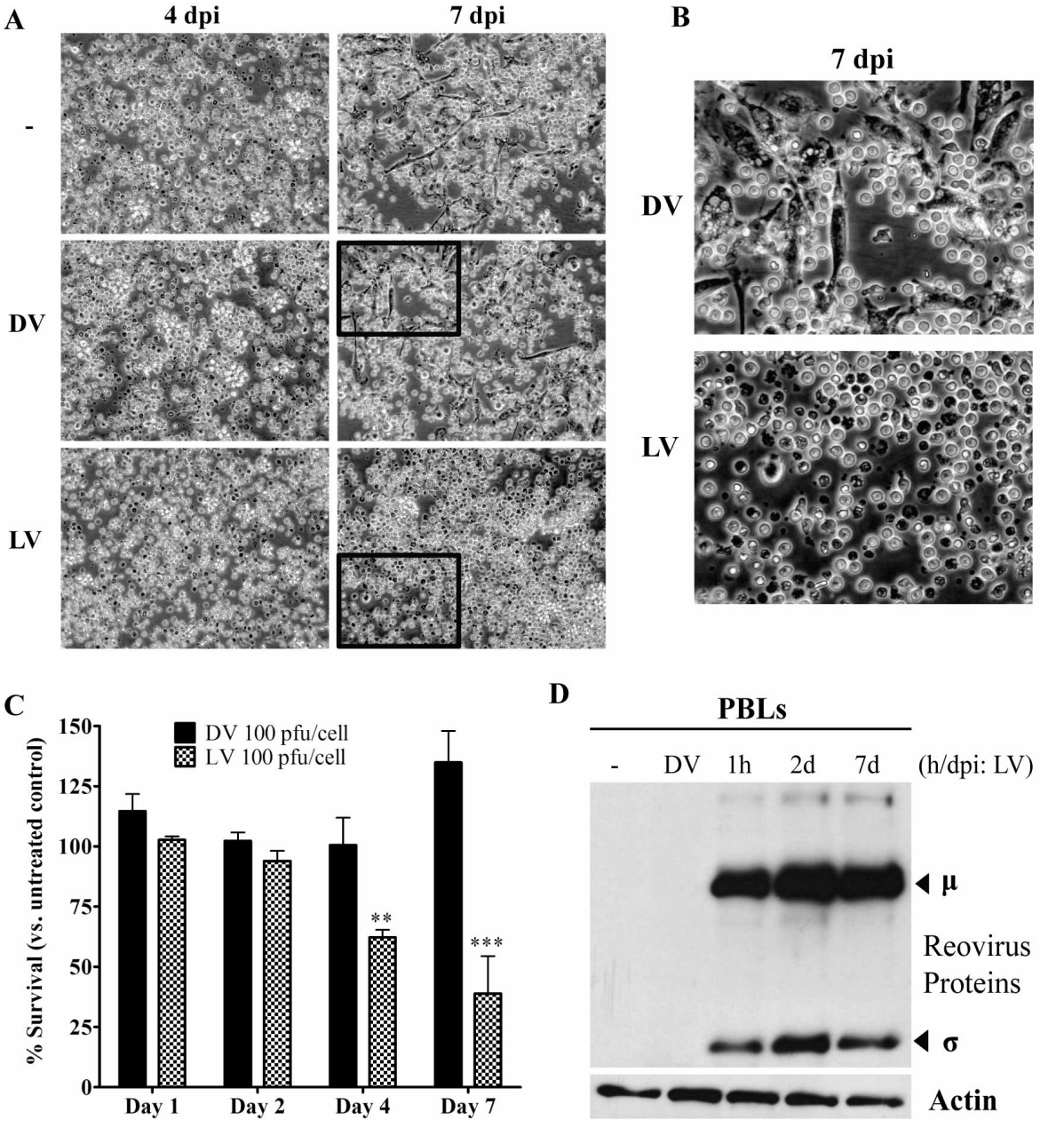
A
4 dpi
7 dpi
-
DV
LV
B
7 dpi
DV
LV
C
DV 100 pfu/cell
LV 100 pfu/cell
% Survival (vs. untreated control)
150
125
100
75
50
25
0
**
***
Day 1
Day 2
Day 4
Day 7
D
PBLs
- DV 1h 2d 7d (h/dpi: LV)
μ
Reovirus Proteins
σ
Actin

Figure 8. Peripheral Blood Lymphocytes do Not Support Reovirus Replication.

A) Peripheral blood lymphocytes obtained from donors were infected with 100 pfu/cell DV or LV for 1 to 7 days. At 4 and 7 dpi, photomicrographs were taken to observe morphological changes during infection. n=3.

B) Specific areas in photomicrographs from **A** (black boxes in **A**) were scaled up in size to visualize adherent cells that were present in the DV control but absent in LV infected cells at 7 dpi.

C) Plates seeded following PBL isolation were treated and both suspended and adherent cells in the wells were subjected to no treatment, DV control, or LV at 100 pfu/cell. At the indicated times, cell survival was measured using an ATP-based assay (see Methods). Error bars are SEM. **$p<0.01$ and ***$p<0.001$, where at each time point, LV infected cells were compared to DV control at that time point using t-test (untreated cells at each time point were called 100%). n=3.

D) PBLs were seeded and left untreated, infected with DV control, or LA at 100 pfu/cell, and only suspended cells were collected at the indicated times, lysed, and subjected to Western Blot for qualitative analysis of reovirus infection (*de novo* protein synthesis). n=3.

Note: **A, B,** and **D** are representative and use PBLs from the same donor.

3.1.5 Apoptosis Targeted Drugs Enhance Reovirus Cytolysis in Pediatric Leukemia Cell Lines

At least some pediatric leukemia cell lines support reovirus infection and cytolysis, and therefore can serve as a suitable model for testing the hypothesis that priming apoptosis pathways will promote reovirus-induced cytolysis. In cancer chemotherapy, as well as in other areas of medicine, one popular method of evaluating agent-agent (drug-virus) interaction is using Combination Index (CI) analysis, originally described by Chou and Talalay, 1984[111]. CI analysis provides qualitative and quantitative information on the nature and extent of agent interaction, respectively. Here, a simplified method described by Zhao et al., 2004[110] based on curve shift analysis (Equation B in reference) is used to study the effects of apoptotic drugs on reovirus cytolysis in pediatric leukemia cell lines, as described in the Materials and Methods.

These experiments were performed in three reovirus-sensitive pediatric leukemia cell lines (B1, MOLT3, TIB202) displaying different high risk features (see **Table 1**). Proapoptotic drugs used in these studies included ABT-737 and Obatoclax, two different pan-BCL-2 inhibitors that sensitize or trigger the intrinsic apoptotic pathway depending on dose, as well as tumor necrosis factor-related apoptosis inducing ligand (Trail), a death receptor ligand that stimulates the extrinsic apoptotic pathway.

First, dose response curves for the influence of each of the three proapoptotic drugs on cell survival in cell lines were obtained, **Fig. 9a**. Curves were fitted using non-linear regression analysis to determine the concentrations of drugs required to inhibit cell survival by 10, 25, or 50% (IC10 or IC25, and IC50, respectively) in each cell line. The influence of a range of reovirus concentrations combined with solvent control or a low dose (IC10 or IC25) of each drug on cell survival was assessed in each cell line. For CI analysis, n=3 experiments were performed to measure reovirus dose-response curve shifts in the presence of a low dose of each drug. **Figure 9b-d** illustrates the average dose response curves for virus alone and virus plus ABT-737, Obatoclax, or Trail, as well as error bars representing standard error of the mean for each data point, to provide a visual approximation of data variability, curve fitting, and curve shift. However, for each of the n=3 replicates the change in IC50 was determined and these values were used alongside the concentration (low dose) of drug used and the IC50 of drug alone (values from **Fig. 9a**) to calculate individual CI values listed in **Table 2** according to the CI

equation in the Methods section. Three CI values for n=3 experiments were obtained, and the mean and 95% confidence intervals of the CI based on the data were calculated (**Table 2**).

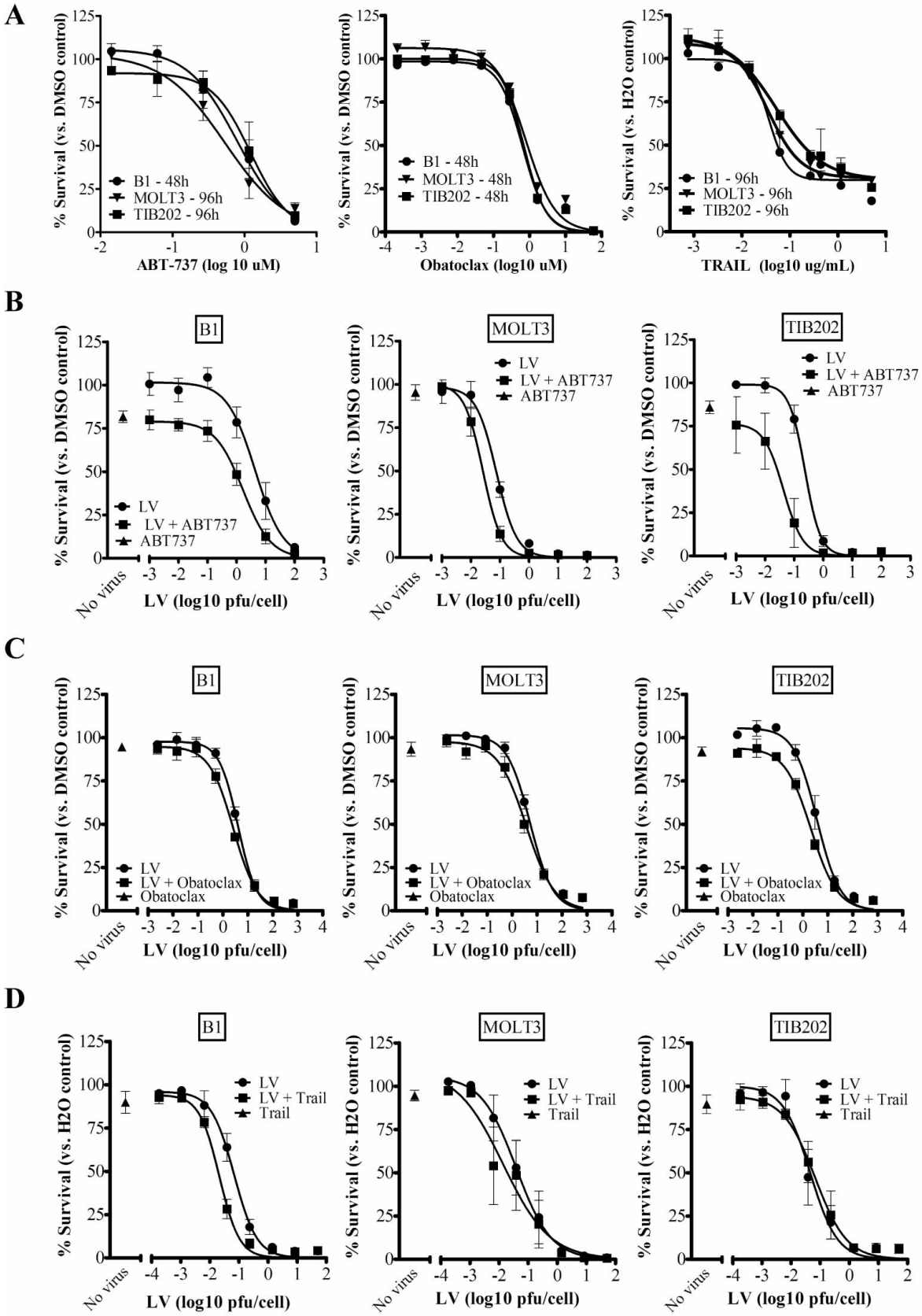
A
% Survival (vs. DMSO control)
B1 - 48h
MOLT3 - 96h
TIB202 - 96h
ABT-737 (log 10 uM)
B1 - 48h
MOLT3 - 48h
TIB202 - 48h
Obatoclax (log10 uM)
% Survival (vs. H2O control)
B1 - 96h
MOLT3 - 96h
TIB202 - 96h
TRAIL (log10 ug/mL)
B
B1
MOLT3
TIB202
% Survival (vs. DMSO control)
LV
LV + ABT737
ABT737
No virus
LV (log10 pfu/cell)
C
B1
MOLT3
TIB202
% Survival (vs. DMSO control)
LV
LV + Obatoclax
Obatoclax
No virus
LV (log10 pfu/cell)
D
B1
MOLT3
TIB202
% Survival (vs. H2O control)
LV
LV + Trail
Trail
No virus
LV (log10 pfu/cell)

Figure 9. Apoptotic Drugs Combine Effectively with Reovirus Infection to Reduce Leukemia Cell Survival.

A) Dose response curves for ABT-737, Obatoclax, and Trail were generated in three reovirus-sensitive leukemia cell lines to determine the concentration of each drug required to inhibit cell survival by 10, 25, and 50% (IC10, IC25, and IC50). These values are used to design the drug-virus combination experiments in **B-D** and for calculation of effective therapeutic combinations using Combination Index analysis, see Methods and **Table 2**. n=3.

B) Curve shift of reovirus dose response curves in B1 (48 hr), MOLT3 (96h), and TIB202 (96h) cells following combination with the pan-BCL-2 inhibitor ABT-737 (IC25 of ABT-737 used). n=3.

C) Curve shift of reovirus dose response curves in B1 (48 hr), MOLT3 (48h), and TIB202 (48h) cells following combination with a different pan-BCL-2 inhibitor Obatoclax (IC10 of Obatoclax used). n=3.

D) Curve shift of reovirus dose response curves in B1 (96 hr), MOLT3 (96h), and TIB202 (96h) cells following combination with an extrinsic apoptotic signaling ligand Trail (IC10 of Trail used). n=3.

The IC50 obtained from non-linear curve fitting of LV alone and LV+drug were obtained from n=3 experiments, as was the dose of reovirus required to reduce cell survival by 50% in the combination setting. These values, combined with the values from **A**, were used to calculate Combination Index values (from n=3) as described in the Methods. CI values are listed in **Table 2**. Errors bars in **A-D** are SEM.

Drug	Cell Line	n=	[Drug] /[IC50 drug]	IC50 LV (pfu/cell)	IC50 LV + Drug (pfu/cell)	CI Values (n=1-3)	CI Value (mean)	95% Confidence Interval (C.I.)	Effect
ABT737	B1 (48h)	1	0.40	8.67E+00	2.91E+00	0.73	0.78	0.64 - 0.92	Synergy
		2		3.41E+00	9.90E-01	0.69			
		3		2.61E+00	1.38E+00	0.93			
	MOLT3 (96h)	1	0.36	1.10E-01	1.42E-02	0.49	0.69	0.44 - 0.94	Synergy
		2		7.22E-02	2.29E-02	0.67			
		3		6.22E-02	3.53E-02	0.92			
	TIB202 (96h)	1	0.45	2.85E-01	8.98E-02	0.76	0.65	0.51 - 0.79	Synergy
		2		2.63E-01	1.84E-02	0.52			
		3		1.62E-01	3.57E-02	0.67			
Obatoclax (48h)	B1	1	0.08	3.24E+00	2.14E+00	0.74	0.74	0.65 - 0.83	Synergy
		2		4.23E+00	2.44E+00	0.66			
		3		5.00E+00	3.66E+00	0.81			
	MOLT3	1	0.06	4.70E+00	4.11E+00	0.93	0.78	0.56 - 1.00	Additive
		2		6.54E+00	5.20E+00	0.85			
		3		4.52E+00	2.26E+00	0.56			
	TIB202	1	0.07	2.20E+00	1.95E+00	0.96	0.69	0.41 - 0.97	Synergy
		2		4.24E+00	2.44E+00	0.65			
		3		5.29E+00	2.07E+00	0.46			
Trail (96hr)	B1	1	0.09	4.66E-02	2.21E-02	0.57	0.42	0.26 - 0.58	Synergy
		2		5.49E-02	1.75E-02	0.41			
		3		1.27E-01	2.46E-02	0.29			
	MOLT3	1	0.06	2.67E-02	8.84E-03	0.39	0.61	0.21 - 1.01	Additive
		2		7.93E-03	2.85E-03	0.42			
		3		2.36E-01	2.28E-01	1.02			
	TIB202	1	0.02	3.30E-02	5.34E-02	1.64	1.64	1.59 - 1.69	Antagonistic
		2		1.96E-02	3.27E-02	1.69			
		3		1.48E-01	2.33E-01	1.60			
Methot-rexate (96h)	B1	1	0.56	1.16E+00	8.44E-01	1.29	0.90	0.52 - 1.28	Additive
		2		8.40E-01	7.26E-02	0.65			
		3		2.52E-01	5.58E-02	0.78			
	MOLT3	1	0.62	1.32E+00	2.49E+00	2.50	1.64	0.79 - 2.49	Additive
		2		1.32E+00	9.02E-01	1.30			
		3		3.12E-01	1.54E-01	1.11			
	TIB202	1	0.65	9.75E-01	3.64E+00	4.38	3.23	2.09 - 4.37	Antagonistic
		2		9.18E-01	1.72E+00	2.51			
		3		7.61E-01	1.64E+00	2.81			
Vincristine (48h)	B1	1	0.28	4.27E+00	3.85E+00	1.18	1.07	0.93 - 1.21	Additive
		2		2.18E+00	1.44E+00	0.94			
		3		6.20E+00	5.10E+00	1.10			
	MOLT3	1	0.28	6.80E+00	7.91E+00	1.45	1.42	1.26 - 1.58	Antagonistic
		2		9.73E+00	9.58E+00	1.27			
		3		6.12E+00	7.78E+00	1.55			
	TIB202	1	0.31	4.45E+00	3.10E+00	1.01	1.32	0.81 - 1.83	Additive
		2		6.26E+00	9.52E+00	1.83			
		3		5.08E+00	4.03E+00	1.10			

Table 2. Evaluation of Drug Combination Effects on Reovirus Cytolysis.

Combination effects were determined to be synergistic if the 95% confidence interval for the CI values (from n=3 replicates of reovirus (LV) IC50 shift with drug present) was <1. If the 95% confidence interval exceeded 1, this indicates antagonism, while an interval overlapping 1 was considered additive. The first term in the CI equation (see methods) is summarized as a ratio of [Drug (used in combination with reovirus)]/[IC50 drug (alone)]. E is exponent.

CI values provide qualitative information on the nature of drug interaction and quantitative information on the extent of drug interaction. Typically, a CI value less than 1 indicates that the combination of reovirus and drug is synergistic, while a value of 1 indicates an additive effect and >1 indicates antagonism. For our interpretation, we concluded that a combination of drug with reovirus was synergistic only if the 95% confidence interval of the mean CI value calculated from n=3 experiments was entirely below 1, while antagonism was concluded if the 95% confidence interval was above 1, and additive if the 95% confidence interval overlapped 1.

Synergistic interaction was found between ABT-737 and reovirus in all three cell lines. Synergy was found for Obatoclax in B1 and TIB202 cells, while the interaction with reovirus was additive in MOLT3 cells. The combination of Trail with reovirus was synergistic in B1 cells, additive in MOLT3 cells, and antagonistic in TIB202 cells.

3.1.6 Chemotherapy Drugs Do Not Synergistically Enhance Reovirus Cytolysis

One way to gauge the potential utility of combining proapoptotic drugs with reovirus as an anticancer strategy is to compare it to the ability of reovirus to combine with current chemotherapy drugs used clinically. Methotrexate (MTX) is a competitive inhibitor of dihydrofolate reductase, while Vincristine is a microtubule destabilizer. Both of these drugs are commonly used in the treatment of pediatric leukemia patients.

Combination Index analysis was used and experiments were performed in the same manner as above. Dose response curves for each drug alone in each cell line were obtained, **Fig. 10a**. A low dose (IC10 or IC25) of each drug was then combined with reovirus in each cell line to observe any shift of the reovirus dose response. **Figures 10b-c** illustrates reovirus dose-response curves for virus alone and virus plus low doses of MTX and Vincristine in pediatric leukemia cells to provide a visual estimate of data variability, dose-response curve fitting, and curve shift. An identical approach was taken for determining combination effects as above for proapoptotic drugs. Briefly, for each of the n=3 replicates the change in reovirus IC50 was determined and these values were used alongside the concentration (low dose) of drug used and the IC50 of drug alone (values from **Fig. 9a**) to calculate individual CI values listed in **Table 2** according to the CI equation in the Methods section. Three CI values for n=3 experiments were

obtained, and the mean and 95% confidence intervals of the CI based on the data was calculated (**Table 2**).

The 95% confidence interval of CI values overlapped a value of 1 in B1 and MOLT3 cells treated with the combination of Methotrexate and reovirus, indicating an additive effect. Combining MTX with reovirus was antagonistic in TIB202 cells (95% of CI values >1). The combination of Vincristine with reovirus was additive in B1 and TIB202 cells, but antagonistic in MOLT3 cells. No synergy was observed between reovirus and MTX or Vincristine in any cell line using the doses and times tested.

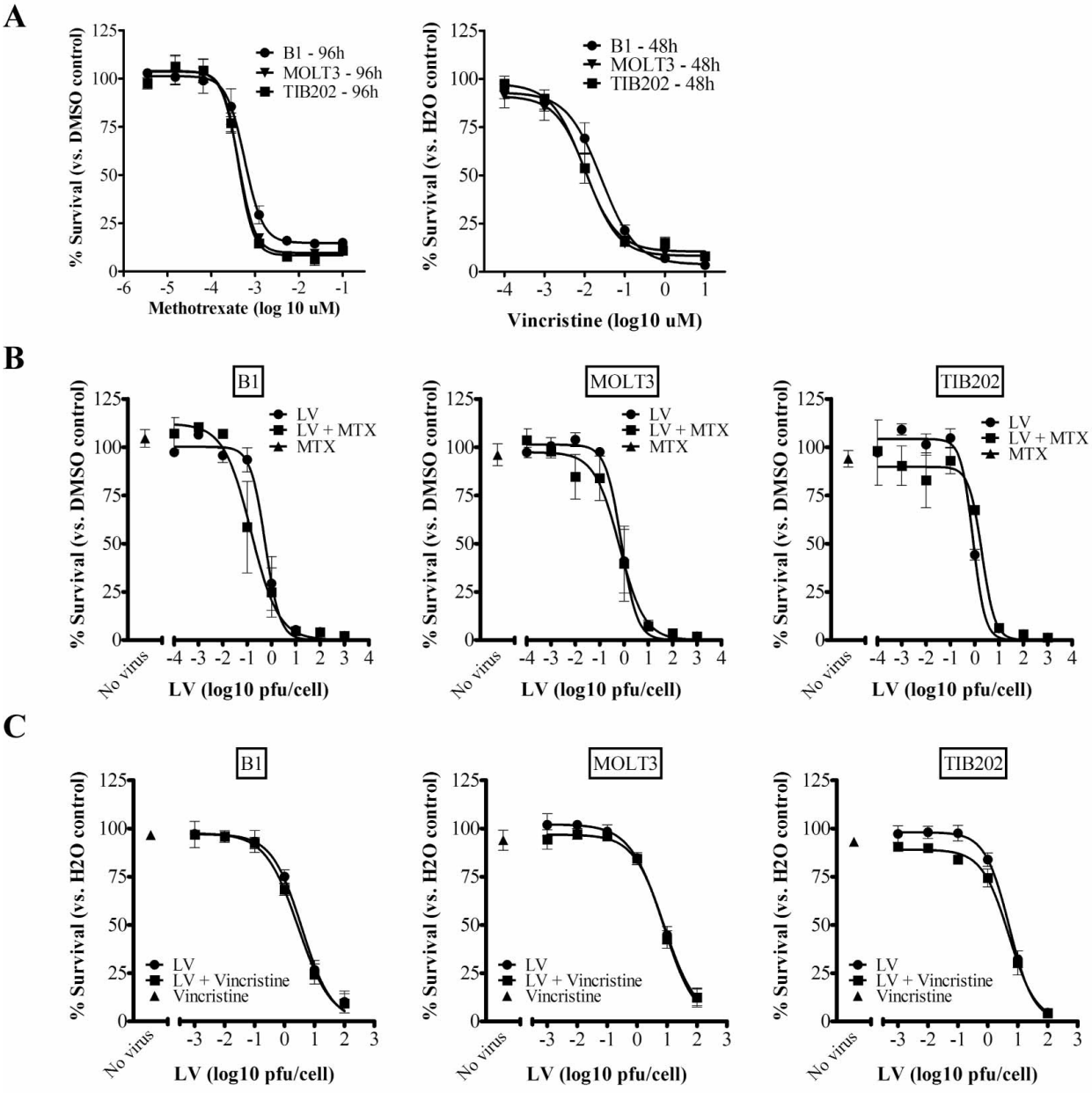
A
% Survival (vs. DMSO control)
B1 - 96h
MOLT3 - 96h
TIB202 - 96h
Methotrexate (log 10 uM)
% Survival (vs. H2O control)
B1 - 48h
MOLT3 - 48h
TIB202 - 48h
Vincristine (log10 uM)
B
B1
MOLT3
TIB202
LV
LV + MTX
MTX
No virus
LV (log10 pfu/cell)
C
LV
LV + Vincristine
Vincristine

Figure 10. Chemotherapy Drugs Do Not Combine Effectively with Reovirus Infection to Reduce Leukemia Cell Survival

A) Dose response curves for Methotrexate and Vincristine were generated in three reovirus-sensitive leukemia cell lines to determine the concentration of each drug required to inhibit cell survival by 10, 25, and 50% (IC10, IC25, and IC50). These values are used to design the drug-virus combination experiments in **B-C** and for calculation of effective therapeutic combinations using the Combination Index as in Zhao et al., 2004[110], see Methods and **Table 2**. n=3.

B) Curve shift of reovirus dose response curves in B1 (96 hr), MOLT3 (96h), and TIB202 (96h) cells following combination with the anti-folate metabolic inhibitor Methotrexate (MTX) (IC10 of MTX used). n=3.

C) Curve shift of reovirus dose response curves in B1 (48 hr), MOLT3 (48h), and TIB202 (48h) cells following combination with the microtubule stabilizing agent Vincristine (IC10 of vincristine used). n=3.

The IC50 obtained from non-linear curve fitting of LV alone and LV+drug were obtained, as was the dose of reovirus required to reduce cell survival by 50% in the combination setting. These values, combined with the values from **A**, were used to calculate Combination Index values as described in the Methods. CI values are listed in **Table 2**. Error bars in **A-C** are SEM.

3.1.7 Apoptosis Targeted Drugs Enhance Markers of Apoptosis Following Reovirus Infection

To determine if enhanced apoptosis is associated with the combination of proapoptotic drugs with reovirus, the influence of the pan-BCL-2 inhibitor ABT-737 and the death receptor ligand Trail on reovirus infection-induced markers of apoptosis was assessed in the B1 cell line. ABT-737 combined with reovirus led to increased levels of the active 17 kDa fragment resulting from cleavage of procaspase-3 and the caspase-dependent cleavage fragment (89 kDa) of PARP, characteristic markers of apoptosis (**Fig. 11a**). Notably, the addition of ABT-737 did not affect reovirus replication within B1 cells as assessed by reovirus protein synthesis (**Fig. 11b**) and production of progeny virions (**Fig. 11c**). Trail addition to reovirus infection also led to enhanced PARP cleavage compared to either agent alone, and this effect was partially rescued by addition of the pan-caspase inhibitor Z-VAD-FMK (ZVAD) (**Fig. 11d**). Trail had no apparent influence on *de novo* viral protein synthesis in the presence or absence of ZVAD (**Fig. 11e**).

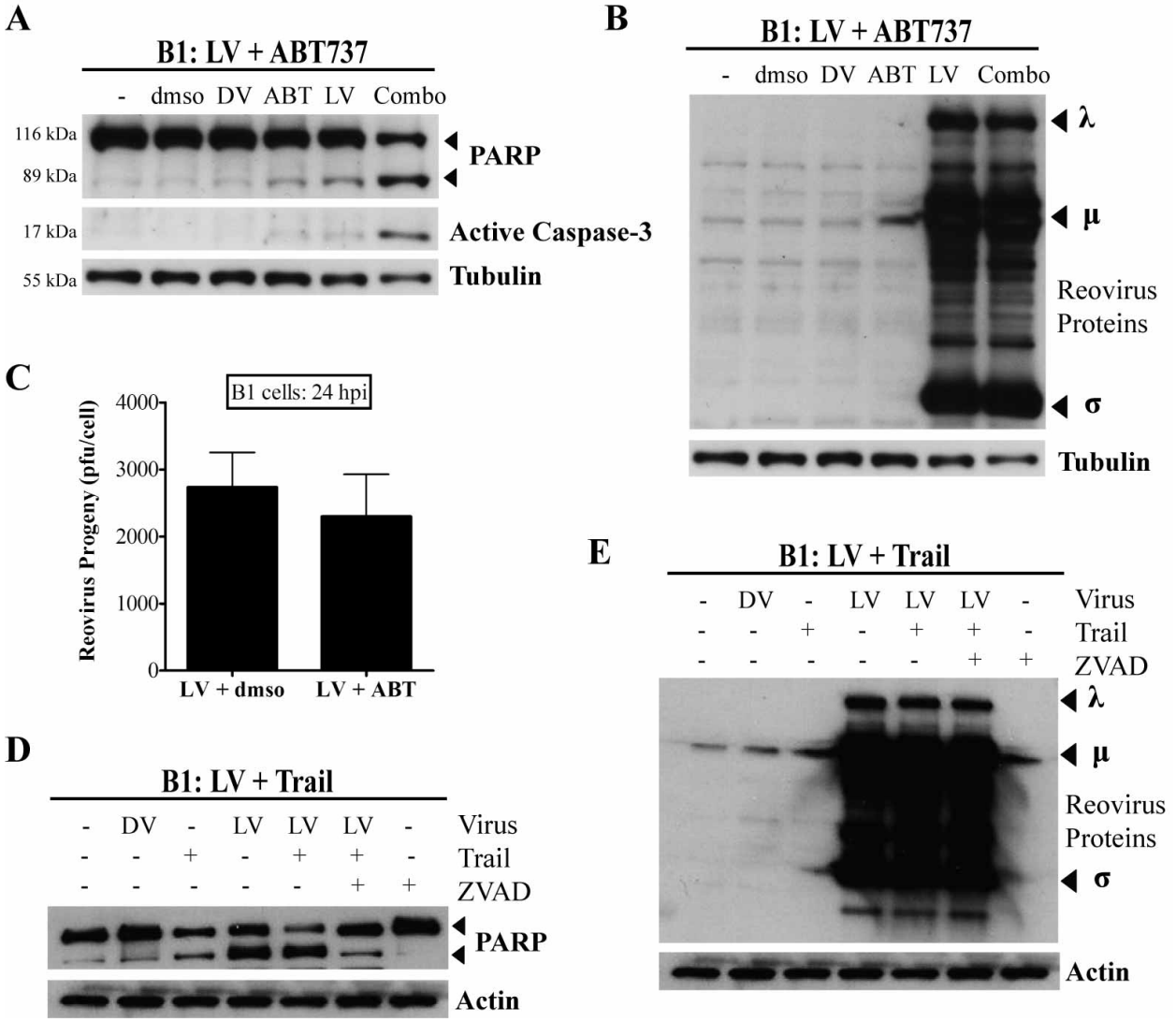
A
B1: LV + ABT737
- dmso DV ABT LV Combo
116 kDa
89 kDa
PARP
17 kDa
Active Caspase-3
55 kDa
Tubulin
B
B1: LV + ABT737
- dmso DV ABT LV Combo
λ
μ
Reovirus Proteins
σ
Tubulin
C
B1 cells: 24 hpi
Reovirus Progeny (pfu/cell)
4000
3000
2000
1000
0
LV + dmso
LV + ABT
D
B1: LV + Trail
- DV - LV LV LV - Virus
- - + - + + - Trail
- - - - - + + ZVAD
PARP
Actin
E
B1: LV + Trail
- DV - LV LV LV - Virus
- - + - + + - Trail
- - - - - + + ZVAD
λ
μ
Reovirus Proteins
σ
Actin

Figure 11. Apoptosis Priming Drugs Enhance Markers of Apoptosis Induction during Reovirus Infection of Leukemia Cell Lines

A) ABT-737 (0.34 μM) combined with live virus (LV, 10 pfu/cell) displays enhanced active (cleaved) caspase-3 and cleavage of PARP into an 89 kDa fragment in B1 cells treated for 24 hours and analyzed by Western Blot. n=2.

B) Addition of proapoptotic ABT-737 does not influence *de novo* reovirus protein synthesis in B1 cells treated as in **A.** n=2.

C) ABT-737 does not affect production of reovirus progeny assessed by plaque assay. B1 cells were treated as above for 24 hours. Error bars are SEM. n=3.

D) Trail (50 ng/mL) combined with LV (10 pfu/cell) displays enhanced cleavage of PARP compared to either treatment alone. B1 cells were treated for 24 hours and analyzed by Western Bot. Cleavage of PARP in the combination setting was partially rescued by the pan-caspase inhibitor Z-VAD-FMK (ZVAD, 25 μM), supporting caspase-dependent apoptosis occurring during reovirus-Trail combination treatment. n=2.

E) Addition of the apoptotic stimulant Trail does not influence *de novo* reovirus protein synthesis in B1 cells treated as in **D.** n=2.

3.1.8 Apoptosis Targeted Drugs Enhance Reovirus Cytolysis and Markers of Apoptosis in Adherent Cancer Cells

Apoptosis plays a strong role in the majority of cell lines in which reovirus induces cytolysis. Therefore it was hypothesized that priming apoptotic pathways to enhance reovirus cytolysis might be an applicable strategy in other cancer cell types. This hypothesis was tested in two adherent cell lines: HCT116 colon carcinoma cells that support efficient reovirus infection and cytolysis, and HeLa cervical carcinoma cells that support slower virus replication and cytolysis with delayed kinetics. Using these cell lines, a similar experimental outline to that used in leukemia cell lines was followed. Briefly, a low dose of proapoptotic drug that alone causes minimal harm to inhibiting cell survival (measured as the number of cells in treatment compared to control as 100%, see methods) is combined with reovirus, and cell number and markers of apoptosis were assessed.

First the dose response curves of the proapoptotic drugs ABT-737, Obatoclax, and Trail were obtained in HCT116 and HeLa cells (**Fig. 12a**). A low dose of the pan-BCL-2 inhibitor Obatoclax was able to shift the reovirus dose-response curve in HCT116 cells, supporting that a low dose of Obatoclax can decrease the dose of reovirus required to kill the same number of cells (**Fig. 12b**). In HeLa cells, the addition of Trail to reovirus infected cells enhanced cleavage of full length PARP, although levels of 89 kDa fragment were similar to Trail alone (**Fig. 12c**). Notably, this equivalent or enhanced marker of apoptosis was found despite lower levels of *de novo* viral protein synthesis. Decreased viral protein levels may be due to suppressed early viral replication steps in the presence of Trail, but a more likely explanation is that treated cells are dying more quickly and extensively in this condition, which inhibits later stages of virus replication such as efficient viral protein synthesis. Interestingly, a higher dose of Obatoclax (used due to the shorter treatment time for protein analysis) combined with reovirus in HeLa cells led to a complete inhibition of reovirus infection. However, upon investigation of the literature it was found that high doses of Obatoclax have the off-target effect of inhibiting lysosomal cathepsins[127]. Cathepsins are required for proteolytic processing of reovirus virions and entry into host cytoplasm[22], and their inhibition prevents successful infection and cytolysis.

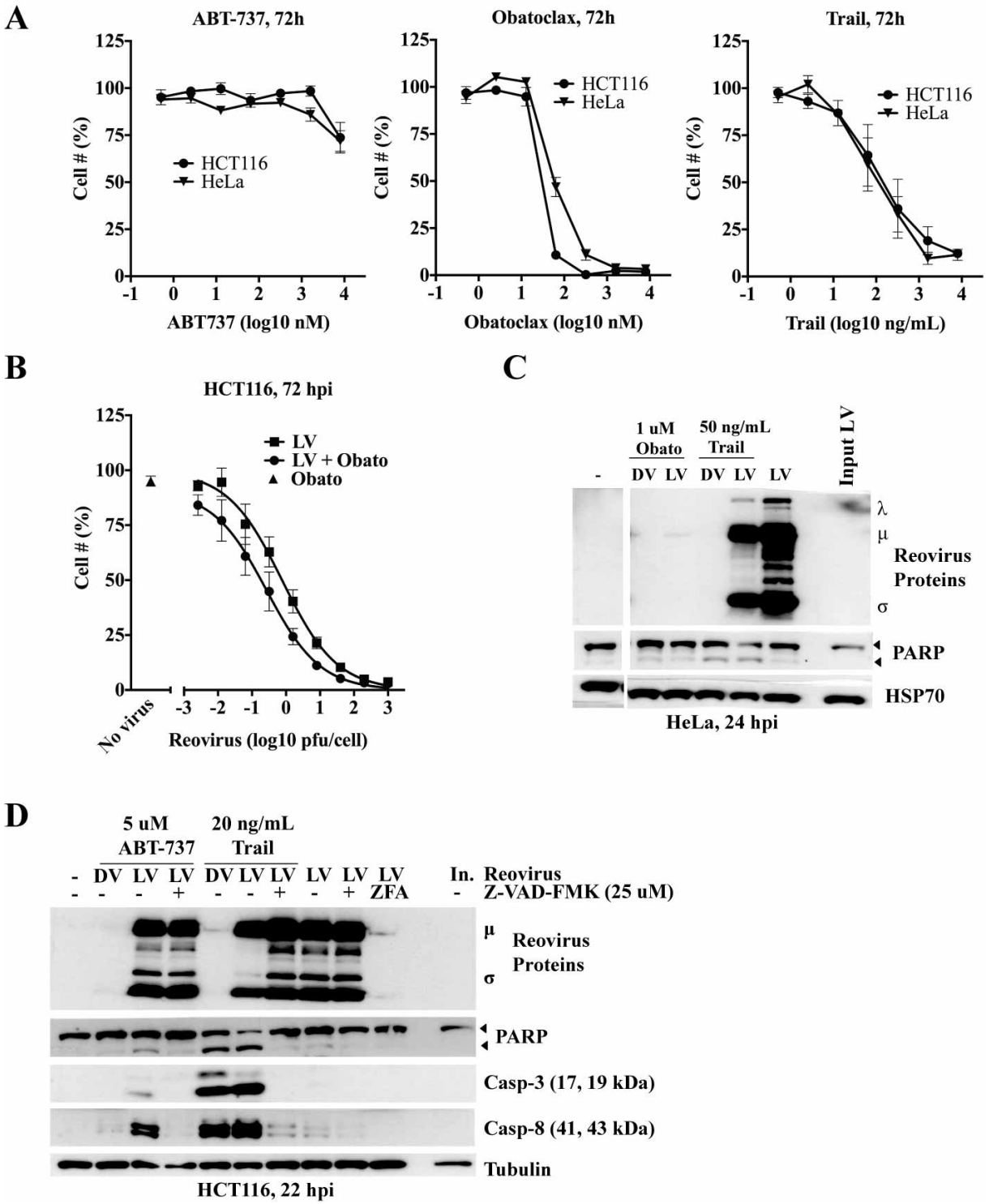
A
ABT-737, 72h
Obatoclax, 72h
Trail, 72h
Cell # (%)
HCT116
HeLa
ABT737 (log10 nM)
Obatoclax (log10 nM)
Trail (log10 ng/mL)
B
HCT116, 72 hpi
LV
LV + Obato
Obato
No virus
Reovirus (log10 pfu/cell)
C
1 uM Obato
50 ng/mL Trail
Input LV
DV LV DV LV LV
λ
μ
σ
Reovirus Proteins
PARP
HSP70
HeLa, 24 hpi
D
5 uM ABT-737
20 ng/mL Trail
DV LV LV DV LV LV LV LV LV
ZFA
In. Reovirus
Z-VAD-FMK (25 uM)
Reovirus Proteins
PARP
Casp-3 (17, 19 kDa)
Casp-8 (41, 43 kDa)
Tubulin
HCT116, 22 hpi

Figure 12. Apoptotic Drugs Promote Reovirus Cytolysis and Apoptotic Markers in Adherent Cancer Cells

A) Dose response curves for ABT-737, Obatoclax, and Trail were generated in two adherent, reovirus-sensitive cell lines: HCT116 and HeLa cells. Curves were used to determine an ideal dose (~IC10) for the experiments in **B-D**. n=3.

B) Curve shift of reovirus dose response curves in HCT116 cells (72 hpi) following combination with the pan-BCL-2 inhibitor Obatoclax (IC10 used). Obatoclax combines effectively with reovirus to decrease cell number. n=3

C) Trail, but not Obatoclax at 1 μM, combined with reovirus (50 pfu/cell) leads to equivalent or slightly enhanced cleavage of PARP. Further experiments found that addition of Obatoclax 3 hours after, but not 3 hours before or simultaneous with viral infection, allowed full viral protein synthesis (data not shown). This is consistent with the recent finding that high doses of Obatoclax inhibit the activity of lysosomal cathepsins[127] normally required for proteolytic disassembly during the reovirus replication cycle[22]. n=2

D) ABT-737 and Trail combine with reovirus (10 pfu/cell) to promote markers of apoptosis, including active (cleaved) caspase-8, caspase-3, and PARP in HCT116 cells. ZVAD (25 μM) suppressed these markers in every case, supporting that enhanced apoptosis underlies the effects of apoptotic priming drugs on reovirus cytolysis. Note: Z-FA-FMK (ZFA) inhibits cathepsin activity and was a negative control for reovirus replication (protein synthesis and cell death markers). n=2

Inhibition of an early stage of reovirus infection was confirmed by addition of Obatoclax 3 hours before and 3 hours after reovirus infection, where successful virus infection was observed only when Obatoclax was added 3 hours after infection (data not shown). In HCT116 cells, addition of ABT-737 or Trail to reovirus led to enhanced cleavage of procaspase-3 into the active 17 kDa fragment, enhanced cleavage of caspase-8 pro-forms (53/55 kDa) into the active 41/43 kDa fragments, and cleavage of PARP into the caspase-specific 89 kDa fragment in HCT116 cells (**Fig. 12d**). These markers of apoptosis were rescued by the pan-caspase inhibitor ZVAD.

3.2 AIM 2: To Probe the Role of Mitochondrial Integrity in Reovirus Cytolysis

A strong role for apoptosis in reovirus-induced oncolysis and reovirus pathology in the central nervous system, liver, and heart of immunocompromised hosts is supported by the literature[33]. A major regulator of apoptosis is the mitochondria. Life or death decisions following many stress stimuli are ultimately made at the mitochondria, where opening of the mitochondrial outer membrane releases numerous proapoptotic factors that execute a programmed cellular disassembly[65].

Evidence already suggests that reovirus-induced cell death by apoptosis is modulated in part by the mitochondria. The strongest support for mitochondrial involvement is i) reovirus-induced apoptosis requires both the extrinsic and the mitochondrial/intrinsic apoptotic pathways[128], ii) the finding that the μ1 reoviral protein can localize to the mitochondrial membrane and lead to efficient MOMP, release of IMS proteins with proapoptotic activity, and cell death independently of BAX/BAK, both in the context of normal viral replication or when ectopically expressed in cells[84], iii) the report that BCL-2 overexpression inhibits reovirus induced apoptosis, suggesting that reovirus-induced MOMP is required for apoptosis and is somehow regulated by BCL-2 family members[74].

The studies in AIM 1 further suggest that priming both the extrinsic and intrinsic apoptotic pathways by manipulating balance within the BCL-2 family proteins can enhance reovirus cytolysis. As the mitochondria act as a site for viral protein localization, death signaling integration, and release of potent proapoptotic proteins, it seems plausible that these organelles play a key role in reovirus-induced apoptosis. The precise nature of mitochondrial regulation of reovirus-induced apoptosis is complicated because reovirus can induce equally efficient

apoptosis in cells lacking BAX and BAK, suggesting a novel mode of MOMP, presumably involving viral μ1/ϕ either directly or indirectly[84]. Thus despite a key role for mitochondria in eliciting reovirus-induced cell death, how they regulate efficient reovirus-induced apoptosis remains unclear.

Mitochondria also play an essential role in efficient ATP production via oxidative phosphorylation a process responsible for the majority of ATP-production in most non-dividing cells. However, proliferating cells such as lymphocytes and many cancer cells benefit from a metabolic switch toward dominant ATP production via glycolysis. While this process is much less efficient for ATP production per glucose molecule, enhanced glucose uptake and the kinetics of ATP production by glycolysis can nevertheless yield enhanced rates of ATP production.

In the case of cancer cells, metabolic pathways are drastically altered such that they support i) rapid proliferation, ii) extensive anabolism, and iii) resistance to apoptosis[98]. The specific changes and contribution of aerobic glycolysis, pyruvate-driven OXPHOS, glutamine-driven OXPHOS and other bioenergetic pathways are quite variable among and flexible within cancer cells, and yield mitochondria with altered or deficient function[103].

Importantly, the preference of reovirus for cancer cells over normal cells remains incompletely understood. Thus I am intrigued by the observation that most cancer cells demonstrate a shift in energy metabolism away from mitochondria[103]. Although mitochondria are clearly involved in reovirus cytolysis, the importance of mitochondrial function on reovirus infection and cytolysis has not been explored. The experiments described below attempt to use different approaches to begin to address this challenge.

Of note, for AIM 2 we changed the cell lines used to study reovirus infection. AIM 2 focuses on the adherent cell lines HCT116 and HeLa, for which reovirus infection has been characterized to some extent previously in our lab. The cell lines used for AIM 2 were changed because of our experimental approach taken. Specifically, the assay used in AIM 1 to quantify cell survival was measured using an ATP-based assay. As AIM 2 intended to manipulate energy metabolism and possibly ATP production, using an ATP-based assay to measure cell number/survival might be inaccurate. Other methods that allow for quantification of cell viability/number include AlamarBlue or MTT/MTS assays, but these assays are also based on mitochondrial redox status/enzyme function that might reasonably be affected during

manipulation of mitochondrial metabolism. Further more, previous work in our lab has shown that these assays can give false positive results, particularly following efficient reovirus cytolysis. Therefore for AIM 2, a different method for cell quantification was chosen that relied on the use of adherent cells. The Crystal Violet (CV) assay involves fixing adherent, healthy cells to culture plates, staining cellular DNA with CV, dissolving stain in 1% SDS, and measuring absorbance at 570 nm. This method requires adherent cells for the fixing step, and because HCT116 and HeLa cells support reovirus infection and were readily available, we chose these cell lines moving forward. As previous work in our lab had characterized reovirus infection in the adherent HCT116 and HeLa cell lines, the quantitative, simple, and reproducible nature of the CV assay using these cell lines allowed for convenient experimentation.

3.2.1 Low Glucose (LG) Adapted Cells Are Resistant to Reovirus Cytolysis and Apoptosis-Inducing Agents

It was hypothesized above that mitochondrial bioenergetic function might regulate reovirus infection in some way. Many cancer cells are significantly glycolytic, which is associated with repression of mitochondrial metabolism as well as resistance to apoptosis[98]. Cancer cells are metabolically plastic, and therefore nutrient limitation is capable of switching energy metabolism readily to maintain ATP levels for cell growth[98]. One method to modulate cell metabolism is by limiting glucose availability, which forces cells to rely on mitochondrial metabolism for ATP production. Depriving cells of glucose in the presence of other oxidizable substrate, such as glutamine or pyruvate, can lead to a number of changes in mitochondrial networking leading to increased and necessary mitochondrial respiration and ATP synthesis[97]. Another method to push cellular metabolism toward reliance and improved function of the mitochondria is through chemical inhibition of glycolysis, such as by using 2-deoxyglucose treatment which inhibits hexokinase. Alternatives to these methods include siRNA knockdown of glycolytic genes, overexpression of glycolytic inhibitors, and others. However, because chronic glucose deprivation and its effect on the mitochondria have been well described, and because this treatment was readily available for our experiments, we chose this method to push cells away from glycolysis and toward reliance on mitochondrial function.

In our experiments, HCT116 and HeLa cells were chronically grown in media with 4 mM glutamine but low glucose (LG) for over one month (see Methods), where the only contribution of glucose was from 10% FBS (final glucose concentration estimated to be ~0.1-0.5 mM). Parental cancer cells growing in high glucose (25 mM glucose and 4 mM glutamine) were used as control to evaluate differences in reovirus infection. The cells cultured in low glucose (LG) were called HCT-LG and HeLa-LG cells. Following LG adaptation, these cells were characterized and used to study reovirus infection in comparison to parental (high glucose) cells.

Untreated HCT116 and HCT-LG cells were compared to look for cellular changes in stress-responsive markers by Western Blot analysis. As seen in **Fig. 13a**, HCT-LG cells showed enhanced levels of phosphorylated eIF2α on serine 21 and phosphorylated eIF4E on serine 209 when compared to HCT116 cells. Both of these marks result from stress signaling and act to suppress protein translation, suggesting that HCT-LG cells might be under a higher level of basal stress. Consistent with this notion, HCT-LG cells also displayed higher levels of LC3-II, a cleavage fragment of LC3 that arises during autophagy, suggesting that these cells have higher levels of basal autophagy in response to low glucose conditions. Cell morphology under the microscope showed visible vacuolization within the cytoplasm of LG-adapted cells (data not shown), which would be consistent with a high level of autophagy.

To provide support for a metabolic switch in LG cells, the influence of drugs targeting mitochondrial respiration was assessed in these cells. LG-adapted cells were significantly more sensitive to Oligomycin A (OA), a mitochondrial F_1F_O-ATP synthase inhibitor, and Rotenone (RN), a Complex I inhibitor, than were HCT116 and HeLa cells under normal growth conditions (**Fig. 13b**). When observed under the microscope, OA and RN were found to induce profound morphological evidence of cell death in LG cells, whereas these agents only seemed to suppress cell proliferation in HCT116 and HeLa cells (data not shown). No direct evidence was obtained to prove a metabolic switch occurred in these cells.

A

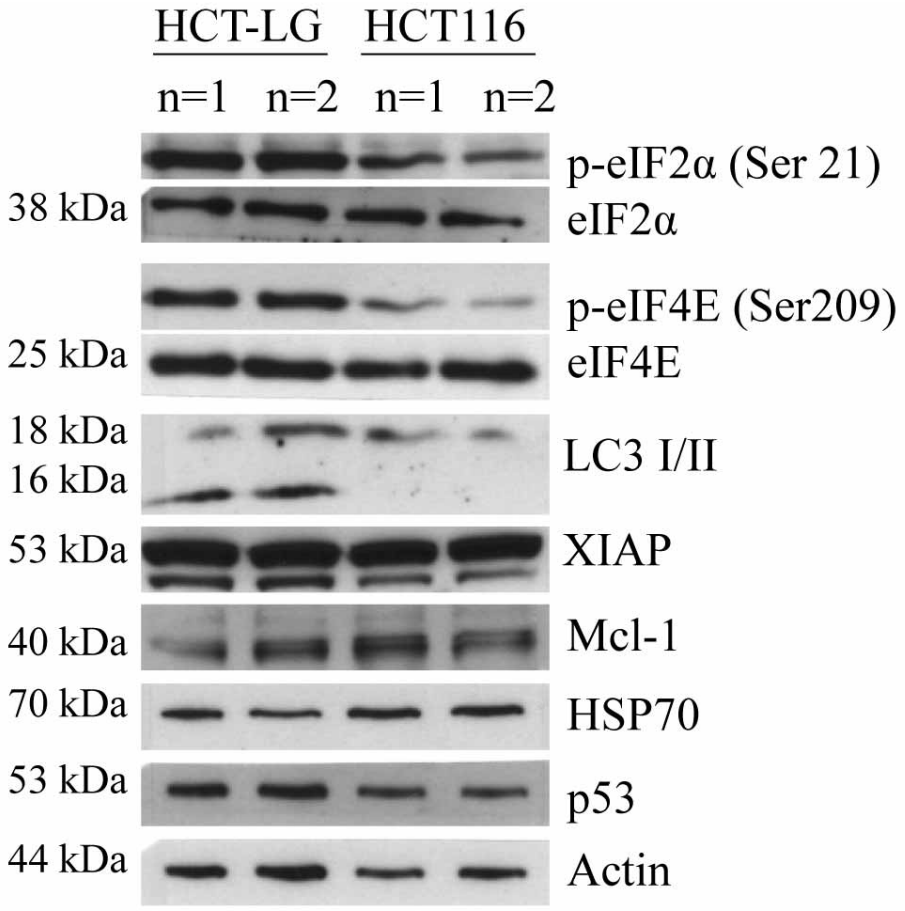
HCT-LG
HCT116
n=1
n=2
n=1
n=2
p-eIF2α (Ser 21)
38 kDa
eIF2α
p-eIF4E (Ser209)
25 kDa
eIF4E
18 kDa
16 kDa
LC3 I/II
53 kDa
XIAP
40 kDa
Mcl-1
70 kDa
HSP70
53 kDa
p53
44 kDa
Actin

B

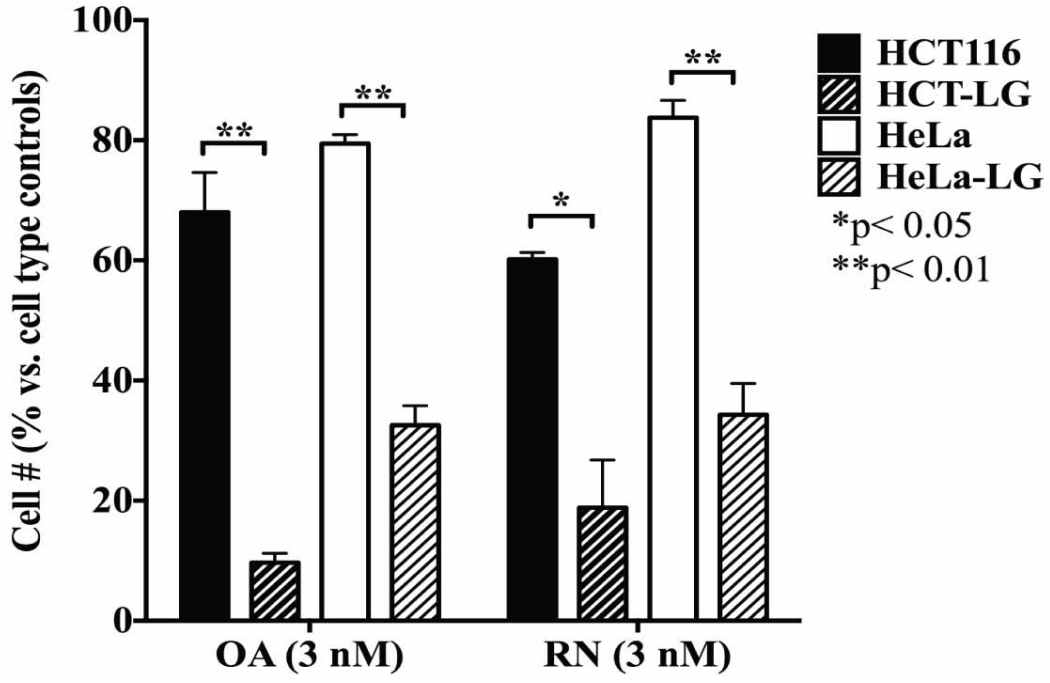
Cell # (% vs. cell type controls)
100
80
60
40
20
0
**
**
*
**
OA (3 nM)
RN (3 nM)
HCT116
HCT-LG
HeLa
HeLa-LG
*p< 0.05
**p< 0.01

Figure 13. Characterizing Low Glucose (LG) Adapted Cells: HCT-LG and HeLa-LG cells.

A) HCT116 and HCT-LG cells were compared for cellular changes in a panel of stress-sensing proteins using Western Blots. Of note, HCT-LG cells had increased phosphorylation of eIF4E and eIF2α, suggesting more limiting protein synthesis machinery, and enhanced LC3 II levels, consistent with enhanced autophagy. n=2.

B) LG cells are significantly more sensitive than normally cultured cells to inhibitors of respiration including Oligomycin A (OA, ATP synthase inhibitor) and Rotenone (RN, Complex I Inhibitor). Cells were treated for 24 hours and assessed by Crystal Violet assay. The results suggest that LG cells are more reliant on mitochondrial oxidative phosphorylation for sustaining cell viability in conditions of low glucose. Error bars are SEM. *$p<0.05$, **$p<0.01$, using a t-test between normal and LG cells for each parental cell type and drug treatment (for example, between HCT-LG and HCT116 treated with OA). n=3 for HCT116 and HeLa, n=4 for HCT-LG and HeLa-LG cells.

Reovirus infection was examined in LG-adapted cells. During reovirus infection of normal and LG cells, it was noted that LG-cells were more resistant to the morphological changes including membrane blebbing, loss of adherence, and accumulation of cell debris normally associated with reovirus-induced apoptosis (**Fig. 14a**). HCT-LG cells were significantly more resistant to loss of cell number induced by reovirus infection at 10 and 100 MOI, but not 1000 MOI, while HeLa-LG cells were more resistant at 100 and 1000 MOI, but not 10 MOI, compared to the respective cell lines cultured with glucose (**Fig. 14b**).

To investigate if suppressed reovirus cytolysis was due to less efficient replication of reovirus, qualitative and quantitative analysis of reovirus replication was measured. Reovirus *de novo* protein synthesis was comparable in LG and normally cultured cells, as shown in **Fig. 14c**. When quantified, viral progeny levels were not significantly different between LG and normal cells at 24 hours post infection (**Fig. 14d**). At 48 hours post infection, production of progeny virus was actually more efficient in HCT-LG cells compared to normal cells, and equivalent in HeLa compared to HeLa-LG cells.

One possible explanation for resistance to reovirus cytolysis in LG cells was a general resistance to apoptosis induction. To test this, the influence of the proapoptotic agents ABT-737, Obatoclax, and Doxorubicin (DOX, a DNA damaging agent) on cell number in HCT116 and HCT-LG cells was measured. As shown in **Fig. 14e**, HCT-LG cells were significantly more resistant to loss of cell number induced by DOX and Obatoclax treatment, but not ABT-737.

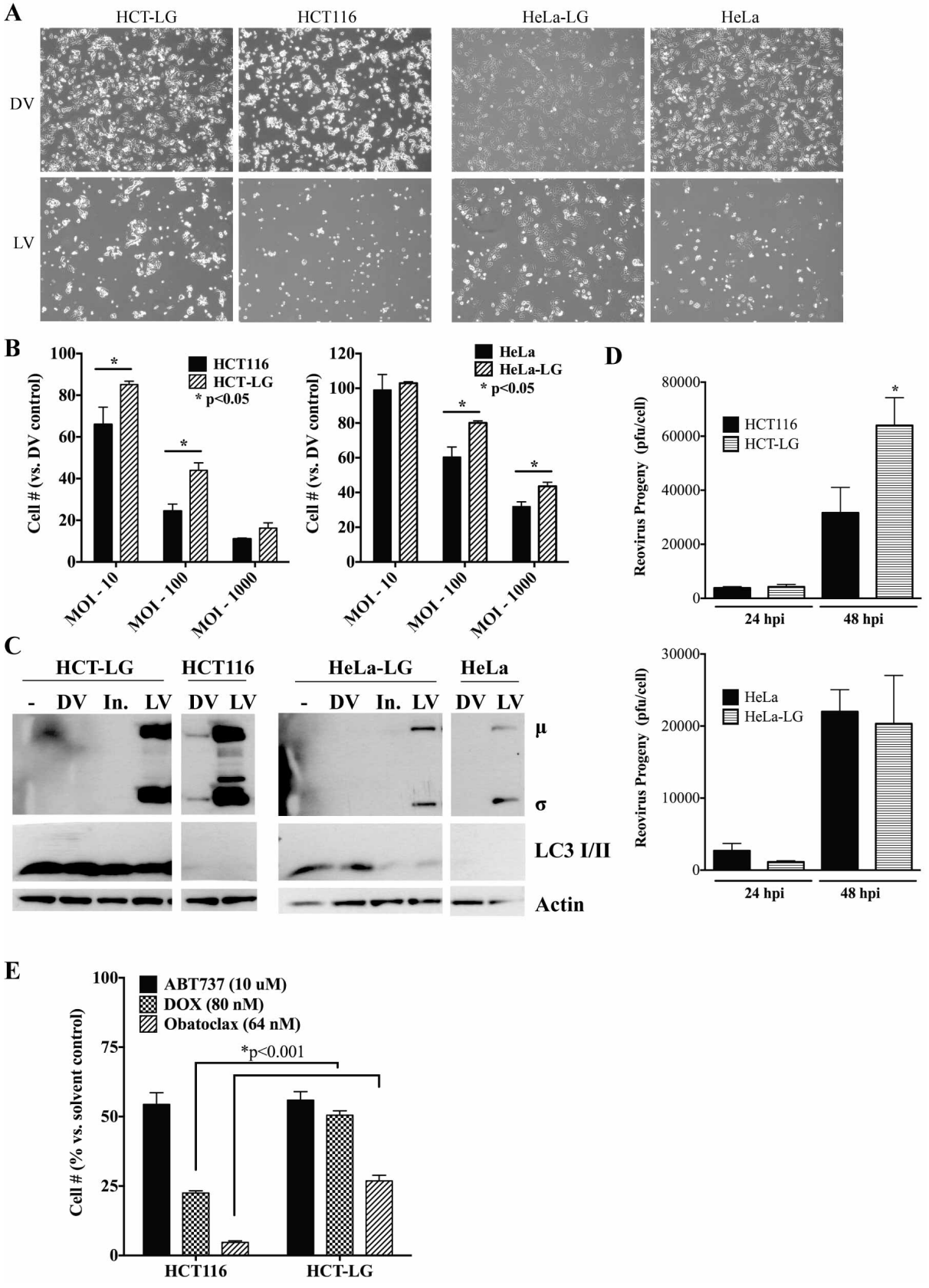
A
HCT-LG
HCT116
HeLa-LG
HeLa
DV
LV
B
Cell # (vs. DV control)
HCT116
HCT-LG
* p<0.05
HeLa
HeLa-LG
* p<0.05
MOI - 10
MOI - 100
MOI - 1000
C
HCT-LG
HCT116
HeLa-LG
HeLa
- DV In. LV DV LV - DV In. LV DV LV
μ
σ
LC3 I/II
Actin
D
Reovirus Progeny (pfu/cell)
HCT116
HCT-LG
24 hpi
48 hpi
HeLa
HeLa-LG
E
ABT737 (10 uM)
DOX (80 nM)
Obatoclax (64 nM)
*p<0.001
Cell # (% vs. solvent control)
HCT116
HCT-LG

Figure 14. LG Cells are Resistant to Reovirus Cytolysis and Apoptotic Drugs.

A) LG cells display partial resistance to reovirus-induced loss of cell number and viability when compared to normally cultured cells, as observed under the microscope and captured by photomicrograph. Cells were infected with 20 pfu/cell for 48 hours. n=2, pictures are representative.

B) LG cells are significantly more resistant to reovirus-induced loss of cell number. Cells were infected with 10, 100, or 1000 pfu/cell for 48 hours and cell number was quantified by crystal violet assay. Error bars are SEM. n=3.

C) Low glucose adapted and normally cultured cells support equivalent reovirus protein synthesis, assessed by Western Blot. *De novo* viral protein synthesis was confirmed by comparison to protein from input (In.) virus. Note, the protein marker LC3I/II was included to confirm differences between LG and normally cultured cells. n=3.

D) Production of progeny reovirus LG cells compared to normally cultured cells as assessed by plaque assay. Cells were infected with 10 pfu/cell for 24 or 48 hours. Error bars are SEM. *$p<0.05$ for HCT-LG vs. HCT116 at 48 hpi. n=3.

E) Cell number was quantified in HCT116 and HCT-LG cells after 24 hour treatment with different apoptosis-inducing drugs. HCT-LG cells were significantly more resistant to the effects of doxorubicin (DOX) and Obatoclax, but not ABT-737. Error bars are SEM. n=3

3.2.2 Mitochondrial Inner Membrane Potential is Decreased during Reovirus Infection

Permeabilization of the outer mitochondrial membrane (MOMP) leads to leakage of proapoptotic proteins from the mitochondrial intermembrane space (IMS) into the cytoplasm. An essential activator of caspase-3-dependent apoptosis is cytochrome c, which is normally localized and functions in the IMS as part of the electron transport chain. Proper localization and function of cytochrome c in mitochondrial respiration is essential for efficient oxidative phosphorylation and ATP production. Loss of cytochrome c from the IMS inhibits electron transport-coupled proton pumping into the IMS that is required for generation of the proton motive force (*pmf*) that drives ATP production through ATP synthase. As a result of cytochrome c release and inhibited proton pumping, the voltage potential across the mitochondrial inner membrane (MIM) decreases in response to agents that induce MOMP.

Reovirus-induced apoptosis is linked to MOMP and previous studies have shown that this is associated with loss of mitochondrial inner membrane potential (Ψ_m)[129]. To confirm that cytolytic reovirus infection leads to loss of Ψ_m in HCT116 and HeLa cells, the Ψ_m-sensitive mitochondrial stain tetramethylrhodamine, methyl ester, perchlorate (TMRM) was loaded into cells and measured by flow cytometry following reovirus infection. Loss of TMRM stain was quantified by determining the percentage of cells below a Ψ_m count of 2000 for HCT116 cells, and 5000 for HeLa cells (along the horizontal axis), which delineates the low end of the Ψ_m peak in control untreated cells. **Figure 15a-b** suggests that reovirus infection induces a time-dependent loss of Ψ_m in HCT116 and HeLa cells over a 48 hour infection period. However, only n=2 experiments were performed, and thus while a trend seems evident, we cannot say with statistical rigor that reovirus leads to loss of Ψ_m in HCT116 and HeLa cells.

It should be noted that in this experiment, the caspase inhibitor ZVAD was included in all samples to suppress rapid caspase-dependent disassembly of cells. One potential consequence of ZVAD treatment could be partial inhibition of loss of Ψ_m during reovirus infection. ZVAD may suppress BCL-2 family-dependent MOMP due to reovirus-induced caspase-8 activation and generation of tBID, a proapoptotic BCL-2 family protein contributing to MOMP and loss of Ψ_m. Therefore, it is possible that an enhanced phenotype, that is, further or more rapid loss of Ψ_m following reovirus infection, might have been observed in the absence of ZVAD.

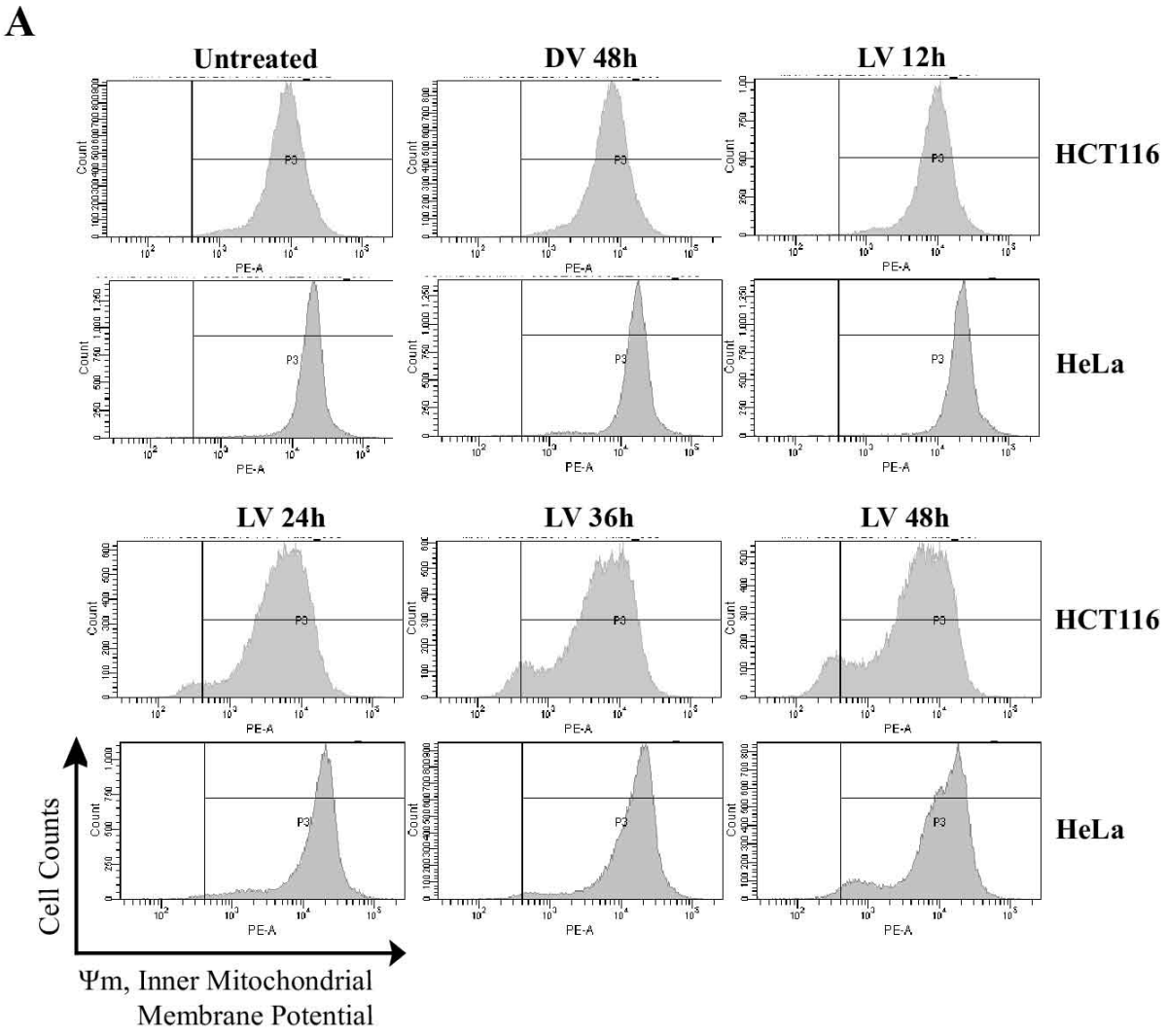
A
Untreated
DV 48h
LV 12h
HCT116
HeLa
LV 24h
LV 36h
LV 48h
HCT116
HeLa
Count
PE-A
P3
Cell Counts
Ψm, Inner Mitochondrial
Membrane Potential

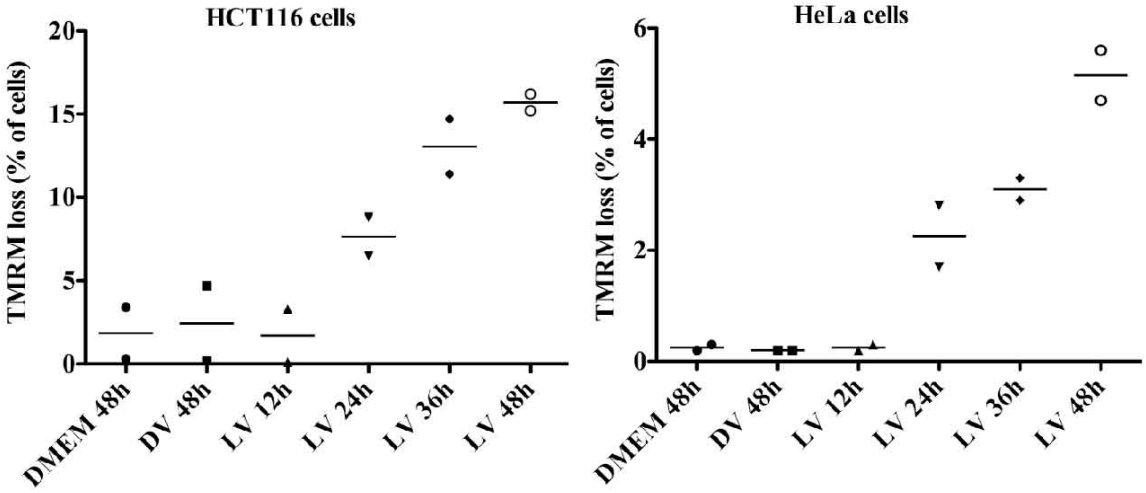
B
HCT116 cells
HeLa cells
TMRM loss (% of cells)
DMEM 48h
DV 48h
LV 12h
LV 24h
LV 36h
LV 48h

Figure 15. Reovirus Infection Leads to Loss of Mitochondrial Inner Membrane Potential

A) Flow cytometry analysis of mitochondrial inner membrane potential measured using the cationic TMRM stain in HCT116 and HeLa cells after treatment with 25 pfu/cell dead or live reovirus for 12 - 48 hours. n=2, images are representative.

B) Quantifying TMRM loss in HCT116 and HeLa cells. Loss of TMRM stain was quantified by determining the percentage of cells below a Ψ_m count of 2000 for HCT116 cells, and 5000 for HeLa cells (along the horizontal axis), which delineates the low end of the Ψ_m peak in control untreated cells. n=2, the mean of 2 data points is presented as a horizontal line.

While the roles of MOMP and cytochrome c release in executing apoptosis during reovirus infection are well studied, a role for functional mitochondrial respiration and mitochondrial ATP synthesis (responsible for maintaining Ψ_m) in reovirus infection has never been investigated. To begin exploring this possibility, the remainder of this thesis investigates the influence of chemically inhibiting mitochondrial respiration and ATP synthesis on reovirus infection, with a focus on the influence of the mitochondrial ATP synthase inhibitor Oligomycin A.

3.2.3 Drugs Targeting Mitochondrial Respiration Differentially Affect Reovirus Cytolysis

To begin assessing a role for mitochondrial function in reovirus infection, the influence of chemical inhibitors of respiratory complexes and mitochondrial ATP synthase on reovirus infection was assessed. These experiments focused primarily on HCT116, with some experiments also performed in HeLa cells. The following drugs were used: Rotenone (RN) is an inhibitor of complex I, Antimycin A (AA) inhibits complex III, Sodium Azide (AZ) inhibits complex IV, and Oligomycin A (OA) inhibits ATP synthase.

The ability of these drugs to decrease HCT116 cell number alone, or in combination with reovirus, was assessed by CV assay in **Figure 16a**. Antimycin A and Sodium Azide combined with reovirus did not significantly affect reovirus infection compared to infection alone. Although a modest enhancement of reovirus-induced effects on cell number was observed for rotenone at low drug concentrations, this was not significantly different than virus infection alone, **Fig. 16a**. Only the combination of Oligomycin A at low (nM) doses with reovirus was able to significantly enhance the loss of cell number compared to drug or reovirus treatment alone. HCT116 cells were infected with reovirus in the presence of each of these drugs and cell morphology was photographed. As shown in **Fig. 16b**, none of the drug treatments by themselves appeared to induce cell death. Combining Antimycin A, Sodium Azide, or Rotenone with reovirus appeared to induce morphological changes very similar to virus infection alone. However, combining Oligomycin with reovirus infection appeard to induce more extensive cell death than virus infection alone, evidenced by a larger proportion of floating, dead cells. .

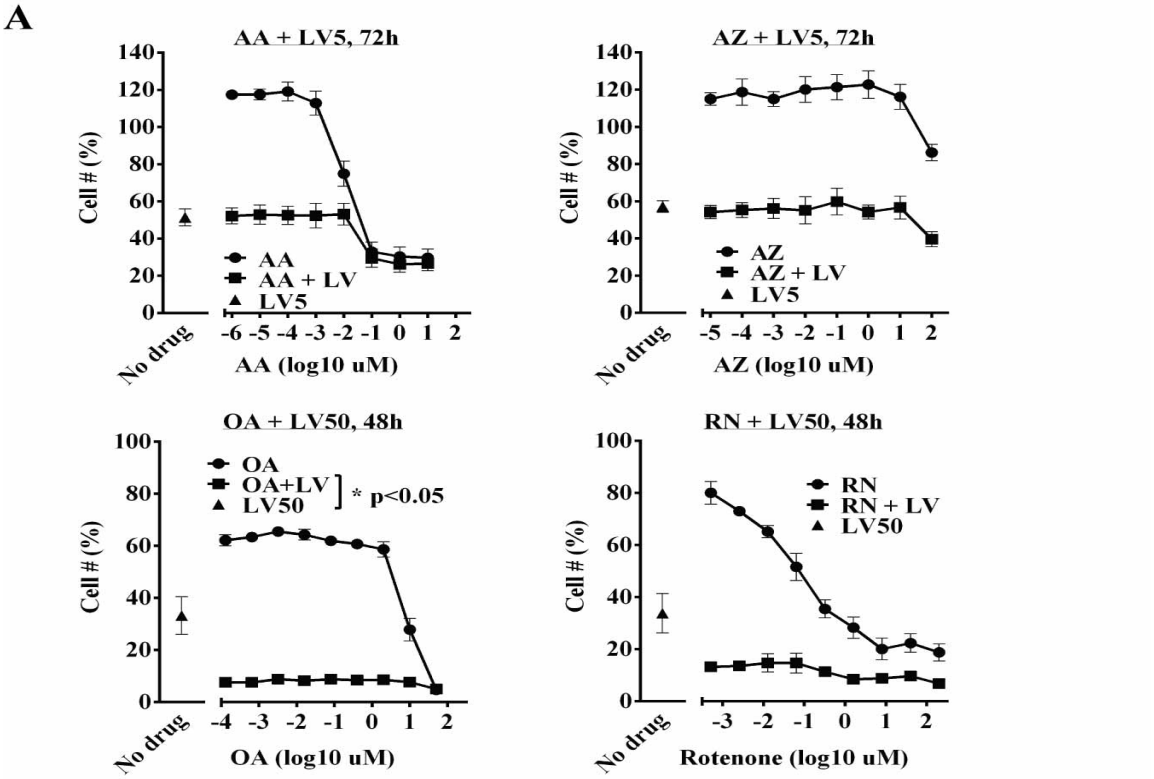
A
AA + LV5, 72h
Cell # (%)
AA
AA + LV
LV5
No drug
AA (log10 uM)
AZ + LV5, 72h
AZ
AZ + LV
LV5
AZ (log10 uM)
OA + LV50, 48h
OA
OA+LV
LV50
* p<0.05
OA (log10 uM)
RN + LV50, 48h
RN
RN + LV
LV50
Rotenone (log10 uM)

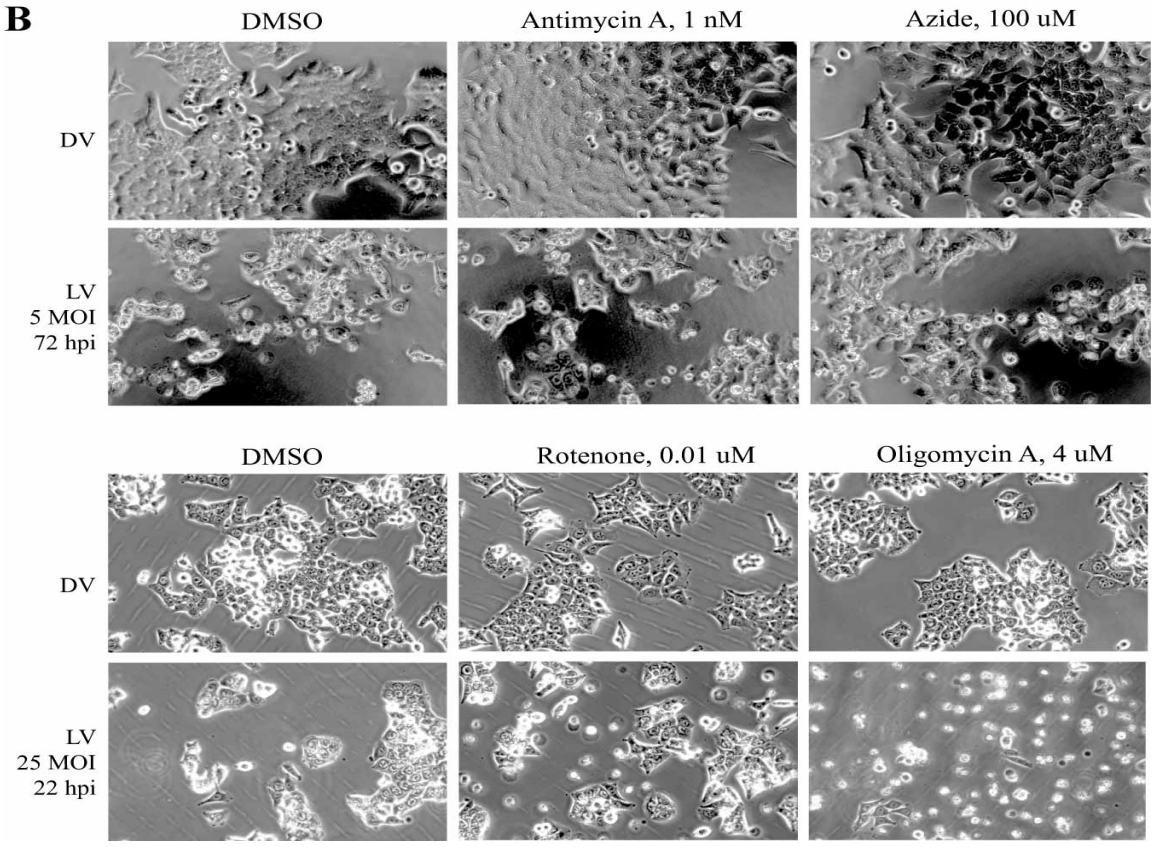
B
DMSO
Antimycin A, 1 nM
Azide, 100 uM
DV
LV
5 MOI
72 hpi
DMSO
Rotenone, 0.01 uM
Oligomycin A, 4 uM
DV
LV
25 MOI
22 hpi

Figure 16. Respiration Inhibitors Differentially Affect Reovirus Cytolysis in HCT116 Cells.

A) The effect of drugs targeting respiration on cell number in the absence or presence of live virus for 48 or 72 hours was determined by CV assay. The effect of reovirus alone was also determined. Error bars are SEM. n=3.

B) Photomicrographs of HCT116 cells treated with respiration inhibitors and infected with dead or live virus at the indicated doses for the indicated times. An observable enhancement in cytolysis was present when Oligomycin A was combined with live virus infection. n=2.

Note that for data points in **A** where error bars do not appear, this is because the software program used (GraphPad Prism 5) does not display error bars when they are smaller than the size of the symbol used. Therefore for all data points that appear to be lacking error bars, these data points have very small error bars that are omitted by the program.

3.2.4 ATP Synthase Inhibition by Oligomycin Enhances Reovirus Cytolysis

High doses of Oligomycin alone potently killed cells (loss of cell number in **Fig. 16a**, and data not shown), possibly due to the additional off-target inhibition of plasma membrane Na/K ATPase and ionic transport[130]. However, at a broad range of lower doses, Oligomycin alone led to only a modest decrease in cell number (~40% decrease after 48 hours in HCT116 cells, **Fig. 16a**) compared to untreated controls. Interestingly, this decrease did not seem to be associated with any cell death morphology and cells displayed healthy morphology indistinguishable from control cells (**Fig. 16b**). Instead, Oligomycin treated cells appeared to proliferate more slowly than control cells during the course of the experiment when observed under a phase contrast microscope (data not shown). A previous study found that Oligomycin induces partial growth suppression due to cell cycle arrest at G_1 as a result of low ATP levels[131]. Therefore it was unclear whether Oligomycin plus reovirus improved the loss of cell number in HCT116 cells compared to reovirus alone when the suspected inhibition of cell number by Oligomycin alone was accounted for.

To test more directly whether the addition of Oligomycin significantly enhanced loss of cell number induced by reovirus, HCT116 cells were treated as in **Figure 17** and cell number was measured by CV assay. All data were either normalized to the dead virus plus ethanol (DV+EtOH) control as 100% cell number (**Fig. 17a**) or data were normalized to the matched DV solvent/drug control as 100% (**Fig. 17b**). Even when LV+OA were normalized to the DV+OA sample, LV+OA decreased HCT116 cell number significantly more than LV+EtOH.

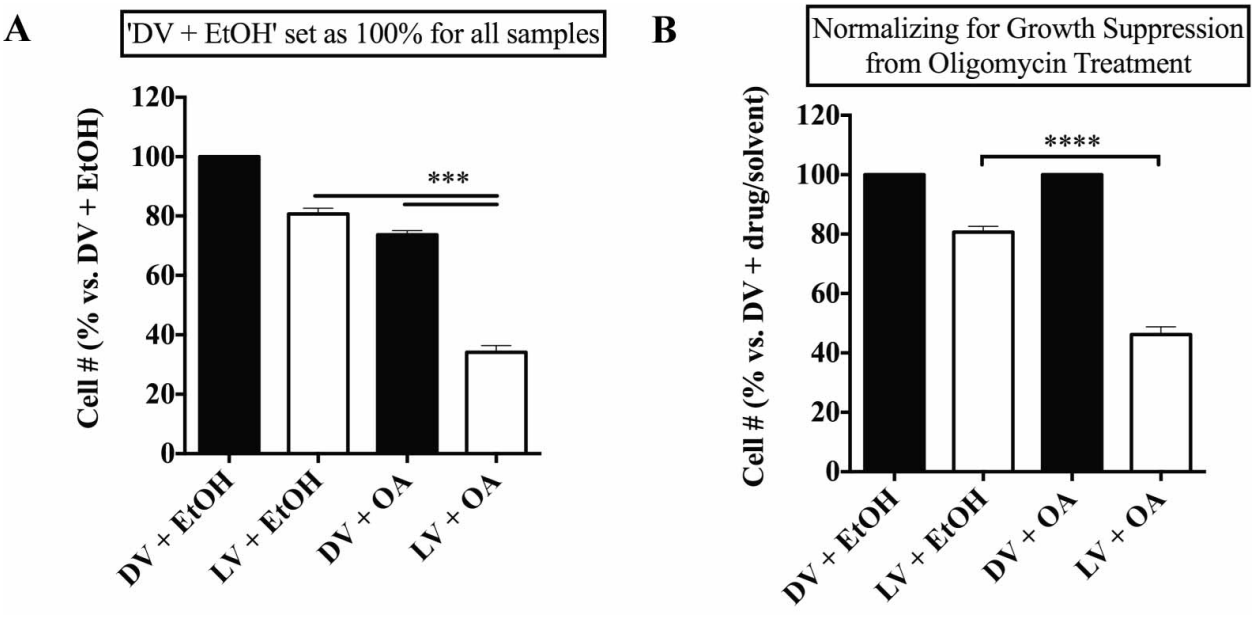
A
'DV + EtOH' set as 100% for all samples
Cell # (% vs. DV + EtOH)
120
100
80
60
40
20
0
***
DV + EtOH
LV + EtOH
DV + OA
LV + OA
B
Normalizing for Growth Suppression from Oligomycin Treatment
Cell # (% vs. DV + drug/solvent)
120
100
80
60
40
20
0
****
DV + EtOH
LV + EtOH
DV + OA
LV + OA

Figure 17. Oligomycin Promotes Reovirus Cytolysis in HCT116 Cells.

A) The effect of Oligomycin treatment combined with reovirus infection was assessed by quantifying cell number 24 hours after treatment/infection using CV assay. It was noted that Oligomycin treatment alone seemed to suppress cell growth under the microscope over the course of treatment, which is supported by the significant decrease in cell number when quantified. Error bars are SEM, ***$p<0.001$ using One-way ANOVA with Holm-Sidak post-test to assess significance (see Methods). n=3.

B) Data were normalized to account for the effect of Oligomycin treatment on cell number. Ie. LV+EtOH was normalized to DV+EtOH, while LV+OA was normalized to DV+OA. When normalized, we can see that there is a true significant enhancement of reovirus-induced cytolysis in the presence of Oligomycin. Error bars are SEM, ****$p<0.0001$ using One-way ANOVA with Holm-Sidak post-test to assess significance between samples (see Methods). n=3.

We wanted to characterize the influence of Oligomycin treatment alone on cancer cells. In HCT116 and HeLa cells, OA treatment suppressed the increase in cell number over time in each cell line, **Fig. 18a**. This decrease in cell number in Oligomycin treated cells relative to control was significant over time in HCT116 cells but not in HeLa cells. The suppressive effect of Oligomycin was also stronger in HCT116 cells.

ATP levels were measured over a range of doses of Oligomycin and Rotenone in HCT116 and HeLa cells using an ATP-based luciferase assay. Oligomycin and Rotenone had only mild effects on ATP levels measured relative to control solvent-treated HCT116 and HeLa cells measured after 48 hours of treatment, **Fig. 18b**. ATP levels were also measured over time in cells treated with a constant dose of OA or RN. The influence of OA and RN on ATP levels over time was mild, and typically the levels were maintained at 80% or higher compared to control, **Fig. 18c**. In HeLa cells, OA induced a larger drop in ATP levels to ~60% of control by 6 hours, but these levels rebounded to ~95% of control by 22 hours of treatment (**Fig. 18c**).

To test if Oligomycin treatment might be enhancing apoptosis more generally, the influence of OA on doxorubicin (DOX), ABT-737, and Trail treatment was assessed in HCT116 and HeLa cells, **Figure 18d**. OA decreased cell number by itself by roughly ~40% in HCT116 cells and ~20% in HeLa cells. The combination of OA with DOX and ABT-737 was not significantly different than either Oligomycin alone or the drug alone controls in HCT116 cells. While OA+Trail was significantly more effective that OA alone in HCT116 cells, it was not significantly different that Trail treatment alone. In HeLa cells, OA+DOX was significantly more effective than OA alone but not DOX treatment alone, while OA+ABT-737 was not significantly different from either OA or ABT-737 controls. OA+Trail was significantly more effective than OA treatment but not the Trail alone control in HeLa cells.

To assess the influence of Oligomycin and reovirus on cell cycle progression, DNA content was measured by propidium iodide staining. Representative results of DNA content analysis from one experiment are shown in **Fig. 19a** and the proportion of cells in S-phase from n=2 experiments are summarized in **Fig. 19b**. Oligomycin appeared to cause a slight decrease in the percent of HCT116 cells in S phase and almost no effect in HeLa cells. However, only n=2 results were obtained and no statistical analysis could be performed. Reovirus infection alone or with OA only slightly influenced the percentage of cells in S-phase in each cell line.

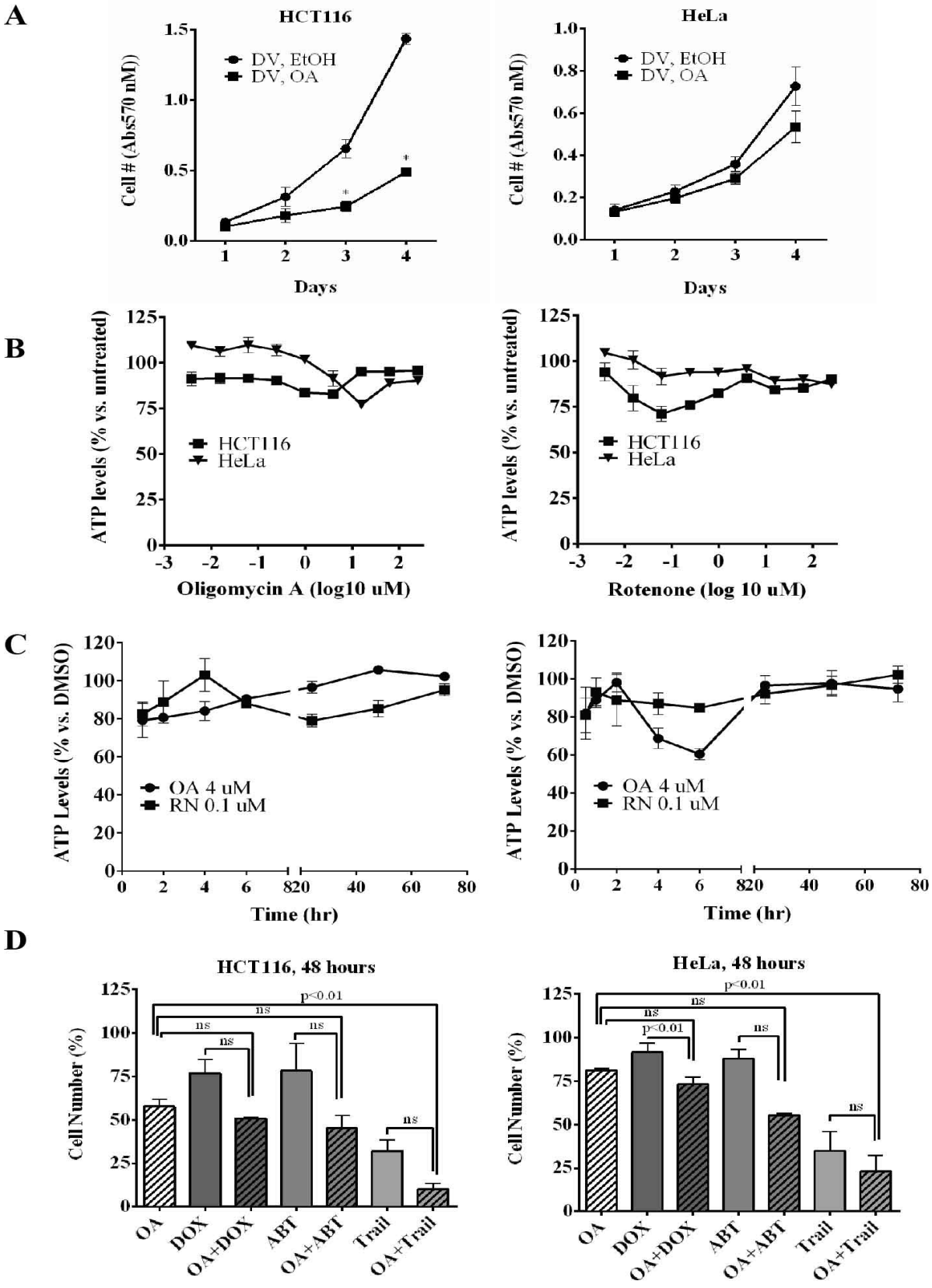
A
HCT116
DV, EtOH
DV, OA
Cell # (Abs570 nM))
Days
HeLa
DV, EtOH
DV, OA
Cell # (Abs570 nM))
Days
B
ATP levels (% vs. untreated)
HCT116
HeLa
Oligomycin A (log10 uM)
ATP levels (% vs. untreated)
HCT116
HeLa
Rotenone (log 10 uM)
C
ATP Levels (% vs. DMSO)
OA 4 uM
RN 0.1 uM
Time (hr)
ATP Levels (% vs. DMSO)
OA 4 uM
RN 0.1 uM
Time (hr)
D
HCT116, 48 hours
Cell Number (%)
p<0.01
ns
ns
ns
ns
ns
OA
DOX
OA+DOX
ABT
OA+ABT
Trail
OA+Trail
HeLa, 48 hours
Cell Number (%)
p<0.01
ns
ns
p<0.01
ns
ns
OA
DOX
OA+DOX
ABT
OA+ABT
Trail
OA+Trail

Figure 18. Oligomycin Treatment Causes Growth Suppression Despite Maintained ATP Levels.

A) The effect of Oligomycin A (OA) on cell number was determined by CV assay in HCT116 and HeLa cells over four days. * $p<0.05$ using t-test for each time point. Error bars are SEM. n=3.

B) Relative ATP levels were determined 48 hours post treatment with Oligomycin (OA) and Rotenone (RN) in HCT116 and HeLa cells using the Cell Titer-Glo Luminescent Cell Viability assay based on ATP levels (see Methods). Note, the effect of each drug on cell number was calculated in parallel experiments by CV assay and ATP data were normalized to cell number. Error bars are SEM. n=3.

C) Relative ATP levels were determined over a time course of treatment with OA or RN in HCT116 (left panel) and HeLa cells (right panel) as above. Error bars are SEM. n=3.

D) The effect of OA treatment on cell death induced by Doxorubicin (DOX, 50 nM)), ABT-737 (5 μM), or Trail (20 ng/mL) was determined in HCT116 and HeLa cells by CV assay. One-way ANOVA was performed using Holm-Sidak post test for multiple comparisons as in Methods. Error bars are SEM. n=3.

Note that for data points in **A-C** where error bars do not appear, this is because the software program used (GraphPad Prism 5) does not display error bars when they are smaller than the size of the symbol used. Therefore in all cases where n=3 and data points appear to be lacking error bars, these data points have very small error bars that are omitted by the program.

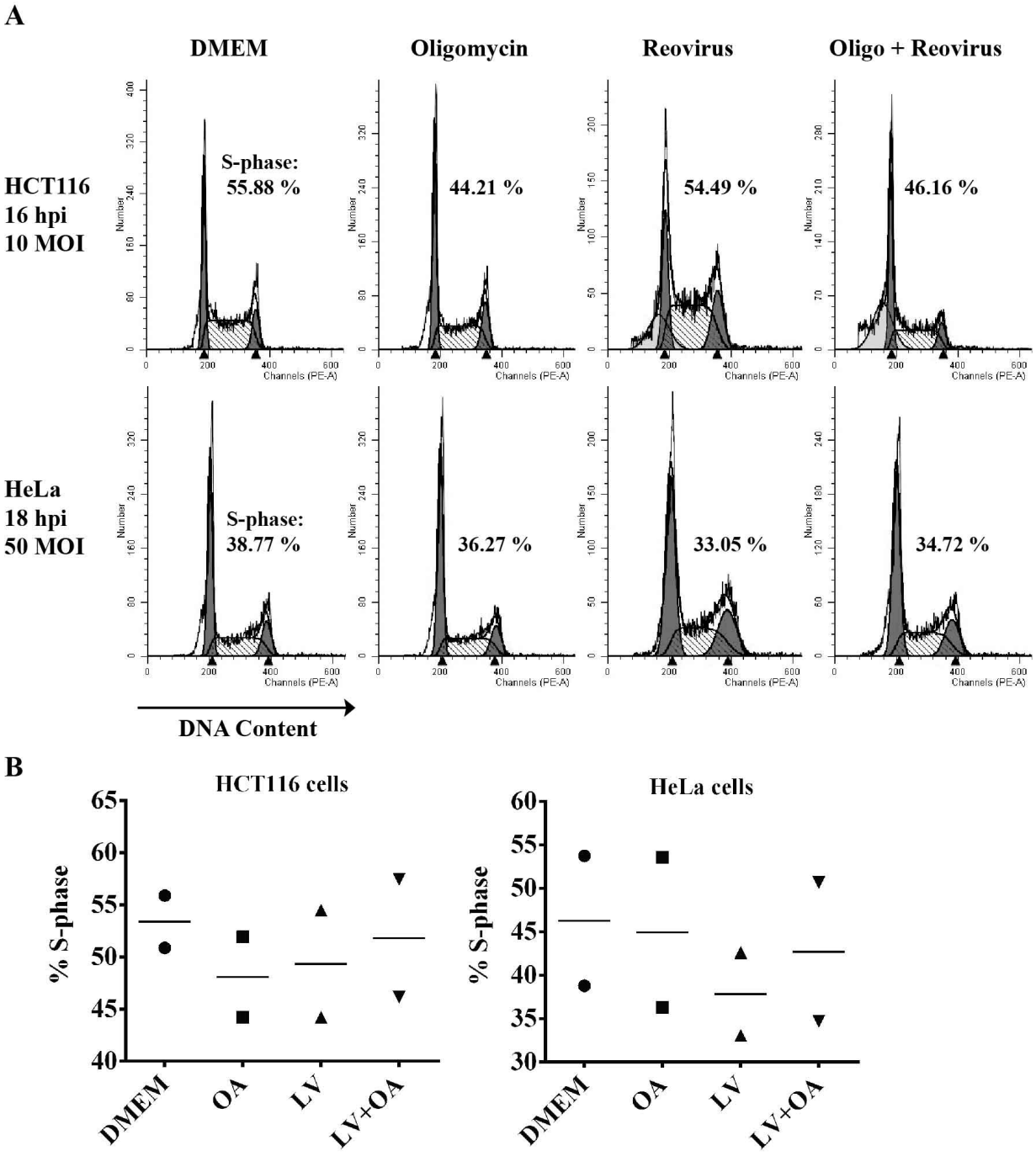
A
DMEM
Oligomycin
Reovirus
Oligo + Reovirus
HCT116
16 hpi
10 MOI
S-phase:
55.88 %
44.21 %
54.49 %
46.16 %
HeLa
18 hpi
50 MOI
S-phase:
38.77 %
36.27 %
33.05 %
34.72 %
Number
Channels (PE-A)
DNA Content
B
HCT116 cells
HeLa cells
% S-phase
DMEM
OA
LV
LV+OA

Figure 19. Oligomycin Treatment or Reovirus Infection Do Not Appear to Influence Cell Cycling.

A) Cell cycle analysis was performed on HCT116 and HeLa cells that were untreated (DMEM) or treated with Oligomycin (10 nM), infected with reovirus (10 pfu/cell and 50 pfu/cell for HCT116 and HeLa cells, respectively), or the combination of Oligomycin and reovirus for 16 hours (HCT116) or 18 hours (HeLa) as described in Methods. Inset are the percentage of cells calculated to be in S phase according to analysis using ModFit LT version 3.2 software as performed by the Flow Cytometry facility. n=2, data are representative.

B) The percentage of cells in S-phase based on the ModFit LT analysis from two replicate experiments from **A**. The individual points are shown, and the horizontal line is the mean of two data points. n=2.

3.2.5 Oligomycin, But Not Rotenone or Obatoclax, Enhances Loss of Mitochondrial Inner Membrane Potential during Reovirus Infection

To address whether Oligomycin treatment influences loss of inner mitochondrial membrane potential occurring during reovirus infection, flow cytometry was used as described above and in Methods. Loss of TMRM stain was quantified by determining the percentage of cells below a Ψ_m count of 2000 (along the horizontal axis), which delineates the low end of the Ψ_m peak in control untreated cells. As shown in **Figure 20a-b** reovirus infection leads to loss of mitochondrial inner membrane potential in HCT116 cells. Oligomycin treatment alone hyperpolarized mitochondria, which was an expected finding since inhibition of mitochondrial ATP synthase prevents proton flux from the IMS into the matrix downstream of mitochondrial respiration, leading to a higher negative charge inside the mitochondria and increased accumulation of the cationic TMRM stain within mitochondria. Unexpectedly, Rotenone treatment alone did not appear to depolarize mitochondria, **Fig. 20a**. Depolarization following Rotenone treatment has been shown previously and has been used as indirect confirmation of respiration inhibition. This may suggest that the dose of Rotenone used in our experiments (0.1 μM) was too low and did not have a strong inhibitory effect on mitochondrial function. Combining Rotenone or Obatoclax with reovirus did not significantly affect inner membrane potential (Ψ_m). On the other hand, Oligomycin treatment combined with reovirus significantly enhanced the percentage of cells with decreased Ψ_m **(**TMRM loss) at 24 and 48 hpi.

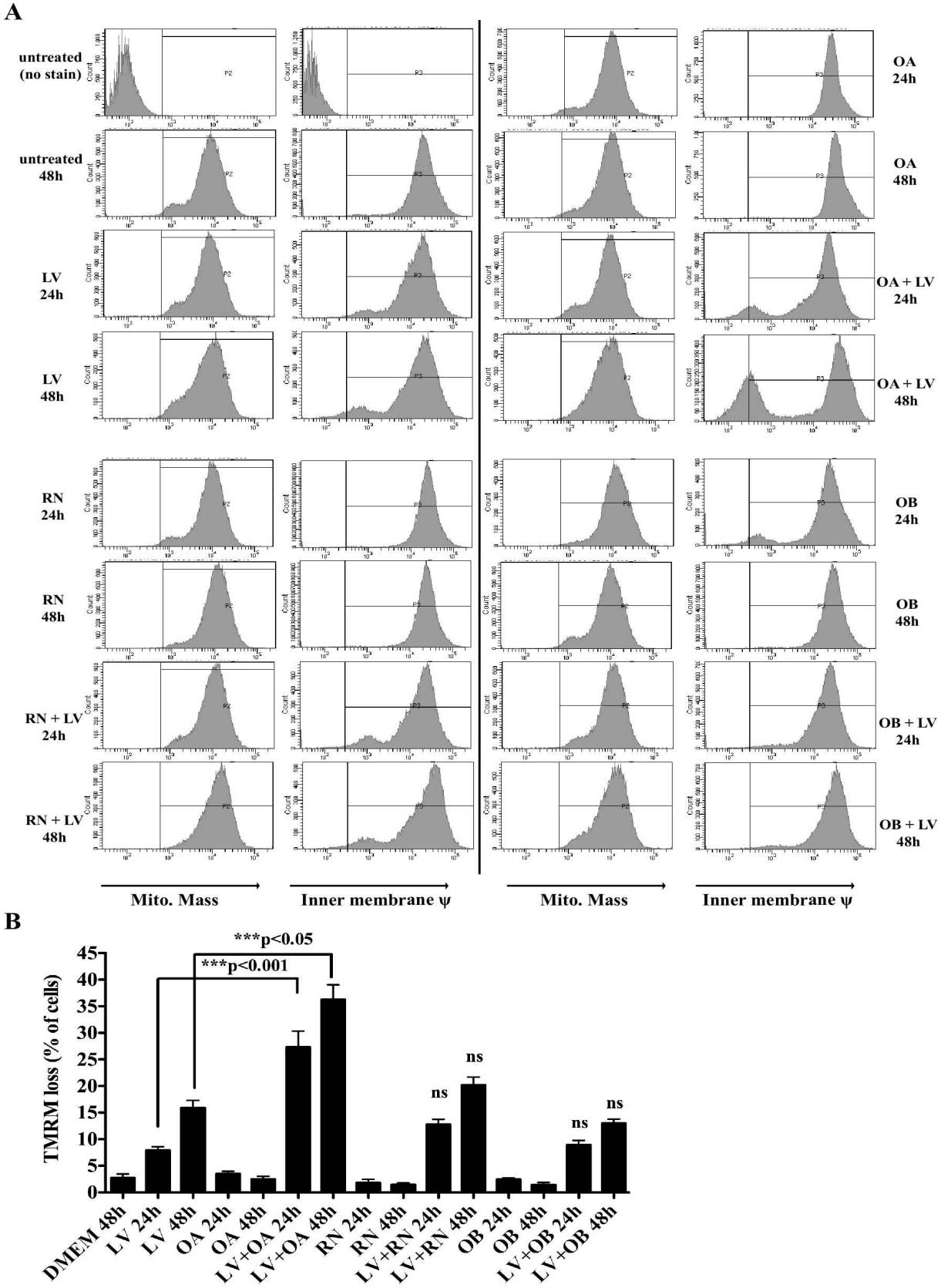
A
untreated (no stain)
untreated 48h
LV 24h
LV 48h
RN 24h
RN 48h
RN + LV 24h
RN + LV 48h
OA 24h
OA 48h
OA + LV 24h
OA + LV 48h
OB 24h
OB 48h
OB + LV 24h
OB + LV 48h
Mito. Mass
Inner membrane ψ
Mito. Mass
Inner membrane ψ
B
***p<0.05
***p<0.001
TMRM loss (% of cells)
0
5
10
15
20
25
30
35
40
45
ns
ns
ns
ns
DMEM 48h
LV 24h
LV 48h
OA 24h
OA 48h
LV+OA 24h
LV+OA 48h
RN 24h
RN 48h
LV+RN 24h
LV+RN 48h
OB 24h
OB 48h
LV+OB 24h
LV+OB 48h

Figure 20. Oligomycin Augments Loss of Mitochondrial Inner Membrane Potential during Reovirus Infection

A) Flow cytometry analysis of mitochondrial mass and inner membrane potential (TMRM stain) in HCT116 cells after treatment with Oligomycin (OA, 4 μM), Rotenone (RN 0.1 μM), or Obatoclax (OB, 15 nM) alone or in combination with reovirus (LV, 25 pfu/cell) for 24 and 48 hours. Untreated cells and cells infected with LV alone were also included. All treatments contained the caspase inhibitor ZVAD to prevent rapid cellular disassembly. n=3, images are representative.

B) Quantifying TMRM loss in HCT116 cells. Loss of TMRM stain was quantified by determining the percentage of cells below a Ψ_m count of 2000 (along the horizontal axis), which delineates the low end of the Ψ_m peak in control untreated cells. Data were analyzed using one-way ANOVA with Holm-Sidak post test to compare treatments. 'ns' indicates no significant difference compared to LV control at the indicated time point. n=3, error bars are SEM.

3.2.6 Oligomycin May Enhance Caspase Activation during Reovirus-Induced Apoptosis

The finding that Oligomycin enhanced loss of Ψ_m during reovirus infection provided support for the idea that Oligomycin enhances reovirus-induced apoptosis. HCT116 cells were infected with reovirus alone or in the presence of Oligomycin or Rotenone for 24 hours and subjected to Western Blot. Oligomycin, but not rotenone, enhanced caspase-specific PARP cleavage induced by reovirus infection in HCT116 cells, **Figure 21a**.

Reovirus protein levels measured by Western Blot in the same set of samples appeared to be much lower in the presence of Oligomycin but nearly equivalent in the presence of Rotenone. Plaque assays were used to quantify the influence of combining Oligomycin or Rotenone treatment with reovirus on production of infectious reovirus progeny in HCT116 cells. As shown in **Figure 21b**, both Oligomycin and Rotenone treatment significantly decreased levels of infectious progeny virus by 4-5 fold.

To provide further support for enhanced caspase activity when Oligomycin is combined with reovirus infection, early caspase activity was measured in HCT116 cells using a pan-active caspase stain and detection by flow cytometry. Combining Oligomycin treatment with reovirus appeared to enhance the percentage of cells displaying caspase activity at 14 hours compared to virus alone, which displayed a lower but detectable level of caspase activity, **Figure 22a-b** Caspase activity following reovirus or reovirus plus Oligomycin was inhibited by the pan-caspase inhibitor ZVAD, as expected. Of note, this experiment was only replicated twice (n=2), therefore we cannot say with statistical rigor that Oligomycin enhances early caspase activity in reovirus infection cells although this might be the case and would be consistent with our other data.

To confirm that increased apoptosis underlies the enhancement of reovirus oncolysis by Oligomycin, the influence of caspase inhibition by ZVAD was assessed in HCT116 cells following a 24 hours infection. As shown in **Figure 23**, ZVAD did not significantly affect the decrease in cell number induced by Oligomycin (DV+OA). However, ZVAD significantly inhibited reovirus induced cell death alone, and also with the combination of reovirus and Oligomycin, as well as Trail treatment (positive control). In each case, cell number was rescued to within 10% of control values, supporting that each of these treatments induced caspase-dependent apoptosis leading to cell death and decreasing cell number.

A

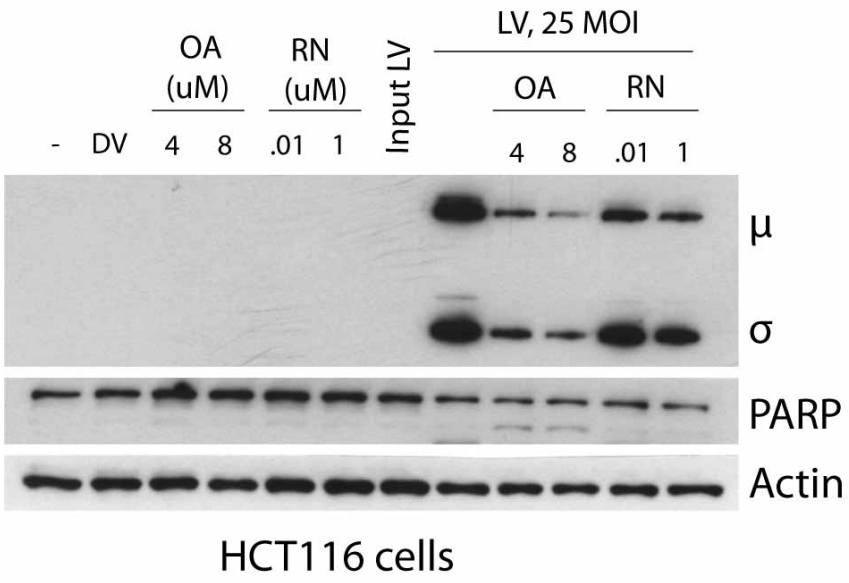
OA (uM)
RN (uM)
Input LV
LV, 25 MOI
OA
RN
- DV 4 8 .01 1
4 8 .01 1
μ
σ
PARP
Actin
HCT116 cells

B

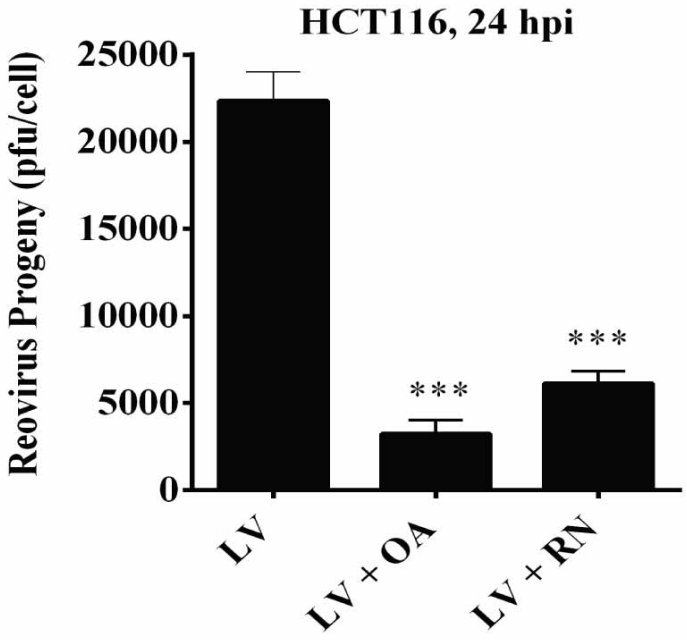
HCT116, 24 hpi
Reovirus Progeny (pfu/cell)
25000
20000
15000
10000
5000
0
***
***
LV
LV + OA
LV + RN

Figure 21. Oligomycin Enhances Markers of Apoptosis Despite Suppressed Reovirus Replication.

A) The influence of Oligomycin (OA) and Rotenone (RN) treatment on reovirus *de novo* protein synthesis and PARP cleavage in HCT116 cells treated for 24 hours was assessed by Western Blot. PARP cleavage was enhanced despite dampened reovirus protein synthesis when Oligomycin was combined with reovirus. n=2.

B) Reovirus progeny production in HCT116 cells infected with reovirus (10 pfu/cell) alone, or combined with Oligomycin (OA, 4 μM) or Rotenone (RN, 0.1 μM) was assess by Plaque Assay. Error bars are SEM. ***$p<0.001$, using One-way ANOVA with Holm-Sidak post-test to assess significance between samples (see Methods). n=3.

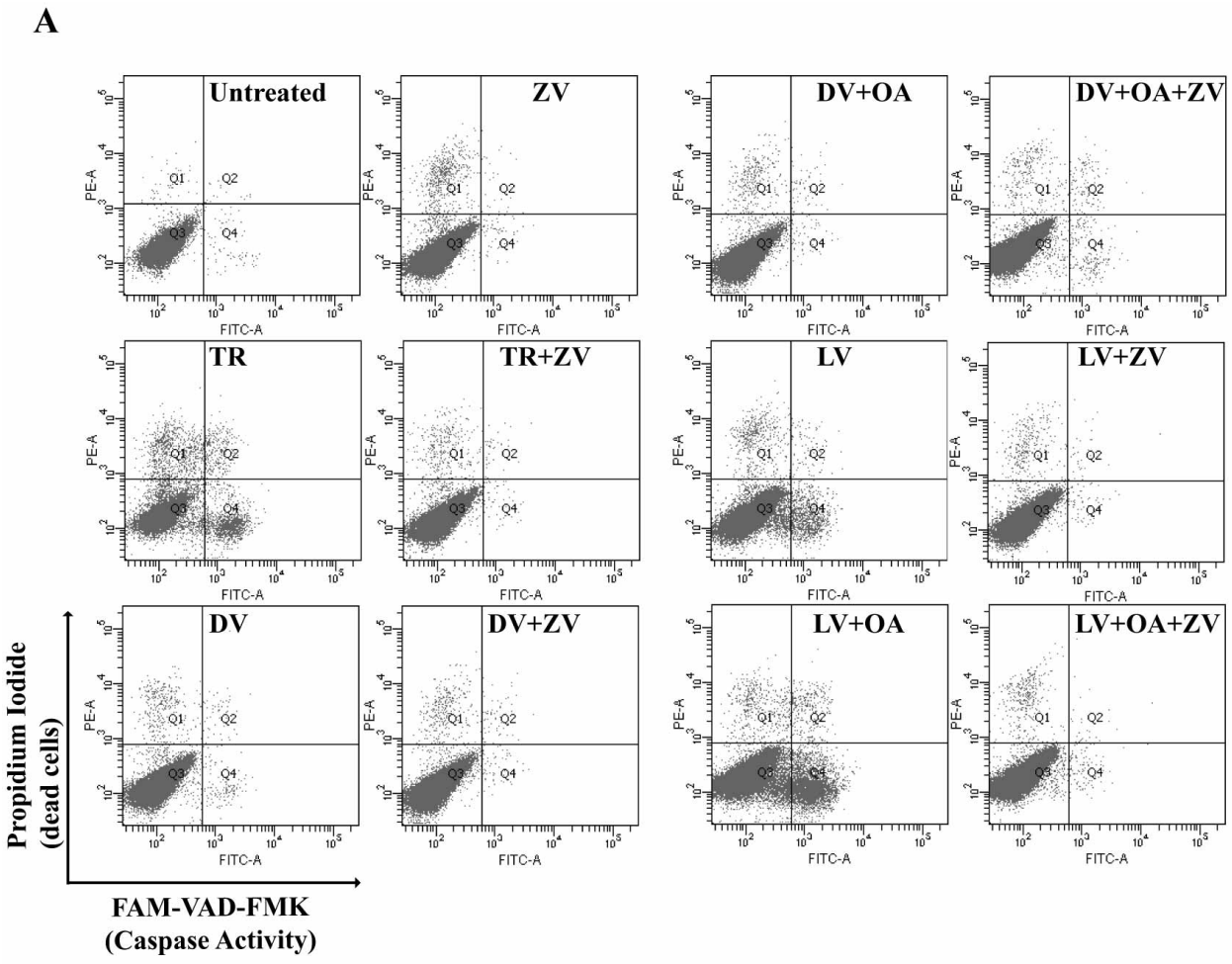
A
Untreated
ZV
DV+OA
DV+OA+ZV
TR
TR+ZV
LV
LV+ZV
DV
DV+ZV
LV+OA
LV+OA+ZV
Q1
Q2
Q3
Q4
PE-A
FITC-A
Propidium Iodide
(dead cells)
FAM-VAD-FMK
(Caspase Activity)

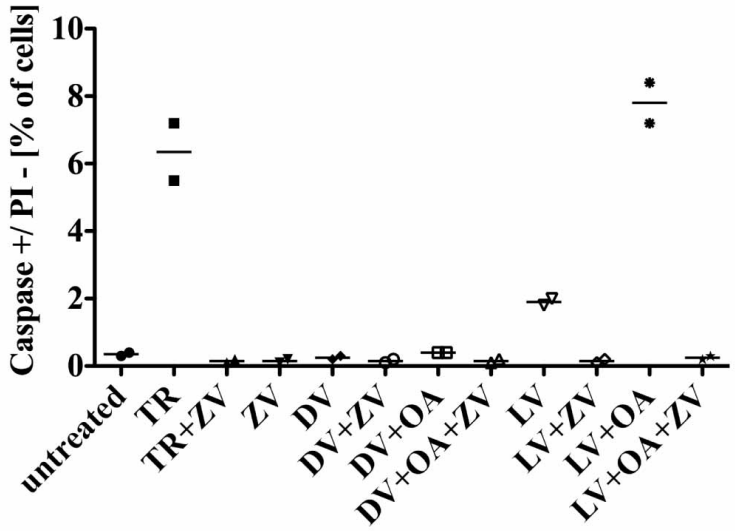
B
Caspase +/ PI - [% of cells]
10
8
6
4
2
0
untreated
TR
TR+ZV
ZV
DV
DV+ZV
DV+OA
DV+OA+ZV
LV
LV+ZV
LV+OA
LV+OA+ZV

Figure 22. Oligomycin Appears to Promote Early Caspase Activation during Reovirus Infection.

A) Pan-caspase activation (FAM-VAD-FMK staining) and non-apoptotic cell death (PI staining) was assessed in HCT116 cells 14 hours post treatment with Oligomycin (OA, 10 nM), dead (DV) or live reovirus (LV, 25 pfu/cell), the pan-caspase inhibitor Z-VAD-FMK (ZV, 50 μM), or the indicated combinations of these agents using the Apo LOGIX FAM-VAD-FMK flow cytometry-based assay. Trail (TR, 2 μg/mL) was used as a positive control for caspase activation.

B) Quantifying Caspase activity +/ PI- cell population (Q4 in **A**) from two experimental replicates. Data points are indicated where the horizontal line represents the mean. n=2.

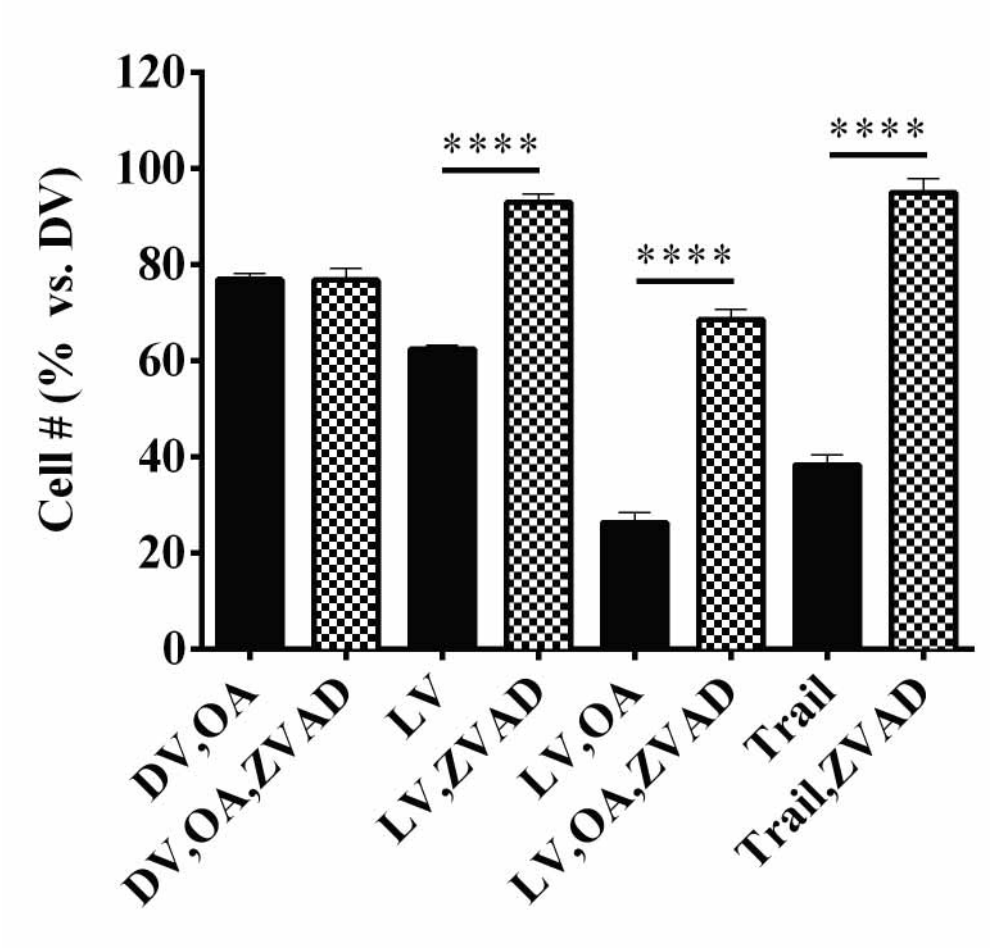
Cell # (% vs. DV)
120
100
80
60
40
20
0
****
****
****
DV,OA
DV,OA,ZVAD
LV
LV,ZVAD
LV,OA
LV,OA,ZVAD
Trail
Trail,ZVAD

Figure 23. Caspase inhibition with ZVAD suppresses cell death induced by the combination of Oligomycin and reovirus.

HCT116 cells were pre-treated with ZVAD (100 μM) for 1 hour then infected with 10 pfu/cell (DV or LV) and treated with OA (10 nM) or Trail (2 μg/mL) or the combinations as indicated for 24 hours and cell number was quantified by crystal violet assay. Error bars are SEM. n=3.

3.2.7 Oligomycin Enhancement of Reovirus-Induced Apoptosis Does Not Require BAX or BAK

Previous studies have found that reovirus can induce MOMP leading to caspase-dependent apoptosis independently of the typically essential MOMP effectors BAX and BAK[84]. To test the requirement of BAX and BAK in the enhancement of early caspase activation and cell death observed when Oligomycin is combined with reovirus, isogenic HCT116 wildtype (WT) and $BAX^{-/-}/BAK^{-/-}$ double knockout (DKO) cells were employed. WT and DKO cells were obtained from Dr. David Andrews (University of Toronto) and the DKO cells were generated from a $BAX^{-/-}$ unselected subclone of HCT116 cells subjected to BAK gene targeting by homologous recombination using a recombinant Adeno Associated Virus vector to engineer STOP codons into the BAK genes, preventing functional protein expression (see Methods for more details)[89, 108].

WT and DKO cells were treated with 10 nM Oligomycin or infected with reovirus at 10 pfu/cell, or with the combination treatment for 24 hours, at which point cells were observed inside culture plates using crystal violet staining (**Fig. 24 a(i)**) as well as higher magnification phase contrast microscopy of cells directly before staining procedures (**Fig. 24a(ii)**). WT and DKO cells were similary sensitive to reovirus alone. Interestingly, loss of cell number due to reovirus in DKO cells was similarly sensitized by Oligomycin treatment. This effect was quantified in **Figure 24b**. WT and DKO cells were similarly sensitive to the effects of Oligomycin treatment or infection alone or in combination, as well as the inhibitory influence of ZVAD. Importantly, the positive control Trail treatment induced significant cell death (~55% decrease in cell number compared to control) in WT cells but had no effect in DKO cells, consistent with the requirement for intrinsic BAX/BAK dependent MOMP in efficient apoptosis induction following extrinsic apoptotic stimuli. These data point to a BAX/BAK independent influence of Oligomycin on reovirus-induced apoptosis.

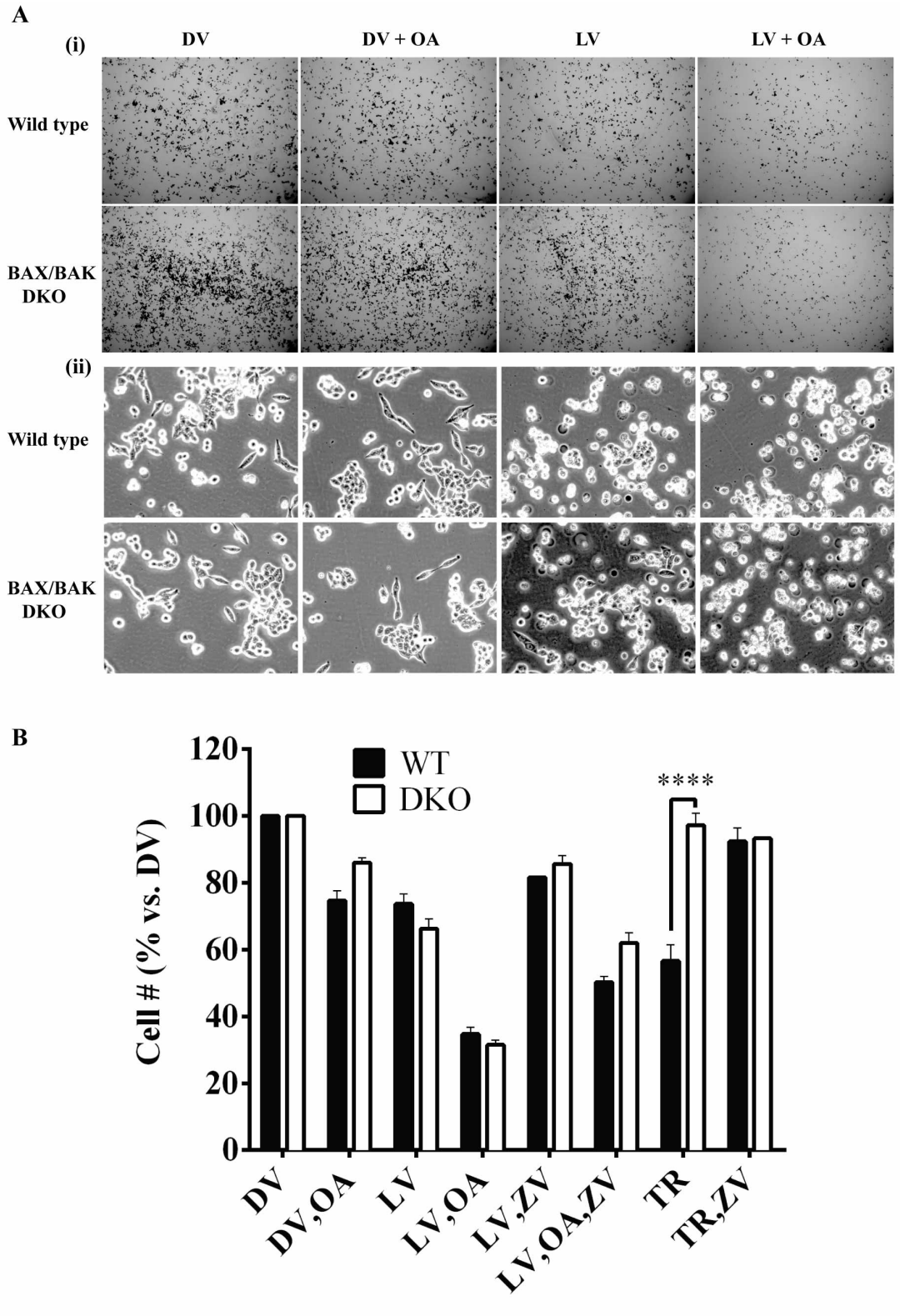
A
(i)
DV
DV + OA
LV
LV + OA
Wild type
BAX/BAK DKO
(ii)
Wild type
BAX/BAK DKO
B
Cell # (% vs. DV)
120
100
80
60
40
20
0
WT
DKO
****
DV
DV,OA
LV
LV,OA
LV,ZV
LV,OA,ZV
TR
TR,ZV

Figure 24. Oligomycin augmentation of reovirus cytolysis is similar in wildtype (WT) and BAX/BAK double knockout (DKO) HCT116 cells.

A) BAX/BAK knockout or wildtype HCT116 cells were infected with 10 pfu/cell dead or live virus and/or treated with OA (10 nM) for 24 hours, and cells were fixed with 3:1 MeOH: Acetic Acid and stained with crystal violet for visualization of cell number using phase contrast microscopy imaging (upper panel (i)). Lower panel is higher magnification images of the same cells immediately before fixing and staining, where cell death induced by live virus alone, and virus plus OA looks similar between WT and DKO cells. n=2, images are representative.

B) Cell number was measured following 24 hour treatment with reovirus and/or OA as above, or Trail (TR, 2 μg/mL) or ZVAD (ZV, 50 μM, cells were pre-treated for 1 hour and during experiment) as indicated in histogram. The combination of Oligomycin and reovirus, or reovirus alone, exhibited similar decreases in cell number. The positive control Trail was the only treatment that was significantly suppressed in DKO cells, as expected. Error bars are SEM. ****$p<0.0001$ using t test between WT and DKO cells for each treatment. n=3.

3.2.8 Combination of Oligomycin and Reovirus May Be an Effective Enhancer of Cell Death in Reovirus-Sensitive Cells

The above data suggest that Oligomycin promotes reovirus-induced apoptosis and cell death in HCT116 cells, possibly suggesting a novel strategy for promoting the anticancer effects of reovirus. However, it was unclear how Oligomycin might influence the anticancer effect of reovirus in cell lines that were differentially sensitive to reovirus infection. Using a panel of cell lines representing low reovirus sensitivity (HT29, MKN74 cells), medium sensitivity (TE1, HeLa, MKN1), or high sensitivity (HCT116, L929, DLD1, GCIY, TE8), the influence of reovirus, Oligomycin, or the combination on cell number over 4 days of treatment was assessed by CV assay, **Figure 25**. At the doses used, reovirus alone decreased cell number considerably, and completely in 4 of 5 high sensitivity cell lines. It was thus difficult to elucidate any influence of Oligomycin combination in these cell lines, and future experiments should use lower doses of viruses to elucidate a contribution from Oligomycin in these cell lines. In moderately sensitive cell lines reovirus induced very large decreases in cell number. Oligomycin, which alone decreased cell number to variable extents among cell lines (presumably through suppressed proliferation), appeared to promote loss of cell number in combination with reovirus. However, using 1-way ANOVA to compare treatment means on Day 4, cell number was not significantly different between LV,OA and both LV,EtOH and DV,OA controls. In the low reovirus sensitivity group, Oligomycin also appeared to promote reovirus-induced loss of cell number compared to either agent alone, but this effect was not statistically significant. The most notable combination was observed in the low reovirus sensitive HT29 colon cancer cell line. As seen in **Figure 25**, reovirus alone or Oligomycin alone had little influence on HT29 cell number over four days of treatment, however the combination of these agents seemed to show a large decrease in cell number over four days compared to controls. However, as only n=2 was performed for HT29, no statistical difference could be accurately assessed. From these data it should be noted that there was no obvious relationships between reovirus sensitivity, Oligomycin sensitivity, or sensitivity to combination treatment. Oligomycin appeared to suppress cell proliferation to different extents, but this was not clearly related to its ability to promote reovirus cytolysis.

Low Reovirus Sensitivity

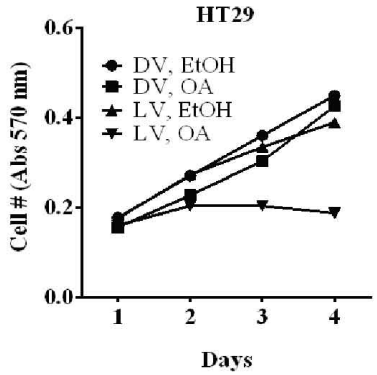

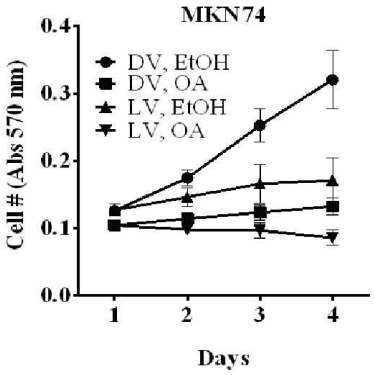

Medium Reovirus Sensitivity

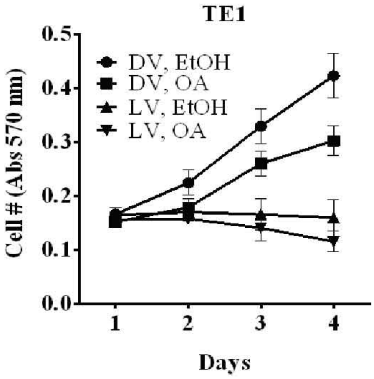

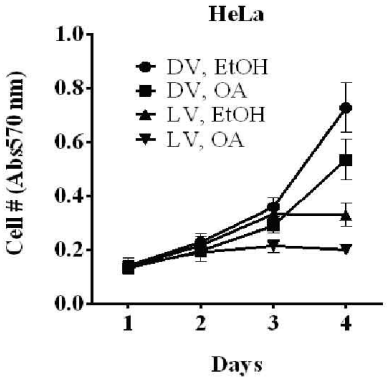

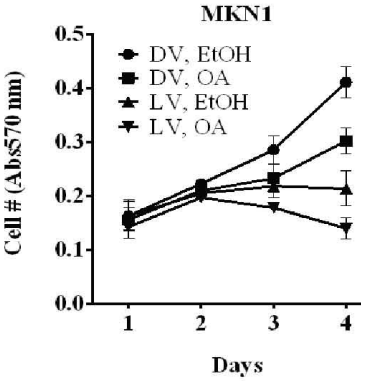

High Reovirus Sensitivity

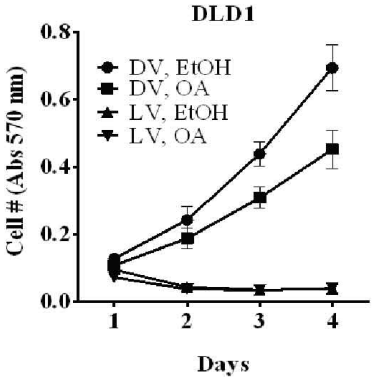

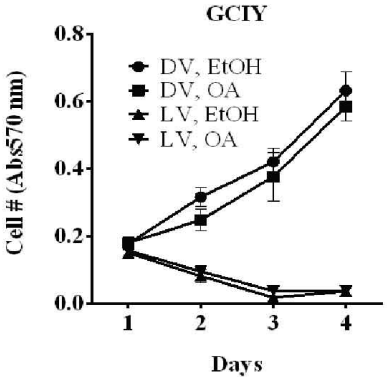

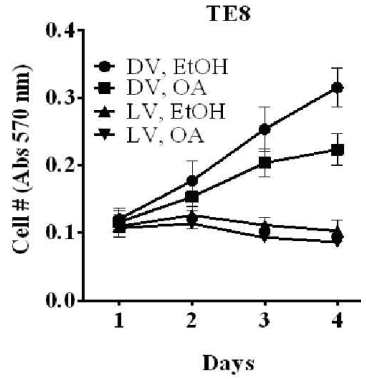

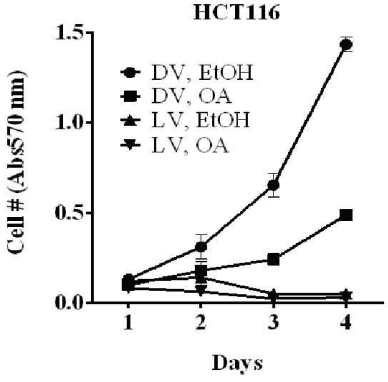

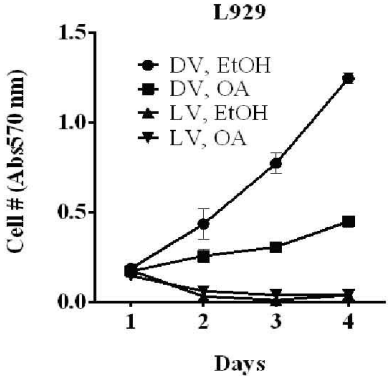

Figure 25. Oligomycin Has a Variable Influence on Reovirus-Induced Anticancer Effects in Cancer Cell Lines of Variable Reovirus Sensitivity.

On day 0 cells were infected with LV or DV control, treated with OA (10 nM) or EtOH control, or the combination, and cell number was quantified by crystal violet assay on each of the next four days. The following cell lines were infected with 10 pfu/cell: HCT116, L929, GCIY, DLD1, and MKN1. All other cell lines were infected with 100 pfu/cell. Using ANOVA to compare treatment means on day 4 revealed that LV,OA was not significantly different from both LV,EtOH and DV,OA controls. Error bars are SEM. n=3 for all cell lines except HT29 (n=2). Note that for data points where error bars do not appear is because the software program used (GraphPad Prism 5) does not display error bars when they are smaller than the size of the symbol used. Therefore in all cases where n=3 and data points appear to be lacking error bars, these data points have very small error bars that are omitted by the program.

Chapter Four: **DISCUSSION**

4.1 Discussion of AIM 1: Priming Apoptotic Pathways Enhances Reovirus Cytolysis

4.1.1 Reovirus in Pediatric Leukemia Cell Lines

Pediatric leukemia cell lines were evaluated as a model system for AIM 1. Flow cytometry analysis of JAM-A expression supported that the majority (5/6) of cell lines, but not the CEM cell line, should allow reovirus entry (**Fig 5)**. Detection of *de novo* reovirus protein synthesis by Western Blot demonstrated that all 6 cell lines appeared to support reovirus protein synthesis, though to different extents (**Fig. 6a**). Here, it was surprising to find that CEM cells appeared capable of supporting a low level of reovirus protein synthesis above the DV and 1hr LV controls. Since these cells appeared to lack JAM-A (n=2), we would expect that these cells could not support reovirus entry and thus infection and viral protein synthesis. Although we did not investigate this further, one possibility is that the detectable protein expression is a result of a very low level of virus entry and infection in a few CEM cells. In line with this possibility, in other experiments using immunofluorescent detection of reovirus proteins in JAM-A negative, non-transformed HS68 fibroblasts, I observed a very low frequency of infection (estimated ~1 in 1000 cells) (data not shown). Despite the observed low level of viral protein synthesis, there was no detectable level of infectious progeny virus in these cells (**Fig. 6b)**, suggesting that the majority of cells are inefficiently infected. The other pediatric leukemia cell lines supported significant reovirus replication to varied levels, **Figure 6b**.

Active RAS pull-down assays (**Fig. 5b**) did not support a clear correlation between RAS activity and efficient reovirus oncolysis in pediatric leukemia cells. Although signaling through the RAS pathway has been suggested as a primary determinant in susceptibility to reovirus[14, 18], other studies suggest that efficient reovirus oncolysis may be mediated by other factors, including cell entry, efficient proteolytic disassembly and tumor suppressor status[21, 22, 26]. Therefore, factors other than JAM-A expression and RAS activation likely play a role in susceptibility of pediatric leukemia cell lines to reovirus infection. However, it should be noted that our assessment of active RAS would only detect elevated signaling upstream or within the RAS protein and does not assess downstream signaling that could impinge on reovirus oncolysis.

These data suggested that 5/6 pediatric leukemia cell lines appear to support reovirus infection and production of progeny virus. As efficient reovirus infection induces cytolysis of cancer cells, we wanted to investigate the ability of reovirus to kill pediatric leukemia cells. Cell morphology visualized by microscopy demonstrated abundant cell debris and membrane blebbing in 4/6 of the cell lines following infection with reovirus, **Figure 7a**. Quantification of cell survival demonstrated that reovirus induces cytolysis in 4/6 cell lines. Reovirus typically induces apoptosis in efficiently infected cells, and we found PARP cleavage by Western Blot, a marker of apoptosis, in 4/6 cell lines following infection (**Fig. 7c**). This was consistent with the expected mode of cytolysis by induction of apoptosis, however using a single marker of cell death is not conclusive evidence. Other apoptosis markers such as caspase-3 activity, DNA fragmentation, or inhibition of cell death and PARP cleavage using a caspase inhibitor (such as Z-VAD-FMK used in later studies) would have provided further support for induction of apoptosis.

These data support that at least some pediatric leukemia cells might be targeted by reovirus therapy, and that further preclinical *in vivo* studies are warranted to investigate this possibility. Of note, our data suggest that confirming cell surface expression of JAM-A in leukemia cells would be one important determinant in the decision to treat patients, and agrees with the literature that supports a requirement of JAM-A for efficient reovirus infection[134-136]. We expect that many pediatric leukemia cell lines might support reovirus targeting, as JAM-A is ubiquitously expressed in the human body and in most cancer cells, and is typically required to initiate infection with wildtype reovirus[133].

One interesting finding from these initial studies was that Jurkat cells were resistant to reovirus-induced cytolysis despite supporting reovirus replication to comparable levels as observed in some cytolysis-sensitive cell lines. In follow up experiments it was noted that infection with a dose higher than 100 pfu/cell led to efficient death of Jurkat cells (data not shown). Our studies and others have shown that higher initial doses of reovirus lead to faster, and sometimes more extensive apoptosis in cancer cell lines. This likely reflects both virus replication-independent and replication-dependent effects, because viral load during infection preceding replication initiates proapoptotic signaling, but UV-inactivated virus (incapable of replication) at all but extreme (1000 pfu/cell or higher) doses, does not induce apoptosis[33]. It is

currently unclear why Jurkat cells support such a high level reovirus infection but resist infection-induced apoptosis. Our studies did not further explore reovirus infection in this cell line, but future study employing Jurkat cells might help identify links between reovirus replication and apoptosis. Generally speaking, differential cytolytic responses to equivalent reovirus replication and the dose-dependent effects of reovirus infection likely play a role in the variable clinical responses observed with oncolytic reovirus, where efficiency of reovirus delivery to tumor, virus replication within tumor, and the characteristics of a given tumor regulate the antitumor efficacy of reovirus. Further study to elucidate mechanisms controlling efficient reovirus infection and cytolysis in cancer cells is needed.

An important consideration for treating patients is the safety of a given treatment. In the context of reovirus therapy, reovirus has been reported not to harm PBLs or hematopoietic progenitor cells *in vitro* or *in vivo*[122, 123] and demonstrates an excellent safety profile in clinical trials[34]. Furthermore, a clinical trial has been initiated to explore the safety of using reovirus in pediatric patients with solid tumors, which is expected to provide evidence for the safety of reovirus in pediatric cancer patients. Our studies only tested reovirus infection in peripheral blood lymphocytes. We did not investigate other important 'normal cell' controls such as donor-derived hematopoietic stem cells, cultured skin fibroblasts, or reovirus infection in mice, which would more completely address the safety of reovirus in normal tissues. Future study should confirm previous similar studies demonstrating the relative safety of reovirus in these systems.

In our experiments with PBLs, we confirmed the inability of reovirus to replicate in these cells (**Figure 8**). However, we did note reovirus-induced cytolytic effects in an adherent cell population present following PBL isolation. It is possible that these are adherent monocytes carried over during PBL isolation, but this was not confirmed in our studies. The identity of these cells could be determined using cell surface markers by flow cytometry, or by monitoring the ability of these cells to differentiate into dendritic cells or macrophages in response to cytokines, which would also be assessed by flow cytometry. Precisely how these findings relate to the safety of reovirus oncolytic therapy is uncertain. Reovirus infection-induced injury of normal tissues is known. Previous studies have documented reovirus infection-induced tissue injury in immunocompromised mice[137], as well as replication and cytolysis in embryonic stem cells[138]. These studies clearly demonstrate that reovirus is capable of infecting normal tissues. To our

knowledge, this is the first indication that reovirus may be harmful to monocytes *in vitro*. If these cells are monocytes, it is known that the process of monocyte adherence is associated with activation of proto-oncogenes[139], and these changes might promote efficient reovirus infection in a similar manner to cytolysis in cancer or stem cells. However, many questions remain about how reovirus kills both cancer and stem cells, and further study is needed and might be very insightful for regulation of reovirus infection. Notably, further study to identify these adherent cells and characterize reovirus infection in this cell population might also be very useful for our understanding of reovirus infection. Although we do not understand why reovirus harms these adherent cells *in vitro*, despite the known harms on normal tissues in immunocompromised mice, the established safety profile of reovirus in clinical trials in adults is supportive of continued use and optimization of reovirus-based cancer therapy.

These experiments characterized the response of pediatric leukemia cell lines to reovirus infection. It was observed that some cell lines were susceptible to reovirus oncolysis, including those representing high risk disease for which novel therapy is of particular importance. Importantly, pediatric leukemia cell lines were susceptible to reovirus infection and thus were an appropriate model in which to test AIM 1, where it was hypothesized that priming extrinsic and intrinsic apoptotic pathways would promote efficient reovirus cytolysis.

4.1.2 Priming Apoptotic Pathways Promotes Reovirus-Induced Cytolysis

It is well established that i) reovirus induces apoptosis[33], ii) chemotherapy and radiotherapy function primarily by inducing apoptosis in cancer cells[81], and enhanced apoptosis underlies beneficial combinations of reovirus with chemotherapy[77-79] and radiation[80] *in vitro* and *in vivo*. Clinical trials with oncolytic reovirus in combination with chemotherapeutic agents demonstrate improved frequency and efficacy of patient response compared to reovirus monotherapy[34]. The future clinical use of reovirus, as well as other oncolytic viruses, will be as an adjuvant alongside other chemotherapy[3]. Therefore it is important to elucidate the cellular targets of chemotherapy that promote efficient reovirus oncolysis.

We hypothesized that directly targeting the extrinsic and intrinsic pathways of apoptosis would promote reovirus oncolysis. Using three reovirus susceptible pediatric leukemia cell lines, we studied the influence of low doses of the extrinsic apoptosis ligand TRAIL or the BCL-2

inhibitors (BH3 mimetics) ABT-737 and Obatoclax on reovirus cytolysis (measured as cell viability). Generation of dose-response curves for reovirus alone, or in combination with a low dose of each proapoptotic agent, and observing the IC50 shift between these curves, was used to determine the combinatorial effect of virus-drug combinations. Combination Index analysis was used to measure the nature and extent of reovirus-drug interactions[110]. As hypothesized, combining a low dose (IC_{10} or IC_{25}) of ABT-737, Obatoclax, or TRAIL with reovirus promoted reovirus-induced cytolysis in the majority cases (**Figure 8** and **Table 2**). ABT-737 combined with reovirus demonstrated a synergistic decrease in cell survival in 3/3 cell lines. Obatoclax demonstrates synergy with reovirus in B1 and TIB202 cells and additive effects in MOLT3 cells. Combining TRAIL with reovirus was synergistic in B1, additive in MOLT3, and antagonistic in TIB202 cells. Taken together, the combination of low doses of proapoptotic agents with reovirus synergistically enhances cell killing in the majority (6/9) of combinations tested, while 2/9 combinations were additive, and only 1/9 was antagonistic. These data support the hypothesis that priming apoptotic pathways can promote reovirus infection in pediatric leukemia cell lines by tipping the balance within the BCL-2 family towards apoptosis.

The combination of proapoptotic drugs ABT-737 or Trail with reovirus to promote cell killing was associated with enhanced induction of apoptosis as measured by Western Blot analysis of apoptotic markers in B1 cells (**Figure 11**). These data are consistent with idea that enhanced apoptosis underlies the synergistic combination of proapoptotic drugs with reovirus in pediatric leukemia cells. Importantly, it should be noted that only the B1 cell line was investigated, and it would be important to detect enhanced apoptosis markers with other drug/virus combinations and in other cell lines in future studies.

The addition of ABT-737 or TRAIL to reovirus infection did not significantly affect reovirus replication in this cell line as measured by Western Blot and Plaque Assay (**Figure 11**). Therefore it appears that priming apoptotic pathways does not significantly influence reovirus replication, though this should be confirmed in other cell lines. It is important that reovirus-based strategies, including this potential new strategy combining proapoptotic drugs, maintain efficient reovirus replication because one very important beneficial aspect of oncolytic reovirus is self-propagation and spread through tumors. Taken together, these data support the idea that

proapoptotic drugs may be a useful strategy to enhance reovirus cytolysis in pediatric leukemia cells. This warrants further preclinical investigation *in vivo*.

As a first step toward addressing the potential broad applicability of this strategy for other cancer types, combination studies were extended to other cancer cell types. The combinatorial influence of ABT-737, Obatoclax, and TRAIL on reovirus infection in the highly reovirus-sensitive HCT116 colorectal cancer cells and in the moderately reovirus-sensitive HeLa cervical cancer cells was analyzed (**Figure 12**). These experiments demonstrated that addition of proapoptotic drugs to reovirus infection could i) reduce the amount of reovirus required to decrease cell number and ii) promote markers of apoptosis induction as measured by Western Blot, without negatively influencing reovirus replication. These results are consistent with our hypothesis that priming apoptotic pathways can promote reovirus cytolysis, likely through stronger and/or more widespread induction of apoptosis in cancer cells, and suggest that this strategy may be applicable to multiple cancer types. Of note, in these experiments it was observed that a low (IC_{10} ~50 nM) dose of Obatoclax combined beneficially with reovirus as it decreased the amount of reovirus required to reduce HCT116 cell number, measured by a leftward shift in the dose-response curve for reovirus at 72 hpi (**Figure 12**). However, a higher dose (1 μM) of Obatoclax (used in Western Blot analysis in HeLa cells at 24 hpi) completely suppressed reovirus replication and cell death. Further experiments (not shown) were consistent with a report showing that high doses of this drug inhibit the activity of lysosomal cathepsins[127] that are required for proteolytic disassembly during reovirus infection[22]. This off-target strong inhibitory effect of Obatoclax on reovirus infection at high doses is an important finding, and suggests that only lower doses of this drug, or perhaps other proapoptotic drugs altogether, might be the focus of future study in combination with reovirus for cancer therapy.

The combination of reovirus with low doses of chemotherapeutic drugs Methotrexate or Vincristine did not demonstrate synergy in our experiments and in our experiments these combinations were additive or mildly antagonistic (**Table 2** and **Figure 10**). This is in contrast to other studies that have found synergy between reovirus and commonly used chemotherapeutic agents. Pandha et al. 2009 reported synergy between reovirus and various chemotherapeutic agents in a melanoma cell line, although this study did not assess Methotrexate or Vincristine[77]. Heinemann et al. 2011 found synergy between reovirus and Vincristine (as well as other

common chemotherapy agents) in prostate cancer cell lines[140]. Sei et al. 2009 demonstrated synergy between reovirus and vinblastine in some but not all lung cancer cell lines and drug/virus doses tested[79]. Our studies only assessed the influence of a single dose of drug on reovirus infection, thus we cannot exclude potential combination effects that might be observed at other drug-virus combinations or time points in leukemia cell lines. Further, as clinical use of reovirus is as an adjuvant to chemotherapy[34], further study on reovirus with these and other chemotherapy drugs used in the clinic for pediatric leukemia patients, without and with the addition of proapoptotic drugs, will be important to further characterize the potential for priming apoptotic pathways in enhancing reovirus-based therapy in pediatric leukemia. A similar approach could be taken for numerous other cancer types where enhanced apoptosis already underlies the synergistic combinations between reovirus and various chemotherapeutic agents.

4.1.3 Relevance of Work: Is Priming Apoptotic Pathways in Reovirus Infection a Plausible Anticancer Strategy?

Priming the apoptotic pathway to enhance reovirus infection was accomplished by stimulating the extrinsic pathway (TRAIL) or by modulation of the BCL-2 family of proteins with proapoptotic BH3 mimetic drugs (ABT-737 and Obatoclax). This strategy is in contrast to the combination of chemotherapeutic drugs with reovirus. Although chemotherapy usually induces apoptosis to eliminate cancer cells[81], this occurs indirectly downstream as a consequence of the pleiotropic effects of these agents. Reovirus oncolysis requires efficient replication within cancer cells, which is reliant on functional cellular processes including transcription, translation, and energy production. Therefore, it may be that chemotherapy drugs with pleiotropic effects on the cell and its normal functions are not ideal agents for combination with reovirus. Our hypothesis that directly priming apoptotic potential would promote reovirus cytolysis was based on the knowledge that reovirus induces apoptotic signaling involving both extrinsic and intrinsic pathways. Reovirus-induced apoptosis ultimately culminates at the mitochondria, involves BCL-2 proteins, and leads to the release of mitochondrial IMS proteins facilitating cellular disassembly. Therefore, direct priming of either extrinsic or intrinsic apoptotic pathways during reovirus infection might potentiate this pathway and promote reovirus cytolysis without significantly affecting reovirus infection. Importantly, this approach may be beneficial for

decreasing toxicity because only low doses of these proapoptotic agents are needed to synergistically enhance reovirus cytolysis, and the strong selectivity of reovirus for cancer cells is already associated with an excellent safety profile in clinical trials[34].

A report by Chonghaile et al. 2009 found that mitochondrial priming, which is "the pretreatment proximity of tumor cell mitochondria to the apoptotic threshold", correlated with clinical response to chemotherapy[141]. An important conclusion from this paper was that the use of agents that increase mitochondrial priming in cancer cells, even at sublethal doses by themselves, might enhance the response of tumors to conventional chemotherapy agents. Our data support that this strategy would also be beneficial for reovirus-based therapy, at least in the context of pediatric leukemia. A study by Vo et al. 2012 implicated mitochondrial priming as a primary determinant of response to chemotherapy and relapse in AML patients, and suggested that direct targeting of the antiapoptotic BCL-2 proteins, for instance by using the BH3 mimetic drugs ABT-737 or Obatoclax, would have therapeutic benefit[142]. Further, BCL-2 inhibition was found to be an effective approach for targeting primary leukemia stem cells from AML patients[143]. Work from our collaborator (Dr. Narendran, University of Calgary, Canada) has already demonstrated the potential for targeting BCL-2 inhibition in pediatric ALL[144, 145], and other groups have come to the similar conclusion that targeting the apoptotic pathway with BCL-2 inhibitors in combination regimens should have clinical benefit for pediatric acute leukemia patients[146-148].

Resistance to apoptosis is one of the hallmarks of cancer[61] and this can be achieved by overexpression of antiapoptotic BCL-2 family members. Indeed, dysregulation of BCL-2 family members is a common occurrence in hematological malignancies[149]. Thus it is not surprising that targeting the BCL-2 proteins for anticancer efficacy has been extensively investigated and found to be effective in pre-clinical *in vitro* and *in vivo* studies[150]. Promising pre-clinical activity has led to the clinical evaluation of these agents, including ABT-263 and Obatoclax. Clinical study of ABT-263, the orally bioavailable derivative of ABT-737, has yielded substantial clinical benefit in patients with CLL, especially in combination regimens, though benefits for patients with small-cell lung cancer were limited, suggesting an enhanced activity toward hematological malignancies. However, due to common high grade 3-4 thrombocytopenia at high doses in these patients, ABT-263 hasn't been explored clinically in acute leukemia. Abbot laboratories is

currently introducing ABT-199 for clinical use which has increased affinity for BCL-2 and decreased affinity for BCL-XL, which should relieve the high grade thrombocytopenia while maintaining or enhancing anticancer efficacy, with a primary goal of enabling clinical study of ABT-199 for acute leukemias[151]. As ABT-199 still causes apoptosis induction in a similar fashion to ABT-737 and ABT-263, we would expect that combining reovirus with this drug would retain synergistic killing of pediatric leukemia cells, and therefore may present exciting clinical potential. Future study of reovirus in combination with ABT-199 in mouse models of acute leukemia will be important to validate the synergistic killing we observe *in vitro*.

Obatoclax was designed as a pan-BCL-2 protein inhibitor and has been evaluated in clinical trials. Obatoclax has demonstrated limited objective responses against CLL, SCLC, and lymphoma in Phase I trials, though a phase II trial showed no clinical benefit when Obatoclax was used with carboplatin and etoposide in late-stage SCLC patients. Another phase II trial against lymphoma and myelofibrosis found no significant single agent activity of obatoclax. Emerging data from other phase I/II clinical trials suggests that the full potential of Obatoclax will be realized in combination regimens with other anticancer agents[150]. Importantly, it should be noted that although Obatoclax was designed as a pan-BCL-2 inhibitor, it is able to induce cell death independently of BAX/BAK, suggesting multiple mechanisms of action. This is in part reflected by the lack of clinical high-grade thrombocytopenia, which is a clinical marker of BCL-XL inhibition. Recent work has demonstrated reduced expression levels of cathepsins B, D, and L protein following Obatoclax treatment through an unknown mechanism, leading to inhibition of autophagy[127]. These off-target effects of Obatoclax may explain the modest clinical efficacy when compared to ABT-263.

Our experiments showed that the synergy observed between reovirus and ABT-737 was associated with enhanced apoptosis, however we did not assess apoptosis induction in the combination of Obatoclax and reovirus. Another mechanism that could be playing a role in the Obatoclax combination is modulation of autophagy. A recent study suggested that, in addition to apoptosis, reovirus infection induced autophagy in a multiple myeloma cell line; however, whether this induced autophagy was necessary or even involved in cell killing is unclear[123]. It should also be noted that the cathepsin proteins whose activity is reduced by Obatoclax treatment are also involved in endo/lysosomal degradation following endocytosis. This could impact the

ability of reovirus to combine favorably with Obatoclax, as reovirus entry into cells is mediated by endocytosis and requires cathepsin activity for successful infection[22]. Indeed, we have found that high doses of Obatoclax almost completely inhibit reovirus replication and oncolysis in multiple cancer cell lines. If and how modulation of autophagy affects cell survival in reovirus-Obatoclax combination treatment is unclear. Given the nonspecific mechanisms of action by Obatoclax, future study on priming apoptotic pathways in combination with reovirus infection should focus on those agents with more specific and exclusive targeting of the apoptotic pathways, such as ABT-199.

TRAIL-based therapy using either human recombinant hrTRAIL or more commonly DR4/DR5 agonistic antibodies have shown potent anticancer efficacy *in vitro* and *in vivo*, while showing little toxicity, and have been studied in clinical trials[152]. However, resistance to TRAIL signaling in many primary tumors has limited the clinical efficacy of these agents. It is proposed that TRAIL sensitization can be accomplished by modulating the TRAIL signaling pathway. Agents that would promote TRAIL activation include those that lead to upregulation of death receptors 4 and 5 expression. Another way to enhance TRAIL sensitivity is to promote amplification through the mitochondrial pathway of apoptosis by shifting the balance within the BCL-2 family towards apoptosis, such as by using agents like ABT-737 that inhibit antiapoptotic BCL-2 family proteins, or using agents that upregulate proapoptotic BCL-2 family members. Relevant to this notion, reovirus infection has been shown to be mediated by TRAIL, to enhance release of TRAIL from infected tumor cells, to enhance expression of DR4/5, and increase expression or activation of proapoptotic BCL-2 family proteins (NOXA, tBID) leading to induction of apoptosis in a highly cancer cell selective manner[33]. Our data show that combining TRAIL with reovirus can act additively or synergistically to promote reovirus cytolysis in at least some (2/3) pediatric cancer cell lines. It has previously been found that reovirus infection can sensitize TRAIL-resistant gastric cancer cells to TRAIL treatment[129]. Although our findings here found that Trail appears to have cell line specific combinatorial effects with reovirus, future study altering the timing or dosing might reveal improved combination effects of these agents. I suggest that the combination of TRAIL (or possibly DR4/DR5 agonistic antibodies) with reovirus might yield mutually beneficial anticancer effects in a wide range of cancers, including

those that display resistance to either agent as a monotherapy, and further *in vitro* and mouse studies of this combination in different cancer types including pediatric leukemia are warranted.

Together, our data show that some pediatric acute leukemia cell lines can be targeted and killed by reovirus, with greater efficacy when combined with apoptosis-inducing agents in the majority of combinations tested. It remains to be seen whether this combination strategy is more widely applicable to numerous other cell lines or if it would be useful against *in vivo* models of acute leukemia, but our data would suggest positive responses. Although our *in vitro* data are promising, they also exposed two issues that arise in clinical use of reovirus. First, differing sensitivity to cell killing following equivalent reovirus infection is likely at least one factor underlying variable patient responses. Second, we found that one cell line lacked expression of the receptor for reovirus JAM-A, which may prevent efficient infection although this was not investigated. Currently, we lack efficient biomarkers predicting sensitivity to reovirus, but our data and the literature supports that cancer cells require JAM-A to initiate efficient infection with reovirus. Due to the feasibility of obtaining cancerous cells from leukemia patients, we suggest that assessment of JAM-A expression on patient cancer cells should be at least one pre-requisite for administration of reovirus-based anticancer regimens in future clinical trials for pediatric acute leukemia patients.

Apoptotic priming combined with reovirus can effectively kill pediatric leukemia cell lines, suggesting that these cells are dependent on balance within the BCL-2 family proteins to decide life or death. It may be that a certain ratio between pro- and anti-apoptotic BCL-2 proteins predicts sensitivity to reovirus combination treatments. This could be extremely useful as a clinical biomarker for response to reovirus alone or in combination regimens, however, to our knowledge this has not yet been investigated.

Reovirus and chemotherapy drugs sometimes demonstrate synergy against cancer cells in other studies *in vitro* and in mice, whereby one or both anticancer agents attain a mechanistic benefit leading to increased cancer cell killing. However, here we found that reovirus did not demonstrate synergy with methotrexate or vincristine, drugs currently used in the treatment of pediatric leukemia patients. It is important to note that this does not necessarily mean reovirus cannot be used effectively with these agents. It is possible that altering the concentration of drug used with reovirus or the length of treatment could yield enhanced killing of cancer cells. On the

other hand, there is no clear mechanism or model that predicts how these agents interact with reovirus infection. Methotrexate is an antifolate drug causing inhibition of DNA, RNA, and protein synthesis, while vincristine is a microtubule destabilizer causing cell cycle arrest. These agents have various effects within the cell, making interpretation of the interaction with reovirus infection difficult. Despite this, it is likely that clinical introduction of reovirus-based therapy in pediatric leukemia patients will be as an adjuvant to chemotherapy. In this regard, it is encouraging that our data show mostly additive effects on cell killing when reovirus is used with methotrexate or vincristine, which may still offer the potential for decreased toxic doses of chemotherapy and increased anticancer effect. More importantly, we would predict that addition of proapoptotic drugs to prime cancer cells towards death would further promote the combinatorial actions of chemotherapeutic agents and reovirus. Further *in vitro* study is needed to elucidate these possibilities, and *in vivo* cancer models will be important to evaluate the potential of this novel reovirus-based anticancer strategy.

4.1.4 Limitations of AIM 1

One limitation in AIM 1 was that certain experiments including flow cytometry analysis of JAM-A expression and Western Blots in AIM 1 were performed at n=2, with the exception of Western Blot analysis of reovirus protein levels following infection of PBLs that was performed at n=3. Having only two replicates of experimental results does not allow statistical analysis to be performed to compare treatments. Although n=2 replicates may hint at a phenotype or result, typically n>2 is performed to ensure data reproducibility and allow stronger conclusions to be made based on the data. Future work should increase the number of experimental replicates to allow for stronger and more appropriate conclusions.

The combination experiments used in this study investigated the influence of a single, low dose of each proapoptotic or chemotherapy drug on the median effect (IC_{50}) of reovirus at a single time point for each drug. Given this limited approach, it is very encouraging that priming the apoptotic pathway demonstrated synergy with reovirus in the majority (6/9) of cases. However, as noted above for chemotherapy drugs, a more complete picture of how proapoptotic drugs interact with reovirus infection in cancer cells would involve i) different ratios of drug and virus, ii) different time points, iii) staggering treatment times of drug and virus, iv) studying

more cell lines, v) cancer cell lines with more varied sensitivity to reovirus, and vi) cancer cell lines from different tissue origins, such as colorectal, lung, breast, pancreatic, skin, ovarian, brain cancer and others for which reovirus is currently in clinical trials. This type of in depth analysis was not conducted here, as our goal was to provide first evidence of the potential utility of combining proapoptotic drugs with reovirus for improved oncolysis. Indeed, our data show that combinations of drugs modulating the extrinsic or intrinsic pathway of apoptosis with reovirus infection can induce synergistic decreases in leukemia cell survival that are associated with enhanced markers of apoptosis.

Another limitation of these studies was a limited analysis of apoptosis induction. Our experiments typically focused on Western Blot markers of apoptosis induction, including cleavage of caspases and PARP. In certain experiments, we also demonstrated suppression of these markers by the caspase inhibitor Z-VAD-FMK, providing further evidence for caspase activity during cell death following infection. Stronger evidence for apoptosis would include detection of cytochrome c release (or other proapoptotic proteins) from the mitochondrial intermembrane space measured by Western Blot or immunofluorescence, detection of phosphatidylserine exposure on the cell surface by flow cytometry using Annexin-V staining, and confirmation of DNA fragmentation by DNA gel electrophoresis or TUNEL staining. Together, this would provide stronger evidence for apoptosis induction during reovirus infection in pediatric leukemia and other cell lines, and as a mechanism underlying additive or synergistic combination effects when combined with proapoptotic drugs.

4.1.5 Conclusions from AIM 1

In conclusion, our data support that the cancer-selective oncolytic reovirus can infect, replicate in, and kill some pediatric leukemia cell lines. Reovirus oncolysis requires entry into cells and is dependent on virus replication. Combining apoptosis-inducing drugs with reovirus infection results in synergistic killing of pediatric leukemia cell lines, supporting targeting of the apoptotic pathway in treating pediatric leukemia. For the first time, our data introduce reovirus as a novel therapeutic strategy for pediatric leukemia, and I argue that this warrants further pre-clinical study *in vivo*. Further, our data hint at the potential broad applicability of priming

apoptotic pathways in promoting efficient reovirus oncolysis as an anticancer strategy for this and other cancer cell types.

4.2 Discussion of AIM 2: Probing Mitochondrial Function in Reovirus Cytolysis

4.2.1 Low Glucose Adaptation Yields Resistance to Reovirus Cytolysis

Reovirus is selective for efficient replication and induction of apoptosis in cancer cells. Although mitochondria are key to metabolic and cell death processes, are dysregulated in cancer cells, and reovirus-induced apoptotic signaling culminates at the mitochondria, no study has specifically asked whether mitochondrial (dys)function in cancer cells might regulate or be exploited for reovirus infection. To begin to explore this intriguing possibility, we hypothesized that modulating mitochondrial function by manipulating metabolism in cancer cells would impact on efficient reovirus infection.

One method of manipulating metabolism and mitochondrial function is glucose deprivation[97].Depriving cells of glucose in the presence of other oxidizable substrate, such as glutamine or pyruvate leads to a number of changes in mitochondrial networking leading to increased and necessary mitochondrial respiration and ATP synthesis. Other methods to push cellular metabolism toward reliance and improved function of the mitochondria is through chemical inhibition of glycolysis, such as by using 2-deoxyglucose treatment which inhibits hexokinase. However, because chronic glucose deprivation and its effect on the mitochondria have been well described, and because this treatment was readily available, we chose this method to push cells away from glycolysis and toward reliance on mitochondrial function. In our experiments, HCT116 and HeLa cells were chronically grown in media with 4 mM glutamine but low glucose for over one month, where the only contribution of glucose was from 10% FBS (final glucose concentration estimated to be ~0.1-0.5 mM). Parental cancer cells growing in high glucose (25 mM glucose and 4 mM glutamine) were used as controls to evaluate differences in reovirus infection.

Low glucose adapted cells (LG cells) grew more slowly than control cells when observed under the microscope over time. LG cells also demonstrated altered stress response markers by Western Blot (**Fig. 13a**), suggesting that these cells contained changes in many pathways

following low glucose culture. Adaptation to low glucose conditions probably involved selection for cells that were inherently resistant to metabolic stress, resistant to apoptosis, and/or especially efficient at upregulating compensatory survival pathways, such as autophagy. The observation of numerous vacuoles inside cells (observations under the microscope) alongside Western Blot analysis showing enhanced LC3B-II accumulation in LG adapted cells (**Figure 13**) suggests that these cells had upregulated autophagy. Autophagy is a cell recycling program that contributes to cell survival following nutrient stress, including glucose withdrawal[154]. Reovirus infection induces autophagy in multiple myeloma, but the importance of autophagy, if any, in reovirus infection is unclear[123]. LG adaptation was also associated with stress-related phosphorylation of eIF4E and eIF2α at residues that inhibit their ability to initiate protein translation. It is unclear whether these changes are a result of metabolic switching and we performed no experiments to test this. On the other hand, it is also possible that during LG adaptation, clonal selection for tolerant cells or more adaptable cells took place first, accounting for the observed changes present. Using single cells to initiate LG-adapted cultures and comparing these over time during adaptation by measuring gene expression by microarray and protein expression by Western Blot or antibody array would be insightful, but these experiments were not performed here. Therefore, while LG cells have likely adapted to survive in low glucose conditions, it is possible that numerous adaptations have taken place that might contribute to experimental observations and make interpretation difficult.

No direct experiments were undertaken to confirm metabolic switching in LG cells, and this is a large limitation of this work that prevents strong conclusions to be drawn. Experiments such as measuring oxygen consumption using a Respirometer as a measure of respiration and lactate production using Liquid Chromatography-Mass Spectrometry as a measure of glycolysis would have been useful to confirm metabolic switching more directly. Our approach was indirect, and based on the sensitivity of LG and parental cells to chemical inhibitors of rerpiration and mitochondrial ATP synthesis. The Complex I inhibitor Rotenone and the F_1F_O-ATP synthase inhibitor Oligomycin were found to significantly decrease cell number of LG cells compared to parental cells (**Fig. 13b**). We did not confirm that this decrease was due to cell death, but observations under the microscope showed dying and dead LG cells following treatment with these drugs, while parental cells were not dying and instead appeared to be

proliferating more slowly compared to control treatment. This increased sensitivity to OXPHOS inhibitors, while indirect, provides some support that among other changes in LG cells, these cells are more reliant on mitochondrial function for survival.

HCT-LG cells were significantly more resistant to loss of cell number induced by reovirus infection at 10 and 100 MOI, but not 1000 MOI, while HeLa-LG cells were more resistant at 100 and 1000 MOI, but not 10 MOI, compared to the respective cell lines cultured with glucose (**Fig. 14b**). HeLa cells support a less efficient infection that HCT116 cells, and infection with 10 MOI reovirus likely requires more than 48 hours to induce cytopathic effects in HeLa and HeLa-LG cells.

LG cells apppeared more resistant than parental control cells to reovirus cytolysis when observed under the microscope (**Figure 14a-b**). When quantified, HCT-LG cells were significantly more resistant to loss of cell number induced by reovirus infection at 10 and 100 MOI, but not 1000 MOI, while HeLa-LG cells were more resistant at 100 and 1000 MOI, but not 10 MOI, compared to the respective cell lines cultured with high glucose (**Fig. 14b**). The lack of significant difference between HCT-LG and HCT116 at 1000 MOI may be due to the fact that at this high dose the majority of cells were already dead at the time measured (48h). Although we did not confirm this, using 1000 MOI at an earlier time point such as 24 or 36 hours post infection might show a difference. On the other hand, there was no significant difference in cell number between HeLa-LG and parental HeLa cells at 10 MOI and 48 hpi. It is known that HeLa cells support a less efficient infection that HCT116 cells (viral replication and kinetics of cytolysis are slower in HeLa cells based on some work included in this thesis and other work not shown). At 10 MOI reovirus likely requires more than 48 hours to induce cytopathic effects in HeLa and HeLa-LG cells since cell numbers were equivalent to control dead virus treatment. I would predict that extending the time of infection in these cells at this dose of reovirus would demonstrate a difference between HeLa-LG and HeLa cells, but this experiment was not performed.

Relevant to the above discussion and our results with LG cells, reovirus-induced apoptotic signaling is typically induced at a level relative to viral protein expression, and thus increasing the time of infection at a given dose normally increases cell death. Further, increasing the initial dose of infection allows greater accumulation of viral proteins and increased kinetics

of cell death. Based on this reasoning, it was entirely possible that the apparent suppression of reovirus cytolysis in LG cells was related to less efficient reovirus replication. However, the difference in cell number loss between LG and parental cells following reovirus infection does not appear to be related to any inhibition of reovirus replication, which was equivalent or even enhanced in LG cells compared to control cells (**Fig. 14c**). Therefore our results showing that HCT-LG and HeLa-LG cells are resistant to reovirus-induced loss of cell number at certain doses may be showing that these cells are more resistant to induction of apoptosis, leading to slower kinetics of reovirus-induced cytolysis. However, we would expect that given sufficient time, reovirus infection in either parental or LG cells would eventually lead to cytolysis of nearly all cells. This was not tested. Furthermore, our experiments did not confirm if, or to what extent, apoptosis was induced in parental and LG cells, and this should be included in future work. Future experiments should test multiple levels of apoptosis induction, including cytochrome c release, caspase activation, DNA fragmentation, and sensitivity to caspase inhibition following reovirus infection.

These results suggested that LG adaptation might yield resistance to apoptosis, the pathway normally underlying efficient reovirus cytolysis. Although we did not test apoptosis induction directly in these cell lines during reovirus infection, we treated LG and parental cells with three different drugs known to induce apoptosis (**Fig. 14e**). HCT-LG cells were significantly more resistant to the killing effects of the DNA damaging agent Doxorubicin and the BH3 mimetic Obatoclax, but not the BH3 mimetic ABT-737. Although AB737 and Obatoclax have similar modes of action, their affinities for the proapoptotic BCL-2 family members differ. Obatoclax targets each of the antiapoptotic BCL-2 members with modest affinity, while ABT-737 targets BCL-2, BCL-XL, and BCL-W, but not MCL-1. We did not assess the relative expression of these proteins in control or LG cells, but it is possible that during LG cell adaptation these cells modulated expression of BCL-2 family proteins in a manner that does not respond differentially to ABT-737 treatment but does respond differentially to apoptosis induced by DOX, Obatoclax, and reovirus. For instance, increased expression of MCL-1 or decreased expression of proapoptotic BH3-only proteins that are preferentially sequestered by MCL-1, such as NOXA[71]. Indeed, NOXA has been implicated in mediating apoptosis induced by reovirus[93] and doxorubicin[153]. However is it currently unclear what

mechanism(s) underlie the apparent resistance to reovirus cytolysis and apoptosis drugs in LG cells.

The complex and undefined alterations in LG cells make it difficult to understand how this intended metabolic alteration influences reovirus cytolysis. Although we don't directly confirm metabolic changes in cells, the increased sensitivity of LG cells to OXPHOS inhibitors provides some support for a metabolic switch in these cells. Our data showing that LG cells are resistant to reovirus cytolysis and certain apoptotic drugs is intriguing and weakly suggests an association between metabolic adaptation and resistance to apoptosis that could be relevant to reovirus infection. But support for this idea is incomplete and weak and our analysis lacks many control experiments.

Although our experiments do not properly demonstrate metabolic alterations during LG adaptation or establish how this influences reovirus infection, a previous study using an almost identical approach demonstrated considerable metabolic and mitochondrial changes. A report by Rossignol et al. 2004 performed very similar glucose withdrawal experiments in HeLa cells and demonstrated numerous changes in the mitochondria[97]. In comparison to control HeLa cells grown in 25 mM glucose (as in our study), HeLa cells grown completely deprived of glucose (but with glutamine) for 3 weeks (15 doublings) demonstrated the following characteristics: these cells 1) grew 3X slower, 2) upregulated expression of proteins promoting OXPHOS (pyruvate dehydrogenase, voltage-dependent anion channel, respiratory complexes I, II, IV, V (ATP synthase)), 3) showed no difference in expression of glycolytic genes (HKI, HKII, or GLUT1), 4) showed no change in mtDNA content, 5) had condensed mitochondria, increased matrix density, expansion of cristal spaces (orthodox to condensed transition is representative of activation of OXPHOS), and increased amount of cristal membranes, 6) showed no change in mitochondrial mass, and 7) had mitochondria that were more networked, thinner and spread through the cell and formed filamentous ring-like structures (in glucose, mitochondria were more clustered together, and clustered in a perinuclear fashion and not spread throughout the cell). It was found that these glucose deprived cells had no morphological changes within 1 hour, used most endogenous glucose within 24 hours, demonstrated fully condensed mitochondria within 1 week, and had an altered mitochondrial network only after 2 weeks. This timing suggested that

mitochondrial condensation occurred as cells begin to use glutamine as an energy source, and precedes interconnection of the mitochondrial network[97].

As the glucose withdrawal in this paper was extremely similar to our treatment of HeLa and HCT116 cells, we expect that similar adaptations might have occurred in our LG cells. However, significant experimentation would be required to confirm similar changes in our cells, including Electron Microscopy to study mitochondrial structure. Unfortunately, this study did not address or comment on how these mitochondrial alterations following glucose withdrawal would impact sensitivity to apoptosis. However, highly networked mitochondria with condensed, remodelled matrix structure are associated with enhanced respiration and ATP synthesis, as well as sequestration of respiratory complexes including cytochrome c within cristae. This mitochondrial morphology is associated with resistance to cytochrome c release during MOMP and less efficient induction of apoptosis. Therefore it is possible to speculate that LG adaptation performed in our work leads to reliance on mitochondrial metabolism associated with mitochondrial morphology changes that either suppress MOMP and/or cytochrome c release following MOMP during cell death induced by reovirus or other agents. To provide support for this idea in future experiments we could first measure cytochrome c release from the mitochondria in parental and LG cells following treatment with reovirus or other agents. Numerous other experiments, including characterizing BCL-2 family gene and protein expression in LG and parental cells would provide a more complete picture of how LG cells become resistant to reovirus cytolysis. Furthermore, different methods of pushing metabolism toward mitochondrial function and reliance, such as through treatment with 2-deoxyglucose, using small interfering RNA targeting mRNA for the glycolytic enzyme hexokinase, using the pyruvate dehydrogenase kinase inhibitor dichloroacetate to push pyruvate into the mitochondria, or using different combinations of energy substrates (glucose, pyruvate, glutamine) in media, would provide a much more comprehensive picture for how mitochondrial metabolism influences reovirus infection. As mentioned previously, in future experiments to properly interpret the influence of LG adaptation on reovirus infection, each of these new approaches would require use of specific and common endpoints to measure glycolysis, mitochondrial respiration, and reovirus infection parameters. A more comprehensive analysis using multiple

approaches and proper experimentation should allow a better understanding of how pushing metabolism toward the mitochondria influences reovirus infection efficiency.

4.2.2 Oligomycin, But Not Other Respiration Inhibitors, Promotes Reovirus Cytolysis

As a second approach to manipulating mitochondrial metabolism, chemical inhibitors of mitochondrial respiration and ATP synthesis were employed to study their effects on reovirus infection. No previous study has tested how manipulation of respiration or mitochondrial ATP synthesis affects reovirus infection. Loss of mitochondrial inner membrane potential (Ψ_m) is associated with dysfunction of mitochondrial respiration[68], and has been associated with reovirus infection previously[129] and in our studies (**Figure 15**). Although loss of respiratory capacity (Ψ_m) is typically a result of MOMP and cytochrome c release, respiration has also been implicated in regulating apoptosis induction. This is illustrated clearly by Kwong et al. 2007, showing that mtDNA mutations (or ablation of mtDNA) leading to complete respiratory chain dysfunction protect cells from mitochondrial apoptosis, while mtDNA mutations with a partial respiratory function are more sensitive to mitochondrial apoptosis[105]. These effects were hypothesized to be mechanistically a result of altered mitochondrial structure under the control of Ψ_m and electron flux. In line with this, Gottlieb et al. 2003 showed that Ψ_m controls mitochondrial matrix morphology and efficient cytochrome c release, as dissipation of Ψ_m by limiting oxidizable substrates (or with inhibitors of respiration) caused matrix remodelling (condensation), unfolding of the cristae and exposure of cytochrome c to IMS for efficient release upon an apoptotic stimulus. These effects were rescued by artificial regeneration of Ψ_m by acidifying the media, implying regulation by functional respiration[107].

Mitochondrial structure and dynamics have been further implicated in regulating apoptosis. In response to apoptotic stimuli, BAX associates with the mitochondrial fission protein Drp1 to promote fission[155]. Mitochondrial fragmentation as a result of fission mediated by Drp1 is associated with enhanced cytochrome c release and execution of apoptosis[156]. Correspondingly, overexpression of Opa1 results in increased mitochondrial fusion and protects cells from MOMP and cytochrome c release[157]. Generally, cells with highly fragmented mitochondria are more sensitive to MOMP and more highly networked mitochondria are

resistant to apoptosis, due to tight sequestration of cytochrome c within cristae[158]. Furthermore, BCL-2 family proteins also have roles in regulating mitochondrial dynamics and thus influence apoptotic potential indirectly in this manner[158]. Together, there is significant evidence that mitochondrial metabolism and respiratory function can have an influence on apoptosis induction.

Our approach to studying the influence of respiratory chain inhibitors on reovirus infection was to use low doses of these drugs that did not cause observable levels of cell death alone. A previous study found that high doses of Rotenone, Antimycin A, and Oligomycin each induced cell death by themselves[159]. We wanted to use sublethal doses to allow detection of the influence of these inhibitors on reovirus cytolysis. This is because we wanted to measure reovirus cytolysis, and using high doses of drugs that kill cells on their own would not allow a valid interpretation of data.

As shown in **Figure 16**, low doses of Antimycin A and Sodium Azide did not seem to affect reovirus-induced cytolysis (measured as loss of cell number alongside cell morphology). Rotenone also did not have a statistically significant influence on reovirus cytolysis. In contrast, Oligomycin significantly promoted reovirus-induced loss of cell number at a wide range of doses (including 10 nM used in many of our followup experiments).

Here, it is important to note that a serious limitation of this study was that no experiments were performed to confirm the influence of these inhibitors on cell respiration. As our study hypothesized that inhibiting mitochondrial respiration would influence reovirus infection, measurement of oxygen consumption using a Respirometer and lactate production using Mass Spectrometry should have been performed to measure mitochondrial and glycolytic metabolism. Without these endpoints for inhibitor function, it is impossible to truly confirm the inhibitory functions of these drugs or properly address the hypothesis that mitochondrial respiration *per se* affects reovirus cytolysis.

Importantly, it is unclear whether the low doses of Antimycin A, Sodium Azide, Rotenone, or Oligomycin used in our experiments are able to inhibit mitochondrial function, or to what extent. While AA and AZ at low doses did not appear to affect HCT116 cell number, a low dose of Rotenone and to a more severe extent, Oligomycin, lead to a decrease in cell number (**Fig. 16a-b**) that appeared to be due to suppressed cell proliferation (observations under the microscope). This might suggest that AA and AZ at the doses used do not inhibit respiration,

while Rotenone has a mild effect on respiration and Oligomycin has a more severe effect on inhibiting respiration indirectly through inhibitoion of ATP synthase. Unfortunately, without measurements of mitochondrial function (oxygen consumption), this cannot be concluded.

On one hand, if we were to assume that each of the drugs used inhibited respiration equivalently, then the finding that Oligomycin but not the other drugs enhances reovirus cytolysis appears to refute our hypothesis that modulating mitochondrial function affects reovirus infection. Although it is unlikely that each of our drugs would affect respiration to the same extent or in the same way, this was not proven and would require further experiments. It might be the case that higher doses of AA and AZ would have a greater affect on mitochondrial function and therefore influence reovirus infection. However, using higher doses of these other drugs seemed to induce cell death, which would complicate interpretation of any influence on reovirus infection parameters. As mentioned, due to the lack of measurement of mitochondrial function, the original hypothesis could not be adequately addressed by the experiments peformed.

Although our initial data did not support our original hypothesis, we were intrigued by the finding that Oligomycin seemed to promote reovirus cytolysis in HCT116 cells. In an attempt to further understand this finding and how it might relate to regulation of reovirus infection, our studies focused mainly on the influence of Oligomycin on reovirus infection in HCT116 cells.

First we performed experiments to characterize the influence of Oligomycin alone on cells to lend support to its known mechanism of action. Oligomycin treatment reduced cell number significantly in HCT116 and a similar, but insignificant, trend was observed in HeLa cells (**Figure18a**). Cell cycle analysis of Oligomycin treated HCT116 and HeLa cells was inconclusive and more replicates (n>2) would be necessary to determine if Oligomycin decreased the number of cells in S-phase (**Figure 19**). Oligomycin alone did not appear to induce apoptosis, measured by Western Blot analysis (PARP cleavage) and a caspase activation assay (**Figure 21 and 22**). However, it should be noted that each of these experiments were only performed twice (n=2). Lending support to the notion that Oligomycin does not induce apoptotis is the finding that the pan-caspase inhibitor ZVAD does not prevent cell number decrease compared to control treated cells (**Figure 23**). Finally, Oligomycin's effects are not significantly different in BAX/BAK$^{-/-}$ double knockout (DKO) HCT116 cells, which are resistant to

apoptosis[89]. Together, these data support that Oligomycin suppresses cellular proliferation but does not induce apoptosis, which is responsible for the decrease in cell number during treatment.

Oligomycin induced mitochondrial inner membrane hyperpolarization of HCT116 cells (**Figure 20a**), as expected. Somewhat surprisingly, however, was the finding that Oligomycin treatment did not have a notable effect on total ATP levels in cells treated at a range of doses, or for an extended period of time (**Figure 18b,c**). Rotenone was used also in these experiments for comparison, and also had no notable effect on ATP levels. Importantly, while inhibition of mitochondrial ATP synthesis might at first be expected to decrease total ATP levels in cells, previous experiments have demonstrated rapid metabolic changes to maintain ATP levels in cultured cells following Oligomycin treatment. In fact, the findings from our experiments with Oligomycin treatment agree with those in a report by Hao et al. 2010, who showed in a panel of cancer cell lines that Oligomycin (~100 nM) completely inhibits OXPHOS within 1 hr, but has only mild effects (<10% loss) on cellular ATP levels that recover alongside glycolysis upregulation within 2-6 hours, causes growth suppression despite only a small decrease in cells in S-phase, and does not induce apoptosis[160]. Therefore, despite an absence of measurement of mitochondrial function during Oligomycin treatment, our ATP results are consistent with findings in the literature and do not necessarily suggest that mitochondrial function is unaffected by Oligomycin or Rotenone.

Oligomycin treatment, but not Rotenone (or the other drugs) appeared to improve reovirus cytolysis (**Fig. 16-17**) in HCT116 cells. Consistent with this, OA+LV led to significant enhancement of mitochondrial inner membrane potential loss in HCT116 cells, **Fig. 20**. Western Blot evidence of increased PARP cleavage during combination treatment (**Fig. 21a**), early caspase acivation during reovirus infection with OA treament in HCT116 cells (**Fig. 22**), and the inhibitory effect of ZVAD on LV+OA treament in HCT116 cells (**Fig. 23**), all suggests that reovirus-induced apoptosis is somehow primed or enhanced during OA treament.

This is particularly surprising since Western Blot analysis of viral protein levels were dampened in the combination treatment (**Fig. 21a**). Plaque Assay analysis of infectious reovirus uncovered a surprising 4-5X decreases in viral progeny (**Fig. 21b**), suggesting suppressed virus replication concurrently with enhanced induction of apoptosis. It may at first seem contradictory that during Oligomycin treatement, cells are less efficiently infected by reovirus but are capable

of undergoing cell death at a faster rate than virus infection alone. We did not perform experiments to understand this apparent contradiction. Although this may seem contradictory, our data on viral replication and cytolysis in the presence of Oligomycin are sound and can be explained. As previously mentioned in the discussion of AIM 1, reovirus-induced apoptotic signaling is dependent on the level of viral proteins inside of cells, as well as BCL-2 family protein dynamics, and possibly other mitochondrial parameters such as cristae morphology and cytochrome c sequestration. Although increased viral protein synthesis and efficiency of replication is often associated with faster or more extensive apoptosis, other methods for increasing the kinetics or extent of cell death include modulating the balance within the BCL-2 protein family or modulating mitochondrial morphology. Alternatively, it may be that in certain cells a threshold level of viral proteins are required to initiate apoptosis, and anything over this threshold has little influence on the kinetics or extent of apoptosis. Since viral replication appears suppressed significantly in both Oligomycin and Rotenone treated HCT116 cells, we would predict that either a threshold level of replcation is required for cell death in these cells, or perhaps mitochondrial changes have occurred that sensitize cells to more efficient induction of apoptosis.

How Oligomycin and Rotenone treatment lead to suppressed viral protein synthesis and replication is unclear. However one speculation is that this is related to undetected inhibition of mitochondrial ATP synthesis by Oligomycin and to a lesser extent by Rotenone. We propose the following explanation for inhibition of reovirus replication: Reovirus factories that form during infection associate closely with the mitochondria and one hypothesis is that this association facilitates ample ATP supply for efficient viral replication[46]. Although glycolysis upregulation recovers total ATP levels during Oligomycin treatment[160], it is also known that growth suppression is maintained as long as Oligomycin is present in cells. A mechanism explaining this has not yet been found. Intriguingly, a recent report by Estein et al. 2014 demonstrated that under oxygenated conditions, mitochondrial-generated ATP meets baseline steady energy demands, while glycolysis functions to rapidly generate ATP to meet short timescale demands, such as for membrane transport activity[161]. This report demonstrated that aerobic glycolysis (the Warburg Effect) serves a physiological function alongside mitochondrial ATP synthesis to meet energy demands supporting prolific cell division, growth, and migration activities. Although not

addressed in this report, based on these findings it is tempting to speculate that continual OXPHOS suppression by Oligomycin (and to a lesser extent Rotenone) forces cells to rely on and upregulate glycolysis to maintain total ATP levels, but likely does so at the expense of rapid cell growth due to the difficulty in producing ATP efficiently. I further speculate based on the same reasoning (inefficient generation of ATP) that Oligomycin, and to a lesser extent Rotenone, treatment might suppress efficient reovirus replication. Indeed, ATP levels have been shown to regulate reovirus replication in Vero cells, albeit in an altered (serum-free) system[162]. How reovirus replication is suppressed by Oligomycin and Rotenone was not further examined.

Reovirus-induced apoptosis is regulated by MOMP, but has been shown to occur efficiently independently of BAX and BAK protein expression[84]. Therefore it appears that reovirus-induced MOMP occurs through a novel, currently unclear, mechanism. We wanted to determine if the effects of Oligomycin on reovirus cytolysis were maintained in the absence of BAX and BAK. Addition of Oligomycin during reovirus infection in BAX/BAK DKO cells led to an equivalent, significant enhancement in reovirus cytolysis as observed in the isogenic parental HCT116 cell line (**Figure 24**). Therefore, the influence of Oligomycin does not appear to alter the mechanism of BAX/BAK independent apoptosis, and instead appears to enhance an undefined step(s) before or during the mitochondrial events leading to enhanced loss of Ψ_m, caspase activation, and efficient cell death. The precise mechanism is not currently clear. While characterizing Oligomycin we noted that it also seemed to promote the anticancer effects (measured as a decrease in cell number) of other apoptosis inducing drugs including DOX, ABT-737, and TRAIL. However in no cases was the combination of OA+drug significantly more effective than both single agent treatments, **Fig. 18d**. Therefore, the influence of Oligomycin appears to be somewhat selective for promoting apoptosis induction and cytolysis in reovirus-infected HCT116 cells.

Our data with HCT116 cells suggested that addition of Oligomycin to reovirus infection might yield improved anticancer effects. Measuring cell number over time, we observed that Oligomycin alone had variable effects in cancer cell lines, consistent with a previous study showing that Oligomycin-induced growth suppression was proportional to each cell line's dependence on OXPHOS for ATP production[160]. It was not possible to detect an enhancement in highly reovirus-sensitive cell lines, as virus alone induced significant and nearly complete

cytolysis. Future study should use a lower dose of reovirus in these cell lines to elucidate an influence of Oligomycin. Cells lines displaying a medium sensitivity to reovirus infection demonstrated improved effects in combination with Oligomycin, although these effects were small and did not achieve statistical significance. The use of a lower virus dose in future experiments would be more insightful. Finally, in the low-sensitivity HT29 cell line, a large anticancer effect was observed with Oligomycin plus reovirus, though each agent alone had little effect. However, only n=2 was obtained for HT29 and so statistical significance could not be determined. An enhancement seemed apparent in MKN74 cells with the combination treatment, but this effect was less profound compared to HT29 cells and was not statistically significant.

Based on these data there was no clear relationship between Oligomycin sensitivity and reovirus sensitivity, or the ability to combine effectively with reovirus to promote anticancer effects. Although not thorough, these studies provide a first indication that addition of Oligomycin to reovirus yields enhanced anticancer effects in cancer cell lines of different origin. Future experiments will need to elucidate i) how Oligomycin might affect cancer cells treated with lower doses of reovirus, ii) what mechanism(s) are at play that contribute to the enhanced anticancer effects observed here, with a focus on mitochondria, and iii) if Oligomycin and reovirus combinations are worthy of further preclinical investigation in mouse models of cancer.

Notably, the majority of our data showing that Oligomycin promotes apoptosis during reovirus infection was obtained using HCT116 cells. It is possible that this effect is cell line specific, and so future work will need to determine whether a similar effect is more widely applicable to other cancer cell lines. As Oligomycin alone suppresses cell proliferation it will also be important to delineate the contribution of growth suppression versus cytolysis in future studies.

There is always a desire to improve the anticancer effects of reovirus, and one method is through enhanced induction of apoptosis, particularly in cell lines that are infected but not efficiently killed by reovirus (for example, Jurkat cells from AIM 1). However, there are a number of important qualifications regarding the potential application of this novel strategy for enhancing reovirus-induced apoptosis with Oligomycin. As mentioned, it must first be shown with more intensive and direct study that this strategy is applicable to multiple types of cancer cells. For instance, this approach will likely only be applicable to cancer cells that display

previous sensitivity to reovirus infection because our data support that Oligomycin promotes a step(s) in the natural course of infection-induced apoptosis. Second, it might be the case that severe sensitivity to Oligomycin and inefficient ATP production significantly limits reovirus replication such that apoptosis is inhibited. Future experiments will be needed to elucidate whether a threshold level of virus replication is necessary to observe enhanced apoptosis with Oligomycin in cancer cells, and to ensure that addition of Oligomycin will not be inhibitory of reovirus oncolysis. Third, there is always concern over the safety of cancer therapy. On the one hand, reovirus selectively replicates and induces apoptosis efficiently in cancer cells, such that we expect promotion of apoptosis by Oligomycin would only be apparent in cancer cells. However, there are safety concerns regarding the use of Oligomycin because OXPHOS is a prevalent pathway in normal differentiated tissues including skeletal muscle, liver, heart, brain, and others. The toxicological properties of Oligomycin have not been investigated fully, but it has been found to be toxic *in vitro* and in mice at high doses. The 50% lethal dose (LD_{50}) in mice is 1.5 mg/kg injected intraperitoneally and 0.3 g/kg orally, which corresponds to approximately 2000 nM and 400 nM, respectively. Lee et al. 2013 reported that although Oligomycin-induced OXPHOS inhibition induces cell death in neural progenitor cells at high doses (>1 μM), at a low dose of 40 nM (4X the dose used in our experiments) Oligomycin reduced cellular ATP by ~25% but had no effect on reactive oxygen species production, cell proliferation, or cell viability[163]. Although other studies have found that high doses of Oligomycin (and other respiration inhibitors) induce cell death[159], no study we can find has used such low concentrations of Oligomycin. A low concentration of Oligomycin, such as 10 nM used in our studies, seems to inhibit mitochondrial ATP synthesis. However, this low dose may avoid generation of reactive oxygen species due to inhibition of electron flux, and likely avoids the known off-target effect of inhibiting plasma membrane Na/K ATPase, which contributes to cell death at high concentrations[130]. Another concern is whether suppression of mitochondrial function with Oligomycin might actually make cancer cells more aggressive. Indeed, mitochondrial OXPHOS is considered to have an established tumor suppressor function[164]. Sanchez-Arago et al. 2010 showed that HCT116 cells treated with Oligomycin (6 μM) for 48 hours followed by removal of Oligomycin led to numerous transcriptional changes leading to an enhanced glycolytic phenotype, suppressed mitochondrial respiration, enhanced tumor growth *in*

vivo, and resistance to 5-fluorouracil treatment[165]. For these reasons, future *in vitro* experiments elucidating the mechanism and applicability of combining Oligomycin with reovirus in cancer and normal cells will help direct *in vivo* experiments.

Taken together, our studies of respiration inhibitors and their effects on reovirus suggest the following: 1) Oligomycin A, but not Antimycin A, Sodium Azide, or Rotenone, appears to significantly enhance cell killing in HCT116 cells, 2) Oligomycin suppresses cell proliferation but does not induce cell death by itself, 3) Neither Oligomycin or Rotenone significantly alter total ATP levels in cells at the concentrations used, 4) Oligomycin, and to a lesser extent Rotenone, suppresses reovirus replication, 5) Oligomycin enhances reovirus-induced loss of mitochondrial inner membrane potential, caspase activity, and caspase-dependent cell death, and 6) Oligomycin's actions are independent of BAX/BAK. Although a mechanism isn't clear from these studies, Oligomycin seems to be enhancing efficiency of the apoptotic pathway induced by reovirus at an early stage.

One possible explanation is that Oligomycin treatment changes mitochondrial structure and/or MOMP such that cytochrome c release and thus caspase activation is enhanced following reovirus-induced MOMP. This possibility, as well as how these data might relate to regulation of reovirus infection by mitochondria more generally and in the context of the findings in AIM 1 will be addressed below.

4.2.3 Relevance of Work: What Do Metabolic Manipulations Tell Us About Reovirus-Induced Cytolysis?

Significant evidence points to involvement of the mitochondria for integrating and executing reovirus-induced apoptosis, but whether mitochondrial function regulates reovirus infection is unknown. No previous study has explored the hypothesis that mitochondrial metabolism will influence reovirus infection. Reovirus selectively replicates in and kills many cancer cells. Although this is in part due to overactive biosynthetic pathways facilitating efficient reovirus replication, regulation of apoptosis during infection in cancer cells is not well understood. It remains very important to understand regulation of reovirus infection and apoptosis in cancer cells for designing improved and novel therapeutic strategies and to understand patient responses to reovirus.

This thesis considered the possibility that cancer cell mitochondria might more directly regulate reovirus infection efficiency and subsequent cell death. Cancer cell mitochondria are significantly altered as a result of metabolic alterations during carcinogenesis. Thus it was very intriguing to consider the novel hypothesis that altering mitochondrial metabolism in cancer cells would influence reovirus cytolysis. I feel that this hypothesis is quite novel and if answered thoroughly could provide unique insight into the role of metabolism and mitochondria in reovirus infection, potentially shedding light on differential responses to infection. However, our two main approaches of modulating mitochondrial metabolism first with low glucose (LG) adaptation and then using chemical inhibitors of respiration and following reovirus infection thereafter have several limitations.

Our first approach of adapting cells to low glucose was chosen mainly because of its convenience and previous demonstration that this treatment does indeed push cellular metabolism toward reliance on efficient mitochondrial ATP generation. Rossignol et al. 2004 showed that metabolic adaptation to low glucose led to extensive networking of the mitochondria throughout the cell, remodelling of the mitochondrial matrix associated with increased cristal membrane, and enhanced OXPHOS, respiration, and ATP synthesis[97]. This report did not address sensitivity to apoptosis. However one consequence of mitochondrial fusion, networking, matrix condensation, and enhanced respiration is more efficient sequestration of respiratory proteins including cytochrome c within cristae that are not readily released upon MOMP. In our experiments, LG-adapted cells were resistant to cell death induced by reovirus and other agents, suggesting a general mechanism of death resistance. While this finding was consistent with our hypothesis that metabolic modulation could impact reovirus infection, it was not within our scope of study to elucidate what mitochondrial alterations were responsible for suppression of apoptosis. We cannot conclusively say that it is metabolic or mitochondrial changes that influenced resistance to reovirus cytolysis in LG cells as 1) we did not perform experiments to confirm altered metabolism, and 2) it would be difficult to delineate the contribution of mitochondrial changes from the likely numerous other changes occurring in the cells during adaptation, such as increased autophagy.

LG cell adaptation may still be a useful model for studying metabolic changes in reovirus infection, but measurement of endpoints (oxygen consumption, lactic acid production) and using

complementary approaches such as use of different glycolytic inhibitors or controlling oxidizable substrates in both an acute and chronic manner in multiple cell types and then following reovirus infection efficiency would provide much stronger evidence for how pushing cell metabolism toward enhanced mitochondrial function would affect reovirus infection. In future studies using more comprehensive and controlled methods to assess the influence of mitochondrial metabolism on reovirus infection, it would be very interesting to monitor mitochondrial morphology using electron microscopy before and during infection in each metabolic alteration scenario (ie. in LG vs parental cells, or OA vs. control treatment, etc.) to understand mitochondrial changes that occur during such treatment.

Our second approach to modulating mitochondrial metabolism was to use chemical inhibitors of respiration to inhibit mitochondrial function. For this approach, we chose to use concentrations of inhibitors that did not significantly decrease cell number, as we wanted to avoid the complication of drug-induced cell death when measuring reovirus cytolysis. The concentrations of both Antimycin A and Sodium Azide used did not affect cell number alone. However, Rotenone, and much more so, Oligmycin A even at very low concentrations decreased cell number. One serious limitation of this approach, as with the LG approach, was lack of experiments confirming metabolic changes and thus inhibitor action in cells. Thus although it appeared that Oligomycin was the only drug that induced an effect, we cannot say whether this is a property unique to Oligomycin or if the effect of this inhibitor to inhibit respiration was much more profound that the other drugs used. Notably, in certain experiments Oligomycin and Rotenone had similar effects on reovirus infection. For instance, both of these inhibitors led to significant suppression of viral protein synthesis and production of infectious progeny virus (**Fig. 21a-b**), but Oligomycin induced a stronger decrease. But in other experiments Oligomycin and Rotenone had different effects. For instance, Oligomycin, but not Rotenone (or Obatoclax) significantly increased the number of cells with decreased mitochondrial inner membrane potential during reovirus infection in HCT116 cells (**Figure 20**).

Unfortunately, a few experiments were performed in an effort to better characterize Oligomycin's effect on reovirus infection that did not include Rotenone and thus it is difficult to include them in a discussion of how mitochondrial function affects reovirus infection. Furthermore, most experiments peformed in AIM 2 omitted Antimycin A and Sodium Azide

altogether. Because of this, our work is better considered as a description of the effects of Oligomycin on reovirus infection instead of addressing the original hypothesis that inhibiting mitochondrial function would influence reovirus infection efficiency (replication and/or apoptosis).

For this approach to successfully address the hypothesis in future studies, confirming and quantifying the inhibitory effects of each drug is essential. Furthermore, a more comprehensive and controlled experimental design would allow for proper testing of the hypothesis. Complementary approaches to chemical inhibition of mitochondrial function might include siRNA knockdown of pyruvate dehydrogenase or TCA cycle enzymes that prevent generation of oxidizable intermediates fueling electron transport, overexpression of pyruvate dehydrogenase kinase to prevent pyruvate entry into the mitochondria, or the use of mtDNA mutant or knockout cells. The entire purpose of mtDNA is to generate proteins necessary for electron transport chain function, and creating mtDNA null cells (with chronic ethidium bromide treatment) might be interesting for studying reovirus infection. As mentioned before, it would be very interesting to follow mitochondrial morphology by electron microscopy during infection with reovirus and in each of these conditions.

As our approach contained serious limitations and was biased toward exploring the interesting results with Oligomycin, we cannot accurately determine how our results with this drug relate to the original hypothesis. However, our data do suggest that Oligomycin promotes reovirus-induced, caspase-dependent apoptosis in HCT116 cells that appears to be independent of BAX and BAK. The mechanism for Oligomycin's enhancement of reovirus-induced apoptosis, particularly given the significant suppression of viral replication, is elusive. However, based on our observations and data from the literature we cautiously speculate that Oligomycin treatment induces mitochondrial structural changes that allow enhanced cytochrome c release from the mitochondria, thus enhancing caspase activation and cell death kinetics. Oligomycin is known to hyperpolarize the mitochondrial inner membrane, decrease networking of mitochondria, and increase mitochondrial fragmentation and swelling[166]. Interestingly, this report by Reis et al. 2012 found that BAX activation following treatment with apoptotic drugs was most notable in conditions where mitochondria were in a swollen state (induced by other agents). This provides support for the idea that Oligomycin-induced morphology or structural change to

mitochondria lead to enhanced apoptosis, either through efficient MOMP or release of cytochrome c. Indeed, a simple experiment that should be performed in the future is to confirm enhanced release of cytochrome c from the mitochondria during reovirus infection with Oligomycin. However, further study is needed to prove the mechanism by which Oligomycin enhances apoptosis during reovirus infection, and very importantly, experiments need to be done in other cell lines to show that this is not an effect specific for HCT116 cells.

Given the prevalent and pleiotropic roles played by mitochondria, even comprehensive and better controlled experimentation modulating energy metabolism will likely lead to numerous effects within the cell. Given the severe limitations of our work in AIM 2, it is difficult to comment with any confidence on how LG adaptation or sensitivity to respiration inhibitors, particularly Oligomycin, influences reovirus infection in an interpretable way. Therefore extreme care should be taken when interpreting our results. If we were to speculate on a common theme underlying resistance to reovirus cytolysis in LG cells and sensitzation to apoptosis during Oligomycin treatment, it would focus on the link between mitochondrial morphology and induction of apoptosis. Highly networked mitochondria are associated with efficient OXPHOS and mitochondrial metabolism, and in this case cytochrome c is sequestered in mitochondrial cristae such that following MOMP during reovirus infection, cytochrome c release is less efficient. This scenario might be the case in LG cells compared to parental cells. On the other hand, Oligomycin treatment, which has been shown previously to induce mitochondrial fission and swelling, might allow more efficient release of cytochrome c following MOMP. An alternative speculation is that these treatments somehow alter the dynamic balance with the BCL-2 family of proteins, altering the propensity for cells to undergo cell death and thus changing the kinetics of cell death. Further experiments studying cytochrome c release, mitochondrial ultrastructure, BCL-2 family expression, and BH3-domain profiling could help elucidate these possibilities.

Study of the role of mitochondrial metabolism in reovirus infection could be extremely insightful. For instance, do the varied responses to reovirus oncolysis relate to a characteristic(s) of the mitochondria within cancer cells, such as the ratio of glycolytic to oxidative metabolism, or perhaps the ratio of networked versus fragmented versus swollen mitochondria? Mitochondrial morphology demonstrates heterogeneity within and among isogenic cancer cells,

and certainly among cancer cells of different types considering their varied metabolic profiles[98]. Might mitochondrial metabolism or morphology play a role in dictating which cancer cell lines, or individual cells within a cell line, die quickly or slowly in response to reovirus infection? For instance, if reovirus preferentially infects and kills highly glycolytic tumors, then perhaps metabolic features could be used as a biomarker of response to reovirus therapy. This knowledge would open novel opportunities for improved therapy either by modulating metabolism chemically or perhaps through dietary changes. Mitochondrial and metabolic alterations in cancer cells have been well described (see a recent review by Wang, Peralta, and Moraes 2013) and altered metabolism is being evaluated for therapeutic intervention[167]. Current strategies targeting metabolism include those that promote oxidative phosphorylation by promoting glucose flux into the mitochondria (dichloroacetate, oxamate) or by inhibiting glycolysis (2-deoxyglucose, 3-bromopyruvate, lonidamide), while other strategies include inhibiting respiration with metformin[167]. How these drugs influence reovirus infection has not been studied, but our data provide clues that these experiments could be worthwhile. Although these are very interesting questions, I must emphasize that this is entirely conjecture at this point since our work did not adequately address the hypothesis outlined. I believe future work is necessary and warranted.

4.2.4 Conclusions from AIM 2

Although we obtained preliminary evidence that reovirus infection can be influenced by LG adaptation or treatment with Oligomycin, our experimental approach to modulating mitochondrial metabolism was incomplete and lacked important control experiments and was not very comprehensive. Because of these limitations, the hypothesis that mitochondrial metabolism influences reovirus infection could not be adequately addressed and no well-supported conclusions are drawn from the data. Despite this, the finding that certain treatments did affect reovirus replication or cytolysis might suggest that metabolic perturbations can influence reovirus infection in some way(s). I believe that future study is warranted to properly address how mitochondrial metabolism influences reovirus infection in cancer cells.

Chapter Five: **CONCLUSIONS AND FUTURE DIRECTIONS**

This thesis describes novel findings regarding the importance of mitochondria in reovirus infection. **Figure 26** introduces a brief model for proposed mitochondrial regulation of efficient reovirus oncolysis. Targeting apoptotic pathways directly alongside reovirus infection promotes reovirus cytolysis in pediatric leukemia and likely other cancers. Future studies should extend *in vitro* data but must also assess the utility of this strategy *in vivo*. Xenograft pediatric leukemia mouse models can be created in NOD/SCID mice that accurately represent the human disease[168]. Leukemia cells isolated from patient bone marrow biopsy specimens can be inoculated into mice by tail vein injection. Following leukemia engraftment that mimics human disease (for example, 50% human cells in circulation, with significant infiltration of the spleen and infiltration of the liver), reovirus could be added intravenously at levels that are proportional to those used currently in clinical trials. Efficacy could be measured by the percent of human leukemic cells in circulation measured by flow cytometry. This model could then be expanded to assess whether synergy is observed between reovirus and apoptosis-inducing drugs (and/or chemotherapy).

Our data from AIM 1 are stronger than those from AIM 2. We describe some preliminary data suggesting that certain treatments intending to modulate mitochondrial metabolism can influence reovirus infection. However, interpretation of this data is clouded by insufficient control experiments. Future work *in vitro* using multiple methods to modulate metabolism toward and away from the mitochondria in conjuction with endpoint measurements of glycolytic metabolism (lactate production) and oxidative metabolism (oxygen consumption) should be used to investigate the influence of mitochondrial metabolism on reovirus infection. Electron microscopy would be a very insightful technique to monitor mitochondrial ultrastructure changes during metabolic intervention and reovirus infection.

Together, this thesis work further supports that the mitochondrial regulation of cell death is important and can be exploited by proapoptotic drugs to improve reovirus cytolysis. Whether cancer cell metabolism regulates reovirus infection and/or is amenable to therapeutic intervention for improved response to reovirus therapy remains unknown and is still an area in need of clarification. This work sets the stage for further investigation that should culminate in improved understanding and efficacy of reovirus-based cancer therapy.

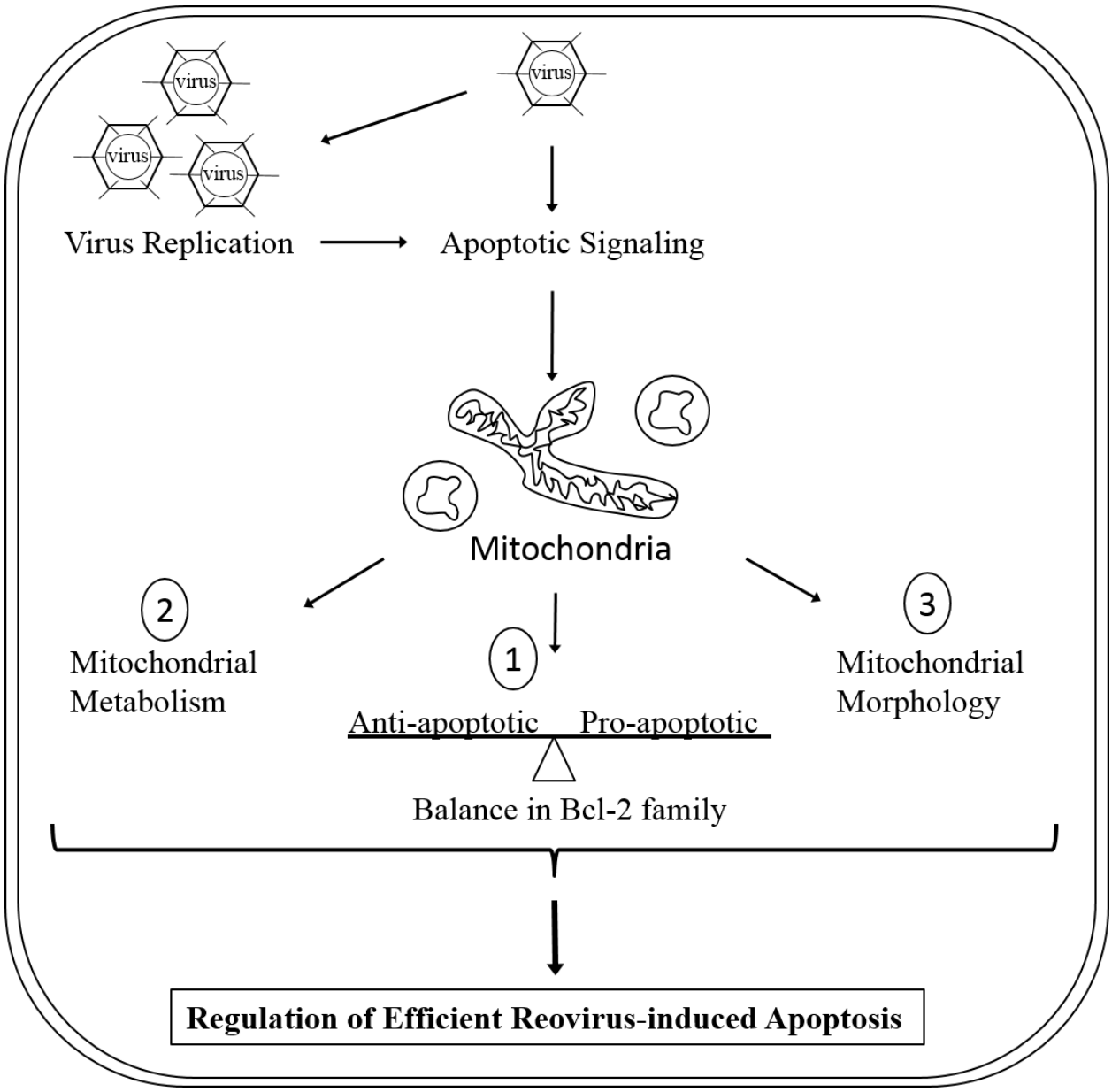
virus
virus
virus
virus
Virus Replication
Apoptotic Signaling
Mitochondria
2
Mitochondrial
Metabolism
1
Anti-apoptotic
Pro-apoptotic
3
Mitochondrial
Morphology
Balance in Bcl-2 family
Regulation of Efficient Reovirus-induced Apoptosis

Figure 26. Model for Mitochondrial Regulation of Efficient Reovirus Oncolysis.

Reovirus infection induces apoptosis that requires mitochondrial-mediated apoptosis. The mitochondria regulate life/death decisions, but also play very important roles in cell metabolism. Reovirus efficiently kills many cancer cells, and cancer cells often demonstrate mitochondrial and metabolic alterations. It is known that reovirus-induced apoptosis is regulated by balance in the BCL-2 family (1) that act at the mitochodnria. This thesis work demonstrates that this regulation can be exploited by directly targeting the anti-apoptotic BCL-2 family of proteins (ABT-737, Obatoclax, Trail). Although we set out to test whether mitochondrial metabolism influences reovirus infection, our experimental approach was insufficient to address this question. Mitochondrial metabolism (2) and mitochondrial morphology ((3), sometimes related to metabolism in literature), do not have described roles in regulating efficient reovirus infection. However, they are included here because they may well be important regulators of reovirus infection, and future study is warranted to investigate this possibility. Intriguing questions about reovirus infection and selectivity for cancer cells remain: I) Do the varied responses to reovirus oncolysis in cancer cells relate to mitochondrial metabolism or morphology? II) Can we modulate these processes to promote efficient reovirus infection? Further investigation should culminate in improved understanding and efficacy of reovirus-based cancer therapy.

References

1. Dock G. The influence of complicating diseases upon leukemia. American Journal of the Medical Sciences 1904;127(4):563-92.

2. Kelly E, Russell SJ. History of oncolytic viruses: Genesis to genetic engineering. Mol Ther 2007 Apr;15(4):651-9.

3. Bell J, McFadden G. Viruses for tumor therapy. Cell Host Microbe 2014 Mar 12;15(3):260-5.

4. Miest TS, Cattaneo R. New viruses for cancer therapy: Meeting clinical needs. Nat Rev Microbiol 2014 Jan;12(1):23-34.

5. Alemany R. Viruses in cancer treatment. Clin Transl Oncol 2013 Mar;15(3):182-8.

6. Guo ZS, Liu Z, Bartlett DL. Oncolytic immunotherapy: Dying the right way is a key to eliciting potent antitumor immunity. Front Oncol 2014 Apr 10;4:74.

7. Gujar SA, Pan DA, Marcato P, Garant KA, Lee PW. Oncolytic virus-initiated protective immunity against prostate cancer. Mol Ther 2011 Apr;19(4):797-804.

8. Gujar SA, Lee PW. Oncolytic virus-mediated reversal of impaired tumor antigen presentation. Front Oncol 2014 Apr 10;4:77.

9. Siegel R, Ma J, Zou Z, Jemal A. Cancer statistics, 2014. CA Cancer J Clin 2014 Jan-Feb;64(1):9-29.

10. Russell SJ, Peng KW, Bell JC. Oncolytic virotherapy. Nat Biotechnol 2012 Jul 10;30(7):658-70.

11. Kobayashi T, Antar AA, Boehme KW, Danthi P, Eby EA, Guglielmi KM, Holm GH, Johnson EM, Maginnis MS, Naik S, et al. A plasmid-based reverse genetics system for animal double-stranded RNA viruses. Cell Host Microbe 2007 Apr 19;1(2):147-57.

12. Kim M, Egan C, Alain T, Urbanski SJ, Lee PW, Forsyth PA, Johnston RN. Acquired resistance to reoviral oncolysis in ras-transformed fibrosarcoma cells. Oncogene 2007 Jun 14;26(28):4124-34.

13. Xia ZJ, Chang JH, Zhang L, Jiang WQ, Guan ZZ, Liu JW, Zhang Y, Hu XH, Wu GH, Wang HQ, et al. Phase III randomized clinical trial of intratumoral injection of E1B gene-deleted adenovirus (H101) combined with cisplatin-based chemotherapy in treating squamous cell cancer of head and neck or esophagus. Ai Zheng 2004 Dec;23(12):1666-70.

14. Strong JE, Coffey M, Tang D, Sabinin P, Lee PWK. The molecular basis of viral oncolysis: Usurpation of the ras signaling pathway by reovirus. EMBO J 1998 06/15;17(12):3351-62.

15. Strong JE, Tang D, Lee PW. Evidence that the epidermal growth factor receptor on host cells confers reovirus infection efficiency. Virology 1993 Nov;197(1):405-11.

16. Strong JE, Lee PW. The v-erbB oncogene confers enhanced cellular susceptibility to reovirus infection. J Virol 1996 Jan;70(1):612-6.

17. Coffey M, Strong JE, Forsyth PA, Lee PW. Reovirus therapy of tumors with activated ras pathway. Science 1998 Nov 13;282(5392):1332-4.

18. Marcato P, Shmulevitz M, Pan D, Stoltz D, Lee PW. Ras transformation mediates reovirus oncolysis by enhancing virus uncoating, particle infectivity, and apoptosis-dependent release. Mol Ther 2007 Aug;15(8):1522-30.

19. Qin Q, Carroll K, Hastings C, Miller CL. Mammalian orthoreovirus escape from host translational shutoff correlates with stress granule disruption and is independent of eIF2alpha phosphorylation and PKR. J Virol 2011 Sep;85(17):8798-810.

20. Shmulevitz M, Pan LZ, Garant K, Pan D, Lee PW. Oncogenic ras promotes reovirus spread by suppressing IFN-beta production through negative regulation of RIG-I signaling. Cancer Res 2010 Jun 15;70(12):4912-21.

21. Song L, Ohnuma T, Gelman IH, Holland JF. Reovirus infection of cancer cells is not due to activated ras pathway. Cancer Gene Ther 2009 Apr;16(4):382.

22. Alain T, Kim TS, Lun X, Liacini A, Schiff LA, Senger DL, Forsyth PA. Proteolytic disassembly is a critical determinant for reovirus oncolysis. Mol Ther 2007 Aug;15(8):1512-21.

23. Smakman N, van den Wollenberg DJ, Borel Rinkes IH, Hoeben RC, Kranenburg O. Sensitization to apoptosis underlies KrasD12-dependent oncolysis of murine C26 colorectal carcinoma cells by reovirus T3D. J Virol 2005 Dec;79(23):14981-5.

24. Twigger K, Roulstone V, Kyula J, Karapanagiotou EM, Syrigos KN, Morgan R, White C, Bhide S, Nuovo G, Coffey M, et al. Reovirus exerts potent oncolytic effects in head and neck cancer cell lines that are independent of signalling in the EGFR pathway. BMC Cancer 2012 Aug 24;12:368,2407-12-368.

25. van Houdt WJ, Smakman N, van den Wollenberg DJ, Emmink BL, Veenendaal LM, van Diest PJ, Hoeben RC, Borel Rinkes IH, Kranenburg O. Transient infection of freshly isolated human colorectal tumor cells by reovirus T3D intermediate subviral particles. Cancer Gene Ther 2008 May;15(5):284-92.

26. Kim M, Williamson CT, Prudhomme J, Bebb DG, Riabowol K, Lee PW, Lees-Miller SP, Mori Y, Rahman MM, McFadden G, et al. The viral tropism of two distinct oncolytic viruses, reovirus and myxoma virus, is modulated by cellular tumor suppressor gene status. Oncogene 2010 Jul 8;29(27):3990-6.

27. Pan D, Pan LZ, Hill R, Marcato P, Shmulevitz M, Vassilev LT, Lee PW. Stabilisation of p53 enhances reovirus-induced apoptosis and virus spread through p53-dependent NF-kappaB activation. Br J Cancer 2011 Sep 27;105(7):1012-22.

28. Clarke P, Meintzer SM, Widmann C, Johnson GL, Tyler KL. Reovirus infection activates JNK and the JNK-dependent transcription factor c-jun. J Virol 2001 Dec;75(23):11275-83.

29. Norman KL, Hirasawa K, Yang AD, Shields MA, Lee PW. Reovirus oncolysis: The ras/RalGEF/p38 pathway dictates host cell permissiveness to reovirus infection. Proc Natl Acad Sci U S A 2004 Jul 27;101(30):11099-104.

30. O'Donnell SM, Holm GH, Pierce JM, Tian B, Watson MJ, Chari RS, Ballard DW, Brasier AR, Dermody TS. Identification of an NF-kappaB-dependent gene network in cells infected by mammalian reovirus. J Virol 2006 Feb;80(3):1077-86.

31. Smith JA, Schmechel SC, Raghavan A, Abelson M, Reilly C, Katze MG, Kaufman RJ, Bohjanen PR, Schiff LA. Reovirus induces and benefits from an integrated cellular stress response. J Virol 2006 Feb;80(4):2019-33.

32. Wallace DC. Mitochondria and cancer. Nat Rev Cancer 2012 Oct;12(10):685-98.

33. Danthi P, Holm GH, Stehle T, Dermody TS. Reovirus receptors, cell entry, and proapoptotic signaling. Adv Exp Med Biol 2013;790:42-71.

34. Black AJ, Morris DG. Clinical trials involving the oncolytic virus, reovirus: Ready for prime time? Expert Rev Clin Pharmacol 2012 Sep;5(5):517-20.

35. Adair RA, Roulstone V, Scott KJ, Morgan R, Nuovo GJ, Fuller M, Beirne D, West EJ, Jennings VA, Rose A, et al. Cell carriage, delivery, and selective replication of an oncolytic virus in tumor in patients. Sci Transl Med 2012 Jun 13;4(138):138ra77.

36. Ilett EJ, Prestwich RJ, Kottke T, Errington F, Thompson JM, Harrington KJ, Pandha HS, Coffey M, Selby PJ, Vile RG, et al. Dendritic cells and T cells deliver oncolytic reovirus for tumour killing despite pre-existing anti-viral immunity. Gene Ther 2009 May;16(5):689-99.

37. Dermody TS, Parker JSL, Sherry B. Chapter 44: Orthoreoviruses. In: D. K. Knipe, P. M. Howley, editors. Fields virology. 6th ed. Wolters Kluwer Health/Lippincott Williams & Wilkins; 2013. .

38. Johansson C, Wetzel JD, He J, Mikacenic C, Dermody TS, Kelsall BL. Type I interferons produced by hematopoietic cells protect mice against lethal infection by mammalian reovirus. J Exp Med 2007 Jun 11;204(6):1349-58.

39. Dionne KR, Galvin JM, Schittone SA, Clarke P, Tyler KL. Type I interferon signaling limits reoviral tropism within the brain and prevents lethal systemic infection. J Neurovirol 2011 Aug;17(4):314-26.

40. Holm GH, Pruijssers AJ, Li L, Danthi P, Sherry B, Dermody TS. Interferon regulatory factor 3 attenuates reovirus myocarditis and contributes to viral clearance. J Virol 2010 Jul;84(14):6900-8.

41. Maginnis MS, Forrest JC, Kopecky-Bromberg SA, Dickeson SK, Santoro SA, Zutter MM, Nemerow GR, Bergelson JM, Dermody TS. Beta1 integrin mediates internalization of mammalian reovirus. J Virol 2006 Mar;80(6):2760-70.

42. Mainou BA, Zamora PF, Ashbrook AW, Dorset DC, Kim KS, Dermody TS. Reovirus cell entry requires functional microtubules. MBio 2013 Jul 2;4(4):10.1128/mBio.00405-13.

43. Mainou BA, Dermody TS. Src kinase mediates productive endocytic sorting of reovirus during cell entry. J Virol 2011 Apr;85(7):3203-13.

44. Connolly JL, Dermody TS. Virion disassembly is required for apoptosis induced by reovirus. J Virol 2002 Feb;76(4):1632-41.

45. Odegard AL, Chandran K, Zhang X, Parker JS, Baker TS, Nibert ML. Putative autocleavage of outer capsid protein micro1, allowing release of myristoylated peptide micro1N during particle uncoating, is critical for cell entry by reovirus. J Virol 2004 Aug;78(16):8732-45.

46. Fernandez de Castro I, Zamora PF, Ooms L, Fernandez JJ, Lai CM, Mainou BA, Dermody TS, Risco C. Reovirus forms neo-organelles for progeny particle assembly within reorganized cell membranes. MBio 2014 Feb 18;5(1):10.1128/mBio.00931-13.

47. Lai CM, Mainou BA, Kim KS, Dermody TS. Directional release of reovirus from the apical surface of polarized endothelial cells. MBio 2013 Apr 9;4(2):10.1128/mBio.00049-13.

48. Sandekian V, Lim D, Prud'homme P, Lemay G. Transient high level mammalian reovirus replication in a bat epithelial cell line occurs without cytopathic effect. Virus Res 2013 May;173(2):327-35.

49. Loo YM, Fornek J, Crochet N, Bajwa G, Perwitasari O, Martinez-Sobrido L, Akira S, Gill MA, Garcia-Sastre A, Katze MG, et al. Distinct RIG-I and MDA5 signaling by RNA viruses in innate immunity. J Virol 2008 Jan;82(1):335-45.

50. Zhang Z, Yuan B, Lu N, Facchinetti V, Liu YJ. DHX9 pairs with IPS-1 to sense double-stranded RNA in myeloid dendritic cells. J Immunol 2011 Nov 1;187(9):4501-8.

51. Liu Y, Lu N, Yuan B, Weng L, Wang F, Liu YJ, Zhang Z. The interaction between the helicase DHX33 and IPS-1 as a novel pathway to sense double-stranded RNA and RNA viruses in myeloid dendritic cells. Cell Mol Immunol 2014 Jan;11(1):49-57.

52. Sun Q, Sun L, Liu HH, Chen X, Seth RB, Forman J, Chen ZJ. The specific and essential role of MAVS in antiviral innate immune responses. Immunity 2006 May;24(5):633-42.

53. Rudd P, Lemay G. Correlation between interferon sensitivity of reovirus isolates and ability to discriminate between normal and ras-transformed cells. J Gen Virol 2005 May;86(Pt 5):1489-97.

54. Smith JA, Schmechel SC, Williams BR, Silverman RH, Schiff LA. Involvement of the interferon-regulated antiviral proteins PKR and RNase L in reovirus-induced shutoff of cellular translation. J Virol 2005 Feb;79(4):2240-50.

55. Poggioli GJ, Dermody TS, Tyler KL. Reovirus-induced sigma1s-dependent G(2)/M phase cell cycle arrest is associated with inhibition of p34(cdc2). J Virol 2001 Aug;75(16):7429-34.

56. Poggioli GJ, DeBiasi RL, Bickel R, Jotte R, Spalding A, Johnson GL, Tyler KL. Reovirus-induced alterations in gene expression related to cell cycle regulation. J Virol 2002 Mar;76(6):2585-94.

57. Clarke P, Richardson-Burns SM, DeBiasi RL, Tyler KL. Mechanisms of apoptosis during reovirus infection. Curr Top Microbiol Immunol 2005;289:1-24.

58. Gujar SA, Marcato P, Pan D, Lee PW. Reovirus virotherapy overrides tumor antigen presentation evasion and promotes protective antitumor immunity. Mol Cancer Ther 2010 Nov;9(11):2924-33.

59. Kyula JN, Roulstone V, Karapanagiotou EM, Melcher AA, Harrington KJ. Oncolytic reovirus type 3 (dearing) as a novel therapy in head and neck cancer. Expert Opin Biol Ther 2012 Dec;12(12):1669-78.

60. Kerr JF, Wyllie AH, Currie AR. Apoptosis: A basic biological phenomenon with wide-ranging implications in tissue kinetics. Br J Cancer 1972 Aug;26(4):239-57.

61. Hanahan D, Weinberg RA. Hallmarks of cancer: The next generation. Cell 2011 Mar 4;144(5):646-74.

62. Lavrik I, Golks A, Krammer PH. Death receptor signaling. J Cell Sci 2005 Jan 15;118(Pt 2):265-7.

63. Guicciardi ME, Gores GJ. Life and death by death receptors. FASEB J 2009 Jun;23(6):1625-37.

64. Meng XW, Peterson KL, Dai H, Schneider P, Lee SH, Zhang JS, Koenig A, Bronk S, Billadeau DD, Gores GJ, et al. High cell surface death receptor expression determines type I versus type II signaling. J Biol Chem 2011 Oct 14;286(41):35823-33.

65. Elmore S. Apoptosis: A review of programmed cell death. Toxicol Pathol 2007 Jun;35(4):495-516.

66. Bender T, Martinou JC. Where killers meet--permeabilization of the outer mitochondrial membrane during apoptosis. Cold Spring Harb Perspect Biol 2013 Jan 1;5(1):a011106.

67. van Delft MF, Smith DP, Lahoud MH, Huang DC, Adams JM. Apoptosis and non-inflammatory phagocytosis can be induced by mitochondrial damage without caspases. Cell Death Differ 2010 May;17(5):821-32.

68. Lartigue L, Kushnareva Y, Seong Y, Lin H, Faustin B, Newmeyer DD. Caspase-independent mitochondrial cell death results from loss of respiration, not cytotoxic protein release. Mol Biol Cell 2009 Dec;20(23):4871-84.

69. Comelli M, Genero N, Mavelli I. Caspase-independent apoptosis in friend's erythroleukemia cells: Role of mitochondrial ATP synthesis impairment in relocation of apoptosis-inducing factor and endonuclease G. J Bioenerg Biomembr 2009 Feb;41(1):49-59.

70. Zanna C, Ghelli A, Porcelli AM, Martinuzzi A, Carelli V, Rugolo M. Caspase-independent death of leber's hereditary optic neuropathy cybrids is driven by energetic failure and mediated by AIF and endonuclease G. Apoptosis 2005 Oct;10(5):997-1007.

71. Shamas-Din A, Kale J, Leber B, Andrews DW. Mechanisms of action of bcl-2 family proteins. Cold Spring Harb Perspect Biol 2013 Apr 1;5(4):a008714.

72. Shamas-Din A, Brahmbhatt H, Leber B, Andrews DW. BH3-only proteins: Orchestrators of apoptosis. Biochim Biophys Acta 2011 Apr;1813(4):508-20.

73. Shamas-Din A, Bindner S, Zhu W, Zaltsman Y, Campbell C, Gross A, Leber B, Andrews DW, Fradin C. tBid undergoes multiple conformational changes at the membrane required for bax activation. J Biol Chem 2013 Jul 26;288(30):22111-27.

74. Rodgers SE, Barton ES, Oberhaus SM, Pike B, Gibson CA, Tyler KL, Dermody TS. Reovirus-induced apoptosis of MDCK cells is not linked to viral yield and is blocked by bcl-2. J Virol 1997 Mar;71(3):2540-6.

75. Beckham JD, Tuttle KD, Tyler KL. Caspase-3 activation is required for reovirus-induced encephalitis in vivo. J Neurovirol 2010 Jul;16(4):306-17.

76. DeBiasi RL, Robinson BA, Sherry B, Bouchard R, Brown RD, Rizeq M, Long C, Tyler KL. Caspase inhibition protects against reovirus-induced myocardial injury in vitro and in vivo. J Virol 2004 Oct;78(20):11040-50.

77. Pandha HS, Heinemann L, Simpson GR, Melcher A, Prestwich R, Errington F, Coffey M, Harrington KJ, Morgan R. Synergistic effects of oncolytic reovirus and cisplatin chemotherapy in murine malignant melanoma. Clin Cancer Res 2009 Oct 1;15(19):6158-66.

78. Thirukkumaran CM, Nodwell MJ, Hirasawa K, Shi ZQ, Diaz R, Luider J, Johnston RN, Forsyth PA, Magliocco AM, Lee P, et al. Oncolytic viral therapy for prostate cancer: Efficacy of reovirus as a biological therapeutic. Cancer Res 2010 Mar 15;70(6):2435-44.

79. Sei S, Mussio JK, Yang QE, Nagashima K, Parchment RE, Coffey M, Shoemaker RH, Tomaszewski JE. Synergistic antitumor activity of oncolytic reovirus and chemotherapeutic agents in non-small cell lung cancer cells. Mol Cancer 2009 Jul 14;8:47.

80. Twigger K, Vidal L, White CL, De Bono JS, Bhide S, Coffey M, Thompson B, Vile RG, Heinemann L, Pandha HS, et al. Enhanced in vitro and in vivo cytotoxicity of combined reovirus and radiotherapy. Clin Cancer Res 2008 Feb 1;14(3):912-23.

81. Westhoff MA, Bruhl O, Nonnenmacher L, Karpel-Massler G, Debatin KM. Killing me softly--future challenges in apoptosis research. Int J Mol Sci 2014 Mar 3;15(3):3746-67.

82. Clarke P, Meintzer SM, Gibson S, Widmann C, Garrington TP, Johnson GL, Tyler KL. Reovirus-induced apoptosis is mediated by TRAIL. J Virol 2000 Sep;74(17):8135-9.

83. Danthi P, Pruijssers AJ, Berger AK, Holm GH, Zinkel SS, Dermody TS. Bid regulates the pathogenesis of neurotropic reovirus. PLoS Pathog 2010 Jul 1;6:e1000980.

84. Wisniewski ML, Werner BG, Hom LG, Anguish LJ, Coffey M, Parker JS. Reovirus infection or ectopic expression of outer capsid protein micro1 induces apoptosis independently of the cellular proapoptotic proteins bax and bak. J Virol 2011 Jan;85(1):296-304.

85. Kim JW, Lyi SM, Parrish CR, Parker JS. A proapoptotic peptide derived from reovirus outer capsid protein {micro}1 has membrane-destabilizing activity. J Virol 2011 Feb;85(4):1507-16.

86. Danthi P, Hansberger MW, Campbell JA, Forrest JC, Dermody TS. JAM-A-independent, antibody-mediated uptake of reovirus into cells leads to apoptosis. J Virol 2006 Feb;80(3):1261-70.

87. Boehme KW, Hammer K, Tollefson WC, Konopka-Anstadt JL, Kobayashi T, Dermody TS. Nonstructural protein sigma1s mediates reovirus-induced cell cycle arrest and apoptosis. J Virol 2013 Dec;87(23):12967-79.

88. Coffey M, Sheh A, Kim IS, Chandran K, Nibert ML, Parker JS. Reovirus outer capsid protein micro1 induces apoptosis and associates with lipid droplets, endoplasmic reticulum, and mitochondria. J Virol 2006 Sep;80(17):8422-38.

89. Wang C, Youle RJ. Predominant requirement of bax for apoptosis in HCT116 cells is determined by mcl-1's inhibitory effect on bak. Oncogene 2012 Jun 28;31(26):3177-89.

90. Connolly JL, Rodgers SE, Clarke P, Ballard DW, Kerr LD, Tyler KL, Dermody TS. Reovirus-induced apoptosis requires activation of transcription factor NF-kappaB. J Virol 2000 Apr;74(7):2981-9.

91. Danthi P, Kobayashi T, Holm GH, Hansberger MW, Abel TW, Dermody TS. Reovirus apoptosis and virulence are regulated by host cell membrane penetration efficiency. J Virol 2008 Jan;82(1):161-72.

92. Stebbing RE, Irvin SC, Rivera-Serrano EE, Boehme KW, Ikizler M, Yoder JA, Dermody TS, Sherry B. An ITAM in a nonenveloped virus regulates activation of NF-kappaB, induction of beta interferon, and viral spread. J Virol 2014 Mar;88(5):2572-83.

93. Knowlton JJ, Dermody TS, Holm GH. Apoptosis induced by mammalian reovirus is beta interferon (IFN) independent and enhanced by IFN regulatory factor 3- and NF-kappaB-dependent expression of noxa. J Virol 2012 Feb;86(3):1650-60.

94. Carew JS, Espitia CM, Zhao W, Kelly KR, Coffey M, Freeman JW, Nawrocki ST. Reolysin is a novel reovirus-based agent that induces endoplasmic reticular stress-mediated apoptosis in pancreatic cancer. Cell Death Dis 2013 Jul 18;4:e728.

95. Kelly KR, Espitia CM, Mahalingam D, Oyajobi BO, Coffey M, Giles FJ, Carew JS, Nawrocki ST. Reovirus therapy stimulates endoplasmic reticular stress, NOXA induction, and augments bortezomib-mediated apoptosis in multiple myeloma. Oncogene 2011 Oct 17.

96. Schulze A, Harris AL. How cancer metabolism is tuned for proliferation and vulnerable to disruption. Nature 2012 Nov 15;491(7424):364-73.

97. Rossignol R, Gilkerson R, Aggeler R, Yamagata K, Remington SJ, Capaldi RA. Energy substrate modulates mitochondrial structure and oxidative capacity in cancer cells. Cancer Res 2004 Feb 1;64(3):985-93.

98. Jose C, Bellance N, Rossignol R. Choosing between glycolysis and oxidative phosphorylation: A tumor's dilemma? Biochim Biophys Acta 2011 Jun;1807(6):552-61.

99. Baracca A, Chiaradonna F, Sgarbi G, Solaini G, Alberghina L, Lenaz G. Mitochondrial complex I decrease is responsible for bioenergetic dysfunction in K-ras transformed cells. Biochim Biophys Acta 2010 Feb;1797(2):314-23.

100. Gaglio D, Metallo CM, Gameiro PA, Hiller K, Danna LS, Balestrieri C, Alberghina L, Stephanopoulos G, Chiaradonna F. Oncogenic K-ras decouples glucose and glutamine metabolism to support cancer cell growth. Mol Syst Biol 2011 Aug 16;7:523.

101. Zheng W, Tayyari F, Gowda GA, Raftery D, McLamore ES, Porterfield DM, Donkin SS, Bequette B, Teegarden D. Altered glucose metabolism in harvey-ras transformed MCF10A cells. Mol Carcinog 2013 Sep 2.

102. Hu Y, Lu W, Chen G, Wang P, Chen Z, Zhou Y, Ogasawara M, Trachootham D, Feng L, Pelicano H, et al. K-ras(G12V) transformation leads to mitochondrial dysfunction and a metabolic switch from oxidative phosphorylation to glycolysis. Cell Res 2012 Feb;22(2):399-412.

103. Boland ML, Chourasia AH, Macleod KF. Mitochondrial dysfunction in cancer. Front Oncol 2013 Dec 2;3:292.

104. Tan AS, Baty JW, Berridge MV. The role of mitochondrial electron transport in tumorigenesis and metastasis. Biochim Biophys Acta 2014 Apr;1840(4):1454-63.

105. Kwong JQ, Henning MS, Starkov AA, Manfredi G. The mitochondrial respiratory chain is a modulator of apoptosis. J Cell Biol 2007 Dec 17;179(6):1163-77.

106. Cosentino K, Garcia-Saez AJ. Mitochondrial alterations in apoptosis. Chem Phys Lipids 2014 Jul;181C:62-75.

107. Gottlieb E, Armour SM, Harris MH, Thompson CB. Mitochondrial membrane potential regulates matrix configuration and cytochrome c release during apoptosis. Cell Death Differ 2003 Jun;10(6):709-17.

108. Zhang L, Yu J, Park BH, Kinzler KW, Vogelstein B. Role of BAX in the apoptotic response to anticancer agents. Science 2000 Nov 3;290(5493):989-92.

109. Alain T, Kim M, Johnston RN, Urbanski S, Kossakowska AE, Forsyth PA, Lee PW. The oncolytic effect in vivo of reovirus on tumour cells that have survived reovirus cell killing in vitro. Br J Cancer 2006 Oct 23;95(8):1020-7.

110. Zhao L, Wientjes MG, Au JL. Evaluation of combination chemotherapy: Integration of nonlinear regression, curve shift, isobologram, and combination index analyses. Clin Cancer Res 2004 Dec 1;10(23):7994-8004.

111. Chou TC, Talalay P. Quantitative analysis of dose-effect relationships: The combined effects of multiple drugs or enzyme inhibitors. Adv Enzyme Regul 1984;22:27-55.

112. Kueng W, Silber E, Eppenberger U. Quantification of cells cultured on 96-well plates. Anal Biochem 1989 Oct;182(1):16-9.

113. Vega-Avila E, Pugsley MK. An overview of colorimetric assay methods used to assess survival or proliferation of mammalian cells. Proc West Pharmacol Soc 2011;54:10-4.

114. Petriz J, Garcia-Lopez J. Flow cytometric analysis of P-glycoprotein function using rhodamine 123. Leukemia 1997 Jul;11(7):1124-30.

115. Guillerman RP, Voss SD, Parker BR. Leukemia and lymphoma. Radiol Clin North Am 2011 Jul;49(4):767,97, vii.

116. Balgobind BV, Zwaan CM, Pieters R, Van den Heuvel-Eibrink,M.M. The heterogeneity of pediatric MLL-rearranged acute myeloid leukemia. Leukemia 2011 print;25(8):1239-48.

117. Pui CH, Mullighan CG, Evans WE, Relling MV. Pediatric acute lymphoblastic leukemia: Where are we going and how do we get there? Blood 2012 Aug 9;120(6):1165-74.

118. Kaspers GJ. Pediatric acute myeloid leukemia. Expert Rev Anticancer Ther 2012 Mar;12(3):405-13.

119. Reaman GH, Sposto R, Sensel MG, Lange BJ, Feusner JH, Heerema NA, Leonard M, Holmes EJ, Sather HN, Pendergrass TW, et al. Treatment outcome and prognostic factors for infants with acute lymphoblastic leukemia treated on two consecutive trials of the children's cancer group. J Clin Oncol 1999 Feb;17(2):445-55.

120. Robison LL. Late effects of acute lymphoblastic leukemia therapy in patients diagnosed at 0-20 years of age. Hematology Am Soc Hematol Educ Program 2011;2011:238-42.

121. Fulbright JM, Raman S, McClellan WS, August KJ. Late effects of childhood leukemia therapy. Curr Hematol Malig Rep 2011 Sep;6(3):195-205.

122. Alain T, Hirasawa K, Pon KJ, Nishikawa SG, Urbanski SJ, Auer Y, Luider J, Martin A, Johnston RN, Janowska-Wieczorek A, et al. Reovirus therapy of lymphoid malignancies. Blood 2002 Dec 1;100(12):4146-53.

123. Thirukkumaran CM, Shi ZQ, Luider J, Kopciuk K, Gao H, Bahlis N, Neri P, Pho M, Stewart D, Mansoor A, et al. Reovirus as a viable therapeutic option for the treatment of multiple myeloma. Clin Cancer Res 2012 Sep 15;18(18):4962-72.

124. Freedman MH, Grunberger T, Correa P, Axelrad AA, Dube ID, Cohen A. Autocrine and paracrine growth control by granulocyte-monocyte colony-stimulating factor of acute lymphoblastic leukemia cells. Blood 1993 Jun 1;81(11):3068-75.

125. Greil J, Gramatzki M, Burger R, Marschalek R, Peltner M, Trautmann U, Hansen-Hagge TE, Bartram CR, Fey GH, Stehr K. The acute lymphoblastic leukaemia cell line SEM with t(4;11) chromosomal rearrangement is biphenotypic and responsive to interleukin-7. Br J Haematol 1994 Feb;86(2):275-83.

126. Shen M, Horbett TA. The effects of surface chemistry and adsorbed proteins on monocyte/macrophage adhesion to chemically modified polystyrene surfaces. J Biomed Mater Res 2001 Dec 5;57(3):336-45.

127. Schwartz-Roberts JL, Shajahan AN, Cook KL, Warri A, Abu-Asab M, Clarke R. GX15-070 (obatoclax) induces apoptosis and inhibits cathepsin D- and L-mediated autophagosomal lysis in antiestrogen-resistant breast cancer cells. Mol Cancer Ther 2013 Apr;12(4):448-59.

128. Kominsky D, Bickel R, and Tyler K. Reovirus-induced apoptosis requires both death receptor- and mitochondrial-mediated caspase-dependent pathways of cell death. Cell Death and Differentiation 2002;9:926-33.

129. Cho IR, Koh SS, Min HJ, Park EH, Srisuttee R, Jhun BH, Kang CD, Kim M, Johnston RN, Chung YH. Reovirus infection induces apoptosis of TRAIL-resistant gastric cancer cells by down-regulation of akt activation. Int J Oncol 2010 Apr;36(4):1023-30.

130. Arato-Oshima T, Matsui H, Wakizaka A, Homareda H. Mechanism responsible for oligomycin-induced occlusion of na+ within na/K-ATPase. J Biol Chem 1996 Oct 11;271(41):25604-10.

131. Gemin A, Sweet S, Preston TJ, Singh G. Regulation of the cell cycle in response to inhibition of mitochondrial generated energy. Biochem Biophys Res Commun 2005 Jul 15;332(4):1122-32.

132. Barrientos A, Moraes CT. Titrating the effects of mitochondrial complex I impairment in the cell physiology. J Biol Chem 1999 Jun 4;274(23):16188-97.

133. van den Wollenberg DJ, Dautzenberg IJ, van den Hengel SK, Cramer SJ, de Groot RJ, Hoeben RC. Isolation of reovirus T3D mutants capable of infecting human tumor cells independent of junction adhesion molecule-A. PLoS One 2012;7(10):e48064.

134. Schulz WL, Haj AK, Schiff LA. Reovirus uses multiple endocytic pathways for cell entry. J Virol 2012 Dec;86(23):12665-75.

135. Barton ES, Forrest JC, Connolly JL, Chappell JD, Liu Y, Schnell FJ, Nusrat A, Parkos CA, Dermody TS. Junction adhesion molecule is a receptor for reovirus. Cell 2001 Feb 9;104(3):441-51.

136. Campbell JA, Schelling P, Wetzel JD, Johnson EM, Forrest JC, Wilson GA, Aurrand-Lions M, Imhof BA, Stehle T, Dermody TS. Junctional adhesion molecule a serves as a receptor for prototype and field-isolate strains of mammalian reovirus. J Virol 2005 Jul;79(13):7967-78.

137. Loken SD, Norman K, Hirasawa K, Nodwell M, Lester WM, Demetrick DJ. Morbidity in immunosuppressed (SCID/NOD) mice treated with reovirus (dearing 3) as an anti-cancer biotherapeutic. Cancer Biol Ther 2004 Aug;3(8):734-8.

138. Kim M, Garant KA, zur Nieden NI, Alain T, Loken SD, Urbanski SJ, Forsyth PA, Rancourt DE, Lee PW, Johnston RN. Attenuated reovirus displays oncolysis with reduced host toxicity. Br J Cancer 2011 Jan 18;104(2):290-9.

139. Shaw RJ, Doherty DE, Ritter AG, Benedict SH, Clark RA. Adherence-dependent increase in human monocyte PDGF(B) mRNA is associated with increases in c-fos, c-jun, and EGR2 mRNA. J Cell Biol 1990 Nov;111(5 Pt 1):2139-48.

140. Heinemann L, Simpson GR, Boxall A, Kottke T, Relph KL, Vile R, Melcher A, Prestwich R, Harrington KJ, Morgan R, et al. Synergistic effects of oncolytic reovirus and docetaxel chemotherapy in prostate cancer. BMC Cancer 2011 Jun 6;11:221,2407-11-221.

141. Ni Chonghaile T, Sarosiek KA, Vo TT, Ryan JA, Tammareddi A, Moore Vdel G, Deng J, Anderson KC, Richardson P, Tai YT, et al. Pretreatment mitochondrial priming correlates with clinical response to cytotoxic chemotherapy. Science 2011 Nov 25;334(6059):1129-33.

142. Vo TT, Ryan J, Carrasco R, Neuberg D, Rossi DJ, Stone RM, Deangelo DJ, Frattini MG, Letai A. Relative mitochondrial priming of myeloblasts and normal HSCs determines chemotherapeutic success in AML. Cell 2012 Oct 12;151(2):344-55.

143. Lagadinou ED, Sach A, Callahan K, Rossi RM, Neering SJ, Minhajuddin M, Ashton JM, Pei S, Grose V, O'Dwyer KM, et al. BCL-2 inhibition targets oxidative phosphorylation and selectively eradicates quiescent human leukemia stem cells. Cell Stem Cell 2013 Mar 7;12(3):329-41.

144. Jayanthan A, Incoronato A, Singh A, Blackmore C, Bernoux D, Lewis V, Stam R, Whitlock JA, Narendran A. Cytotoxicity, drug combinability, and biological correlates of ABT-737 against acute lymphoblastic leukemia cells with MLL rearrangement. Pediatr Blood Cancer 2011 Mar;56(3):353-60.

145. Singh A, Jayanthan A, Farran A, Elwi AN, Kim SW, Farran P, Narendran A. Induction of apoptosis in pediatric acute lymphoblastic leukemia (ALL) cells by the therapeutic opioid methadone and effective synergy with bcl-2 inhibition. Leuk Res 2011 Dec;35(12):1649-57.

146. High LM, Szymanska B, Wilczynska-Kalak U, Barber N, O'Brien R, Khaw SL, Vikstrom IB, Roberts AW, Lock RB. The bcl-2 homology domain 3 mimetic ABT-737 targets the apoptotic machinery in acute lymphoblastic leukemia resulting in synergistic in vitro and in vivo interactions with established drugs. Mol Pharmacol 2010 Mar;77(3):483-94.

147. Del Gaizo Moore V, Schlis KD, Sallan SE, Armstrong SA, Letai A. BCL-2 dependence and ABT-737 sensitivity in acute lymphoblastic leukemia. Blood 2008 Feb 15;111(4):2300-9.

148. Paoluzzi L, Gonen M, Bhagat G, Furman RR, Gardner JR, Scotto L, Gueorguiev VD, Heaney ML, Manova K, O'Connor OA. The BH3-only mimetic ABT-737 synergizes the antineoplastic activity of proteasome inhibitors in lymphoid malignancies. Blood 2008 Oct 1;112(7):2906-16.

149. Goard CA, Schimmer AD. An evidence-based review of obatoclax mesylate in the treatment of hematological malignancies. Core Evid 2013;8:15-26.

150. Davids MS, Letai A. Targeting the B-cell lymphoma/leukemia 2 family in cancer. J Clin Oncol 2012 Sep 1;30(25):3127-35.

151. Davids MS, Letai A. ABT-199: Taking dead aim at BCL-2. Cancer Cell 2013 Feb 11;23(2):139-41.

152. Lemke J, von Karstedt S, Zinngrebe J, Walczak H. Getting TRAIL back on track for cancer therapy. Cell Death Differ 2014 Jun 20.

153. Ehrhardt H, Hofig I, Wachter F, Obexer P, Fulda S, Terziyska N, Jeremias I. NOXA as critical mediator for drug combinations in polychemotherapy. Cell Death Dis 2012 Jun 21;3:e327.

154. Russell RC, Yuan HX, Guan KL. Autophagy regulation by nutrient signaling. Cell Res 2014 Jan;24(1):42-57.

155. Youle RJ, van der Bliek AM. Mitochondrial fission, fusion, and stress. Science 2012 Aug 31;337(6098):1062-5.

156. Frank S, Gaume B, Bergmann-Leitner ES, Leitner WW, Robert EG, Catez F, Smith CL, Youle RJ. The role of dynamin-related protein 1, a mediator of mitochondrial fission, in apoptosis. Dev Cell 2001 Oct;1(4):515-25.

157. Frezza C, Cipolat S, Martins de Brito O, Micaroni M, Beznoussenko GV, Rudka T, Bartoli D, Polishuck RS, Danial NN, De Strooper B, et al. OPA1 controls apoptotic cristae remodeling independently from mitochondrial fusion. Cell 2006 Jul 14;126(1):177-89.

158. Chi X, Kale J, Leber B, Andrews DW. Regulating cell death at, on, and in membranes. Biochim Biophys Acta 2014 Jun 11.

159. Wolvetang EJ, Johnson KL, Krauer K, Ralph SJ, Linnane AW. Mitochondrial respiratory chain inhibitors induce apoptosis. FEBS Lett 1994 Feb 14;339(1-2):40-4.

160. Hao W, Chang CP, Tsao CC, Xu J. Oligomycin-induced bioenergetic adaptation in cancer cells with heterogeneous bioenergetic organization. J Biol Chem 2010 Apr 23;285(17):12647-54.

161. Epstein T, Xu L, Gillies RJ, Gatenby RA. Separation of metabolic supply and demand: Aerobic glycolysis as a normal physiological response to fluctuating energetic demands in the membrane. Cancer Metab 2014 Jun 5;2:7,3002-2-7. eCollection 2014.

162. Burgener A, Coombs K, Butler M. Intracellular ATP and total adenylate concentrations are critical predictors of reovirus productivity from vero cells. Biotechnol Bioeng 2006 Jul 5;94(4):667-79.

163. Lee Y, Oh SB, Park HR, Kim HS, Kim MS, Lee J. Selective impairment on the proliferation of neural progenitor cells by oxidative phosphorylation disruption. Neurosci Lett 2013 Feb 22;535:134-9.

164. Cuezva JM, Ortega AD, Willers I, Sanchez-Cenizo L, Aldea M, Sanchez-Arago M. The tumor suppressor function of mitochondria: Translation into the clinics. Biochim Biophys Acta 2009 Dec;1792(12):1145-58.

165. Sanchez-Arago M, Chamorro M, Cuezva JM. Selection of cancer cells with repressed mitochondria triggers colon cancer progression. Carcinogenesis 2010 Apr;31(4):567-76.

166. Reis Y, Bernardo-Faura M, Richter D, Wolf T, Brors B, Hamacher-Brady A, Eils R, Brady NR. Multi-parametric analysis and modeling of relationships between mitochondrial morphology and apoptosis. PLoS One 2012;7(1):e28694.

167. Wang X, Peralta S, Moraes CT. Mitochondrial alterations during carcinogenesis: A review of metabolic transformation and targets for anticancer treatments. Adv Cancer Res 2013;119:127-60.

168. Lock RB, Liem N, Farnsworth ML, Milross CG, Xue C, Tajbakhsh M, Haber M, Norris MD, Marshall GM, Rice AM. The nonobese diabetic/severe combined immunodeficient (NOD/SCID) mouse model of childhood acute lymphoblastic leukemia reveals intrinsic differences in biologic characteristics at diagnosis and relapse. Blood 2002 Jun 1;99(11):4100-8.